CHAPTER 4

Multiple Sequence Alignment

INTRODUCTION

One of the most important contributions of molecular biology to evolutionary analysis is the discovery that the DNA sequences of different organisms are often related. Similar genes are conserved across widely divergent species, often performing a similar or even identical function, and at other times, mutating or rearranging to perform an altered function through the forces of natural selection. Thus, many genes are represented in highly conserved forms in organisms. Through simultaneous alignment of the sequences of these genes, sequence patterns that have been subject to alteration may be analyzed.

Because the potential for learning about the structure and function of molecules by multiple sequence alignment (msa) is so great, computational methods have received a great deal of attention. In msa, sequences are aligned optimally by bringing the greatest number of similar characters into register in the same column of the alignment, just as described in Chapter 3 for the alignment of two sequences. Computationally, msa presents several difficult challenges. First, finding an optimal alignment of more than two sequences that includes matches, mismatches, and gaps, and that takes into account the degree of variation in all of the sequences at the same time poses a very difficult challenge. The dynamic programming algorithm used for optimal alignment of pairs of sequences can be extended to three sequences, but for more than three sequences, only a small number of relatively short sequences may be analyzed. Thus, approximate methods are used, including (1) a progressive global alignment of the sequences starting with an alignment of the most alike sequences and then building an alignment by adding more sequences, (2) iterative methods that make an initial alignment of groups of sequences and then revise the alignment to achieve a more reasonable result, (3) alignments based on locally conserved patterns found in the same order in the sequences, and (4) use of statistical methods and probabilistic models of the sequences. A second computational challenge is identifying a reasonable method of obtaining a cumulative score for the substitutions in the column of an msa. Finally, the placement and scoring of gaps in the various sequences of an msa presents an additional challenge.

The msa of a set of sequences may also be viewed as an evolutionary history of the sequences. If the sequences in the msa align very well, they are likely to be recently derived from a common ancestor sequence. Conversely, a group of poorly aligned sequences share a more complex and distant evolutionary relationship. The task of aligning a set of sequences, some more closely and others less closely related, is identical to that of discovering the evolutionary relationships among the sequences.

As with aligning a pair of sequences, the difficulty in aligning a group of sequences varies considerably with sequence similarity. On the one hand, if the amount of sequence variation is minimal, it is quite straightforward to align the sequences, even without the assistance of a computer program. On the other hand, if the amount of sequence variation is great, it may be very difficult to find an optimal alignment of the sequences because so many combinations of substitutions, insertions, and deletions, each predicting a different alignment, are possible.

The availability of a subset of the many multiple sequence alignment programs is shown in Table 4.1. A flowchart illustrating the considerations to be made in choosing an alignment method is shown on page 144.

When dealing with a sequence of unknown function, the presence of similar domains in several similar sequences implies a similar biochemical function or structural fold that may become the basis of further experimental investigation. A group of similar sequences may

Table 4.1. *Web sites and program sources for multiple sequence alignment*

Name	Source	Reference
Global alignments including progressive		
CLUSTALW or CLUSTALX (latter has graphical interface)	FTP to ftp.ebi.ac.uk/pub/software[a,d]	Thompson et al. (1994a, 1997); Higgins et al. (1996)
MSA	http://www.psc.edu/[b] http://www.ibc.wustl.edu/ibc/msa.html[c] FTP to fastlink.nih.gov/pub/msa	Lipman et al. (1989); Gupta et al. (1995)
PRALINE	http://mathbio.nimr.mrc.ac.uk/~jhering/praline	Heringa (1999)
Iterative and other methods		
DIALIGN segment alignment	http://www.gsf.de/biodv/dialign.html	Morgenstern et al. (1996)
MultAlin	http://protein.toulouse.inra.fr/multalin.html	Corpet (1988)
PRRP progressive global alignment (randomly or doubly nested)	ftp.genome.ad.jp/pub/genome/saitama-cc	Gotoh (1996)
SAGA genetic algorithm	http://igs-server.cnrs-mrs.fr/~cnotred/Projects_home_page/saga_home_page.html	Notredame and Higgins (1996)
Local alignments of proteins		
Aligned Segment Statistical Evaluation Tool (Asset)	FTP to ncbi.nlm.nih.gov/pub/neuwald/asset	Neuwald and Green (1994)
BLOCKS Web site	http://blocks.fhcrc.org/blocks/	Henikoff and Henikoff (1991, 1992)
eMOTIF Web server	http://dna.Stanford.EDU/emotif/	Nevill-Manning et al. (1998)
GIBBS, the Gibbs sampler statistical method	FTP to ncbi.nlm.nih.gov/pub/neuwald/gibbs9_95/	Lawrence et al. (1993); Liu et al. (1995); Neuwald et al. (1995)
HMMER hidden Markov model software	http://hmmer.wustl.edu/	Eddy (1998)
MACAW, a workbench for multiple alignment construction and analysis	FTP to ncbi.nlm.nih.gov/pub/macaw	Schuler et al. (1991)
MEME Web site, expectation maximization method	http://meme.sdsc.edu/meme/website/	Bailey and Elkan (1995); Grundy et al. (1996, 1997); Bailey and Gribskov (1998)
Profile analysis at UCSD[a,e]	http://www.sdsc.edu/projects/profile/	Gribskov and Veretnik (1996)
SAM hidden Markov model Web site	http://www.cse.ucsc.edu/research/compbio/sam.html	Krogh et al. (1994); Hughey and Krogh (1996)

[a] Lists of additional Web sites for msa are maintained at: http://www.ebi.ac.uk/biocat/, http://www.hgmp.mrc.ac.uk/Registered/Menu/prot-mult.html, http://www.hum-molgen.de/BioLinks/Biocomp.html, http://biocenter.helsinki.fi/bi/rnd/biocomp/. Reviews on the performance of msa software are given in McClure et al. (1994; progressive alignment methods), Gotoh (1996) and Thompson et al. (1999), a review of Web sites is given in Briffeuil et al. (1998) and a review on iterative algorithms is given in Hirosawa et al. (1995) and Gotoh (1999). The performance of msa programs is commonly assessed by comparing the computed msa with a structural alignment of the proteins and by other objective methods (Notredame et al. 1998). Many of these programs are computationally complex and must be set up on a local site.

[b] The Biomedical Supercomputing facility at the University of Pittsburgh Supercomputing Facility provides accounts (see http://www.psc.edu/biomed/seqanal/grants.html) that provide access to several different versions of MSA and profile analysis. MSA 50 150 will align no more than 50 sequences each less than 150 residues long, MSA 25 500 will align no more than 25 sequences each less than 200 residues long, and MSA10 1000 will align no more than 10 sequences each less than 1000 long.

[c] The MSA server at the University of Washington will take up to 8 sequences, each less than 500 long.

[d] CLUSTALW is also available as freeware that runs on PCs and Macintosh computers from the same FTP site.

[e] Profile generating programs are available by FTP from ftp.sdsc.edu/pub/sdsc/biology and are included in the Genetics Computer Group suite of programs (http://www.gcg.com/), although the most recent features of Gribskov and Veretnik (1996) are not included.

define a protein family that may share a common biochemical function or evolutionary origin. Similar proteins have been organized into databases of protein families that are described in Chapter 9.

GENOME SEQUENCING

One application of multiple sequence alignment algorithms is in genome sequencing projects discussed in Chapter 2. Instead of cloning and arranging a very large number of fragments of a large DNA molecule, and then moving along the molecule and sequencing the fragments in order, random fragments of the large molecule are sequenced, and those that overlap are found by a msa program. This approach enables automated assembly of large sequences. Bacterial genomes have been quite readily sequenced by this method, and it has also been used to assemble portions of the *Drosophila* and human genomes at Celera Genomics (Weber and Myers 1997 and see Chapter 10).

The requirements for a msa program for genome projects differ in several respects from those for general sequence analysis. First, the sequences are fragments of the same large sequence molecule, and the sequences of overlapping fragments should be the same except for sequence copying and reading errors, which may introduce the equivalent of substitutions and insertions/deletions between the compared fragments. Thus, there should be one correct alignment that corresponds to that of the genome sequence instead of a range of possibilities. Second, the sequences may be from one DNA strand or the other and hence the complements of each sequence must also be compared. Third, sequence fragments will usually overlap, but by an unknown amount, and, in some cases, one sequence may be included within another. Finally, all of the overlapping pairs of sequence fragments must be assembled into a large, composite genome sequence, taking into account any redundant or inconsistent information. Interested readers may wish to consult a description of the type of methodology (Myers 1995 and see Chapter 10) and a comparison of the methods, including several commercial packages that are useful for managing the sequence data from laboratory sequencing projects (Miller and Powell 1994). The Institutue of Genome Research (http://www.tigr.org/) has also developed and made available software and methods for genome assembly and analysis.

USES OF MULTIPLE SEQUENCE ALIGNMENTS

Just as the alignment of a pair of nucleic acid or protein sequences can reveal whether or not there is an evolutionary relationship between the sequences, so can the alignment of three or more sequences reveal relationships among multiple sequences. Multiple sequence alignment of a set of sequences can provide information as to the most alike regions in the set. In proteins, such regions may represent conserved functional or structural domains.

If the structure of one or more members of the alignment is known, it may be possible to predict which amino acids occupy the same spatial relationship in other proteins in the alignment. In nucleic acids, such alignments also reveal structural and functional relationships. For example, aligned promoters of a set of similarly regulated genes may reveal consensus binding sites for regulatory proteins. Methods for finding such sites in nucleic acid sequences are discussed in Chapter 8.

Another use for consensus information retrieved from a multiple sequence alignment is for the prediction of specific probes for other members of the same group or family of similar sequences in the same or other organisms. There are both computer and molecular biology applications. Once a consensus pattern has been found, database searching pro-

grams (Chapter 7) may be used to find other sequences with a similar pattern. In the laboratory, a reasonable consensus of such patterns may be used to design polymerase chain reaction (PCR) primers for amplification of related sequences.

RELATIONSHIP OF MULTIPLE SEQUENCE ALIGNMENT TO PHYLOGENETIC ANALYSIS

Once the msa has been found, the number or types of changes in the aligned sequence residues may be used for a phylogenetic analysis. The alignment provides a prediction as to which sequence characters correspond. Each column in the alignment predicts the mutations that occurred at one site during the evolution of the sequence family, as illustrated in Figure 4.1. Within the column are original characters that were present early, as well as other derived characters that appeared later in evolutionary time. In some cases, the position is so important for function that mutational changes are not observed. It is these conserved positions that are useful for producing an alignment. In other cases, the position is less important, and substitutions are observed. Deletions and insertions may also be present in some regions of the alignment. Thus, starting with the alignment, one can hope to dissect the order of appearance of the sequences during evolution.

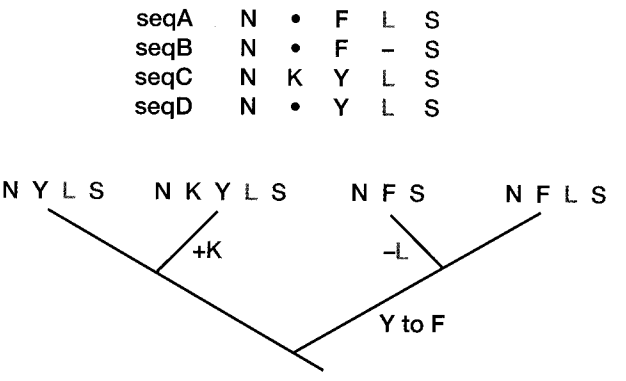

Figure 4.1. The close relationship between msa and evolutionary tree construction. Shown is a short section of one msa of four protein sequences including conserved and substituted positions, an insertion (of K) and a deletion (of L). Below is a hypothetical evolutionary tree that could have generated these sequence changes. Each outer "branch" in the tree represents one of the sequences. The outer branches are also referred to as "leaves." The deepest, oldest branch is that of sequence D, followed by A, then by B and C. The optimal alignment of several sequences can thereby be thought of as minimizing the number of mutational steps in an evolutionary tree for which the sequences are the outer branches or leaves. The mathematical solution to this problem was first outlined by Sankoff (1975). Fast multiple sequence alignment programs that are tree-based have since been developed (Ravi and Kececioglu 1998). However, such an approach depends on knowing the evolutionary tree to perform an alignment, and often this is not the case. Usually, pair-wise alignments are generated first and then used to predict the tree. In this example, the alignment could be explained by several different trees, including the one shown, following one of several types of analyses described in Chapter 6. The sequences then become the outer leaves of the tree, and the inner branches are constructed by this analysis.

METHODS

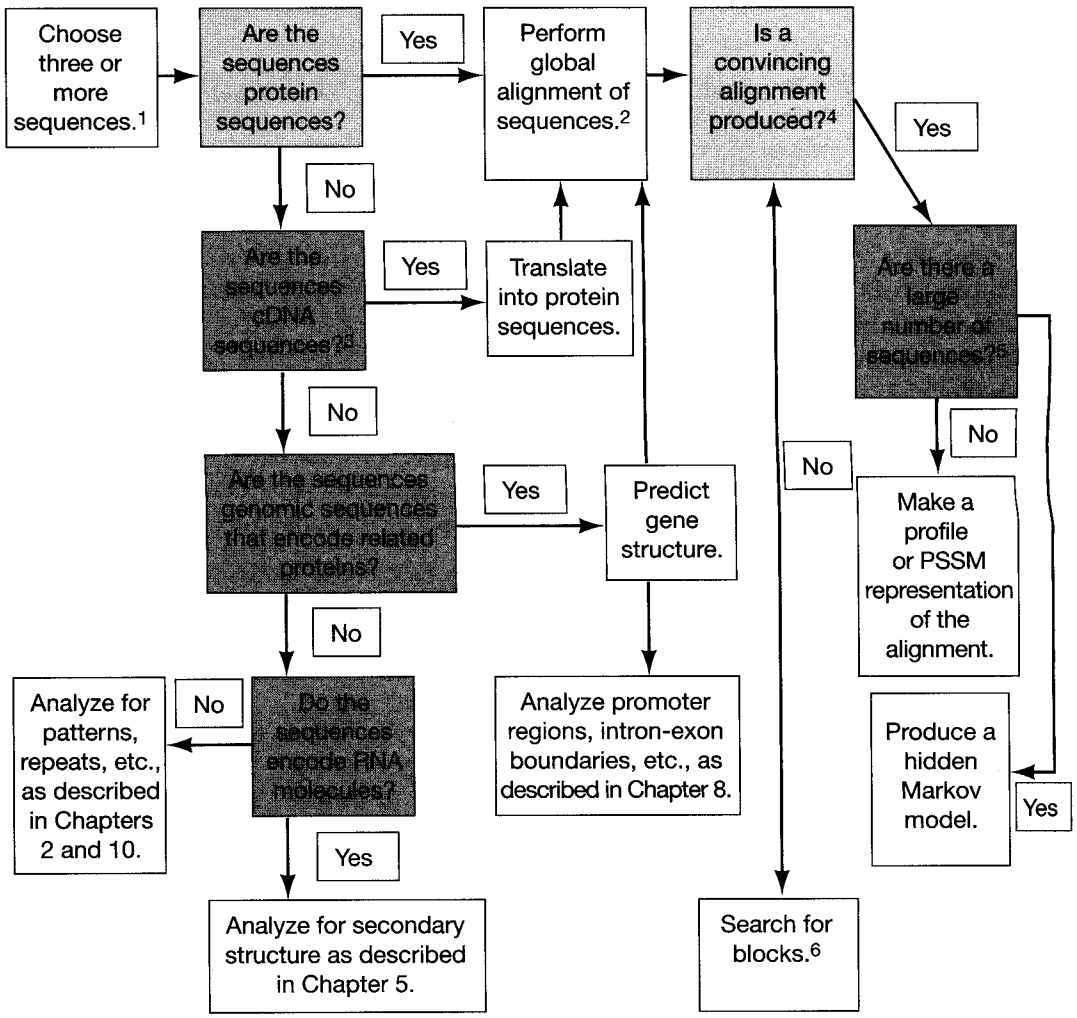

1. The sequence chosen for analysis may already be known to be similar on the basis of pair-wise alignments (Chapter 2), but sequences related by other criteria may also be used. Complex features of the sequences, including repeated or low-complexity regions that interfere with alignments, can be analyzed as described in Chapters 2 and 7. The flowchart describes the production of four classes of multiple sequence alignment.
   a. A global alignment includes the entire range of each sequence in the alignment, and is usually produced by extensions to the dynamic programming global alignment algorithm that is used for aligning pairs of sequences, but other methods are also used.
   b. A sequence block is an alignment of common patterns in protein sequences that includes matches and mismatches in each column found by using pattern-finding algorithms, but no gaps (insertions and deletions) are present.
   c. An alignment of common patterns in protein sequences that includes matches, mismatches, insertions, and deletions may be used to make a type of scoring matrix called a profile.
   d. A hidden Markov model is a probabilistic model of a global alignment of protein sequences or of a conserved local region (similar to a sequence profile) in those sequences that includes matches, mismatches, insertions, and deletions. The model is "trained" to represent the set of sequences.

Methods for finding common patterns in DNA sequences are discussed in Chapter 8.

2. Examples of global alignment, as well as other programs from which to choose, are given in the global alignments and iterative and other methods sections of Table 4.1.
3. cDNA sequences of the same gene from a group of organisms may be multiply aligned by a global method so that synonymous (i.e., change the amino acid) and nonsynonymous (i.e., do not change the amino acid) sequences may be analyzed, as described in Chapter 6 (see also note 2).
4. A convincing alignment should include a series of columns in which a majority of the sequences have the same amino acid or an amino acid that is a conservative substitution for that amino acid, with relatively few examples of other substitutions or gaps in these columns. These columns of alike amino acids should be found throughout the alignment, often clustered into domains. There may also be variable regions in the alignment that represent sequences that diverged more during the evolution of the protein family.
5. This decision rests on whether or not there are enough sequences on which to build a hidden Markov model of the entire alignment or of a well-defined region in the alignment (a profile hidden Markov model). For sequences that are related but show considerable variations in many columns, as many as 100 sequences may be needed to produce a hidden Markov model of the alignment. This number is reduced to approximately 25–50 if there is less variation among the sequences. A scoring matrix representing the sequence variation found in each column of the alignment may also be made. These matrices may accommodate gaps in the alignment (a profile or HMM profile) or may not include gaps (position-specific scoring matrix).
6. For finding patterns common to the sequences, pattern-searching algorithms and statistical methods are used. The former search for a set of matched sequence characters that are present in the sequences. The latter perform an exhaustive analysis of sequence "windows" in the sequences to find the most alike amino acid patterns by the expectation maximization (EM) or Gibbs sampling algorithms. These methods are described in the text.

MULTIPLE SEQUENCE ALIGNMENT AS AN EXTENSION OF SEQUENCE PAIR ALIGNMENT BY DYNAMIC PROGRAMMING

The dynamic programming algorithm described in Chapter 2 provides an optimal alignment of two sequences. In the program MSA (Lipman et al. 1989), application of the global alignment algorithm has been extended to provide an optimal alignment of a small number of sequences greater than two. Gupta et al. (1995) have shown, however, that MSA rarely produces a provable optimal alignment. The number of sequences that can be aligned is limited because the number of computational steps and the amount of memory required grow exponentially with the number of sequences to be analyzed. This limitation means that the program has somewhat limited application to a small number of sequences.

Recall that the dynamic programming method of sequence alignment between two sequences builds a scoring matrix where each position provides the best alignment up to that point in the sequence comparison. The number of comparisons that must be made to fill this matrix without using any short cuts and excluding gaps is the product of the length of the two sequences. Imagine extending this analysis to three or more sequences. For three sequences, instead of the two-dimensional matrix for two sequences, think of the lattice of a cube that is to be filled with calculated dynamic programming scores. Scoring positions on three surfaces of the cube will represent the alignment values between a pair of the sequences, ignoring the third sequence, as illustrated in Figure 4.2. In MSA, positions inside the lattice of the cube are given values based on the sum of the initial scores of the three pairs of sequences.

For three protein sequences each 300 amino acids in length and excluding gaps, the number of comparisons to be made by dynamic programming is equal to $300^3 = 2.7 \times 10^7$, whereas only $300^2 = 9 \times 10^4$ is required for two sequences of this length. This number is sufficiently small that alignment of three sequences by this method is practical. For alignment of more than three sequences, one has to imagine filling an N-dimensional space or hypercube. The number of steps and memory required for a 300-amino-acid sequence (300^N, where N is the number of sequences) then becomes too large for most practical purposes, and it is necessary to find a way to reduce the number of comparisons that must be made without compromising the attempt to find an optimal alignment. Fortunately, Carrillo and Lipman (1988) found such a method, called the sum of pairs, or SP method. Since the publication of the MSA program, Gupta et al. (1995) have substantially reduced the memory requirements and number of steps required. The enhanced version of MSA is available by anonymous FTP from fastlink.nih.gov/pub/msa.

The basic idea is that a multiple sequence alignment imposes an alignment on each of the pairs of sequences. The heavy arrow in Figure 4.2 represents the path followed in the cube to find a msa for three sequences, but the msa can be projected on to the sides of the cube, thus defining an alignment for each pair of sequences. The alignments found for each pair of sequences likewise impose bounds on the location of the msa within the cube, and thus defines the number of positions within the cube that have to be evaluated. Pair-wise alignments are first computed between each pair of sequences. Next, a trial msa is produced by first predicting a phylogenetic tree for the sequences (Saitou and Nei 1987; see Chapter 6 for the neighbor-joining method of tree construction), and the sequences are

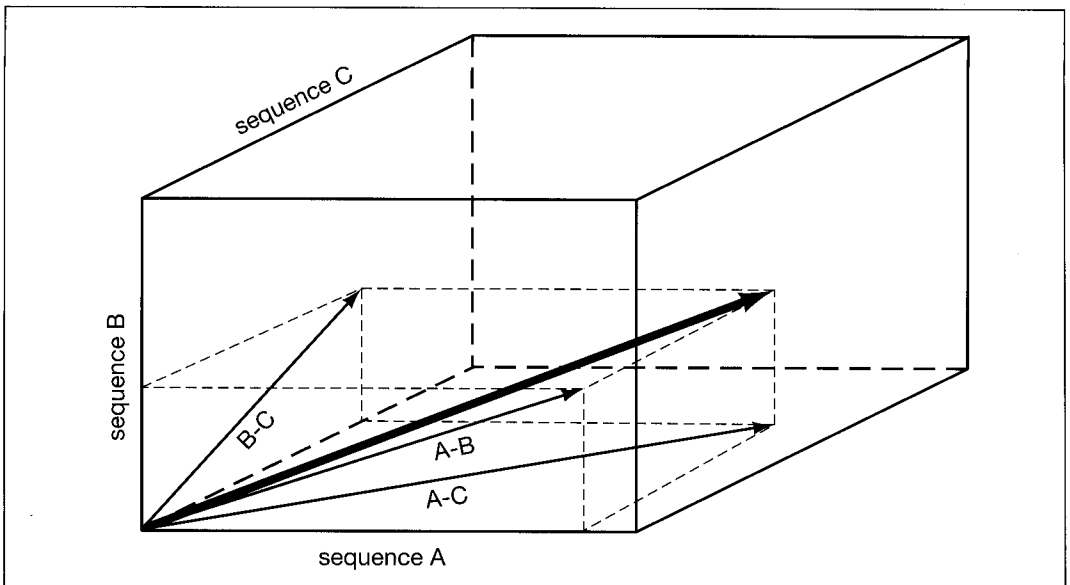

Figure 4.2. Alignment of three sequences by dynamic programming. Arrows on the surfaces of the cube indicate the direction for filling in the scoring matrix for pairs of sequences, A with B, etc., performed as previously described. The alignment of all three sequences requires filling in the lattice of the cube space with optimal alignment scores following the same algorithm. The best score at each interior position requires a consideration of all possible moves within the cube up to that point in the alignment. The trace-back matrix will align positions in all three sequences including gaps.

then multiply aligned in the order of their relationship on the tree. This method is used by other programs described below (e.g., PILEUP, CLUSTALW) and provides a heuristic alignment that is not guaranteed to be optimal. However, the alignment serves to provide a limit to the space within the cube within which optimal alignments are likely to be found. In Figure 4.3, the green area on the left surface of the cube is bounded by the optimal alignment of sequences B and C and a projection of the heuristic alignment for all three sequences. The orange and blue areas are similarly defined for other sequence pairs. The dark gray volume within the cube is bounded by projections from each of the three surface areas. For more sequences, a similar type of analysis of bounds may be performed in the corresponding higher-order space.

In practice, MSA calculates the multiple alignment score within the cube lattice by adding the scores of the corresponding pair-wise alignments in the msa. This measure is known as the SP measure (for sum of pairs), and the optimal alignment is based on obtaining the best SP score. These scores may or may not be weighted so as to reduce the influence of more closely related sequences in the msa. The Dayhoff PAM250 matrix and an associated gap penalty are used by MSA for aligning protein sequences. MSA uses a constant penalty for any size of gap and scores gaps according to the scheme illustrated in Figure 4.4 (Altschul 1989; Lipman et al. 1989). MSA calculates a value ϵ for each pair of sequences that provides an idea of how much of a role the alignment of those two sequences plays in the msa. ϵ for a given sequence pair is the difference between the score of the alignment of that pair in the msa and the score of the optimal pair-wise alignment. The bigger the value of ϵ, the more divergent the msa from the pair-wise alignment and the smaller the contribution of that alignment to the msa. For example, if an extra copy of one

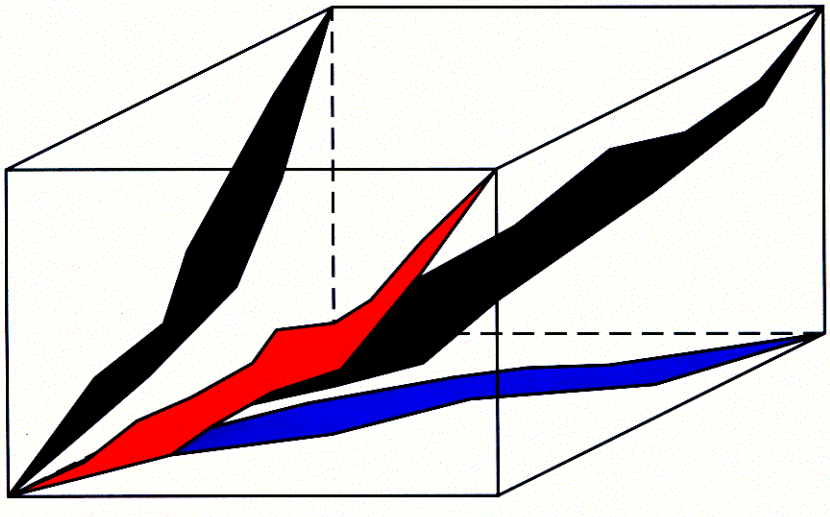

Figure 4.3. Bounds within which an optimal alignment will be found by MSA for three sequences. For MSA to find an optimal alignment among three sequences by the DP algorithm, it is only necessary to calculate optimal alignment scores within the gray volume. This volume is bounded on the one side by the optimal alignments found for each pair of sequences, and on the other by a heuristic multiple alignment of the sequences. The colored areas on each cube surface are two-dimensional projections of the gray volume.

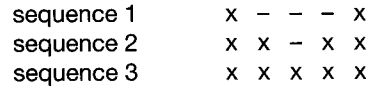

Figure 4.4. Method of scoring gap penalties by the msa program MSA. *x* indicates aligned residues, which may be a match or a mismatch, and – indicates a gap. In this example, each gap cost is 1, regardless of length. The "natural" gap cost is the sum of the number of gaps in all pair-wise combinations (sequences 1 and 2, 1 and 3, and 2 and 3). Note that the alignment of a gap of three in sequence 1 with a gap of length one in sequence 2 scores as gap of 1 because the gap in sequence 1 is longer. The quasi-natural gap cost is the natural cost for the gap plus an additional value for any gap that begins and ends within another. In this example, there is an additional penalty score for the presence of a single gap in sequence 2 that falls within a larger gap in sequence 1. The inclusion of this extra cost for a gap has little effect on the alignments produced but provides an enormous reduction in the amount of information that must be maintained in the DP scoring matrix (Altschul 1989), thus making possible the simultaneous alignment of more sequences by MSA.

of the sequences is added to the alignment project, then ϵ for sequence pairs that do not include that sequence will increase, indicating a lesser role because the contributions of that pair have been out-voted by the alike sequences (Altschul et al. 1989). Weighting the sequence pairs is designed to get around the common difficulty that some pairs in most sets of sequences are similar. Another score δ is the sum of the ϵs and gives an indication of the degree of divergence among the sequences—closely related sequences will have low ϵs and δs and distantly related sequences will have high ϵs and δs.

The MSA program avoids the bias in an alignment due to alike sequences by weighting the pair-wise scores before they are added to give the SP score. These weights are determined by using the predicted tree of the sequences discussed above. The pair-wise scores between all sequence pairs are adjusted to reduce the influence of the more unlike sequence pairs that occupy more distant "leaves" on the evolutionary tree (i.e., by sequences that are joined by more branches) based on the argument that these sequence pairs provide less useful information for computing the msa. This scheme is different from that used by other msa programs (see below), which generally increase the weight of scores from more distant sequences because these sequences represent greater divergence in the evolutionary tree (see Vingron and Sibbald 1993).

In using MSA, several additional practical considerations should be considered (described on MSA Web sites given in Table 4.1): (1) MSA is a heavy user of machine resources and is limited to a small number of sequences of relatively short lengths. (2) In the UNIX command line mode of the program, there are options that allow users to specify gap costs, force the alignment of certain residues, specify maximum values for ϵ, and tune the program in other ways. (3) When the output shows that some ϵ are greater than the respective maximum ϵ, a better alignment usually can be found by increasing the maximum ϵ in question. However, increasing ϵ also increases the computational time. (4) If the program bogs down, try dividing the problem into several smaller ones.

Below is an example from http://www.psc.edu of using MSA to align a group of phospholipase a2 proteins. Note that the program uses the FASTA sequence format. The following steps are used:

1. Calculate all pair-wise alignment scores (alignment costs).
2. Use the scores (costs) to predict a tree.
3. Calculate pair weights based on the tree.

4. Produce a heuristic msa based on the tree.
5. Calculate the maximum ϵ for each sequence pair.
6. Determine the spatial positions that must be calculated to obtain the optimal alignment.
7. Perform the optimal alignment.
8. Report the ϵ found compared to the maximum ϵ.

Example of MSA

```
MSA release 2.1  (PSC revision b) started on Thu Jun 19 14:55:31 1997
Sequence file format is Fasta.
Calculating pairwise alignments.
..........
**********
Calculating weights.

---------------- Tree given from ancestor ----------------
On the left:   Internal Node  Distance to parent =  278.83
On the left:   Internal Node  Distance to parent =   23.63
On the left:   Internal Node  Distance to parent =  118.62
On the left:   SEQ#01         Distance to parent =  230.50
On the right:  SEQ#04         Distance to parent =  205.50
On the right:  SEQ#05         Distance to parent =  238.37
On the right:  SEQ#02         Distance to parent =  256.17
On the right:  SEQ#03         Distance to parent =    0.00

Calculating epsilons.

Sequence     ID        Description
   1        SEQ#01     P1;1POA Phospholipase a2 (EC 3.1.1.4) - Chinese cobra
   2        SEQ#02     P1;1POD Phospholipase a2 (EC 3.1.1.4) - human
   3        SEQ#03     P1;1PPA Phospholipase a2 (EC 3.1.1.4) lys 49 variant
   4        SEQ#04     P1;1BPQ phospholipase A2 (EC 3.1.1.4) mutant (K56M) -
   5        SEQ#05     P1;1PP2R phospholipase A2 (EC 3.1.1.4) (calcium-free)


               ***  Heuristic Multiple Alignment  ***

**********23541      **********************************35214 **35214      ***
NLYQFKNMIQCTVPSR-SWWDFADYGCYCGRGGSGTPVDDLDRCCQVHDNCYNEAEKISGC-----WPYFKTYSY
NLVNFHRMIK-LTTGKEAALSYGFYGCHCGVGGRGSPKDATDRCCVTHDCCYKRLEK-RGC-----GTKFLSYKF
SVLELGKMIL-QETGKNAITSYGSYGCNCGWGHRGQPKDATDRCCFVHKCCYKKLT---DC-----NHKTDRYSY
ALWQFNGMIKCKIPSSEPLLDFNNYGCYCGLGGSGTPVDDLDRCCQTHDNCYKQAMKLDSCKVLVDNPYTNNYSY
SLVQFETLIM-KIAGRSGLLWYSAYGCYCGWGGHGLPQDATDRCCFVHDCCYGKAT---DC-----NPKTVSYTY
```

```
*********35214 ******************14325
ECSQGTLTCKGGNNACAAAVCDCDRLAAICFAG--APYNDNDYNINLKARC-------
SNSGSRITC-AKQDSCRSQLCECDKAAATCFARNKTTYNKKYQYYS-NKHCRGSTPRC
SWKNKAIIC-EEKNPCLKEMCECDKAVAICLRENLDTYNKKYKAYF-KLKCKKPDT-C
SCSNNEITCSSENNACEAFICNCDRNAAICFSK--VPYNKEHKNLD-KKNC-------
SEENGEIIC-GGDDPCGTQICECDKAAAICFRDNIPSYDNKYWLFP-PKDCREEPEPC

Calculating pairwise projection costs.
..........
**********

Calculating multiple alignment.
....1....2....3....4....5....6....7....8....9....0
************************************************

                ***  Optimal Multiple Alignment  ***

NLYQFKNMIQCTVPSR-SWWDFADYGCYCGRGGSGTPVDDLDRCCQVHDNCYNEAEKISGC-----WPYFKTYSY
NLVNFHRMIK-LTTGKEAALSYGFYGCHCGVGGRGSPKDATDRCCVTHDCCYKRLEK-RGC-----GTKFLSYKF
SVLELGKMIL-QETGKNAITSYGSYGCNCGWGHRGQPKDATDRCCFVHKCCYKKL---TDC-----NHKTDRYSY
ALWQFNGMIKCKIPSSEPLLDFNNYGCYCGLGGSGTPVDDLDRCCQTHDNCYKQAMKLDSCKVLVDNPYTNNYSY
SLVQFETLIM-KIAGRSGLLWYSAYGCYCGWGGHGLPQDATDRCCFVHDCCYGKA---TDC-----NPKTVSYTY

ECSQGTLTCKGGNNACAAAVCDCDRLAAICFAG--APYNDNDYNINLKARC-------
SNSGSRITC-AKQDSCRSQLCECDKAAATCFARNKTTYNKKYQYYS-NKHCRGSTPRC
SWKNKAIIC-EEKNPCLKEMCECDKAVAICLRENLDTYNKKYKAYF-KLKCK-KPDTC
SCSNNEITCSSENNACEAFICNCDRNAAICFSK--VPYNKEHKNLD-KKNC-------
SEENGEIIC-GGDDPCGTQICECDKAAAICFRDNIPSYDNKYWLFP-PKDCREEPEPC

End gaps not penalized.
Costfile:                    pam250
Alignment cost:    35132     Lower bound:    34945
Delta:               187     Max. Delta:       285

 Sequences  Proj. Cost  Pair. Cost  Epsilon  Max. Epsi.  Weight  Weight*Cost
   1   2        1864        1825        39          39       1         1864
   1   3        1891        1843        48          57       1         1891
   1   4        1654        1653         1           5       4         6616
   1   5        1814        1787        27          28       2         3628
   2   3        1735        1733         2           8       4         6940
   2   4        1876        1866        10          10       1         1876
   2   5        1713        1712         1           8       2         3426
   3   4        1901        1889        12          21       1         1901
   3   5        1648        1648         0          11       2         3296
   4   5        1847        1842         5           6       2         3694
 Elapsed time =   0.895

 Tree
      A tree is given for the heuristic alignment (not shown).
```

SCORING MULTIPLE SEQUENCE ALIGNMENTS

As discussed above, the SP method provides a way to score the msa by summing the scores of all possible combinations of amino acid pairs in a column of a msa. The method assumes a model for evolutionary change in which any of the sequences could be the ancestor of the others, as illustrated in Figure 4.5. This figure also illustrates a difficulty with the SP method when a substitution table of log odds scores such as BLOSUM62 is used for protein sequences (see Durbin et al. 1998, pp. 139–140). Shown is the effect of adding a small number of amino acid subsitutions to a column that initially has all matching amino acids. Scores in the msa column decrease rapidly as the number of mismatched residue pairs increases. For a larger number of sequences than five with all N, or with one or two C substitutions, these decreases should be greater because there will be more N-N matched pairs relative to mismatched N-C pairs. However, the reverse is true with the SP method of scoring. For n sequences, the number of combinations of pairs in a column is

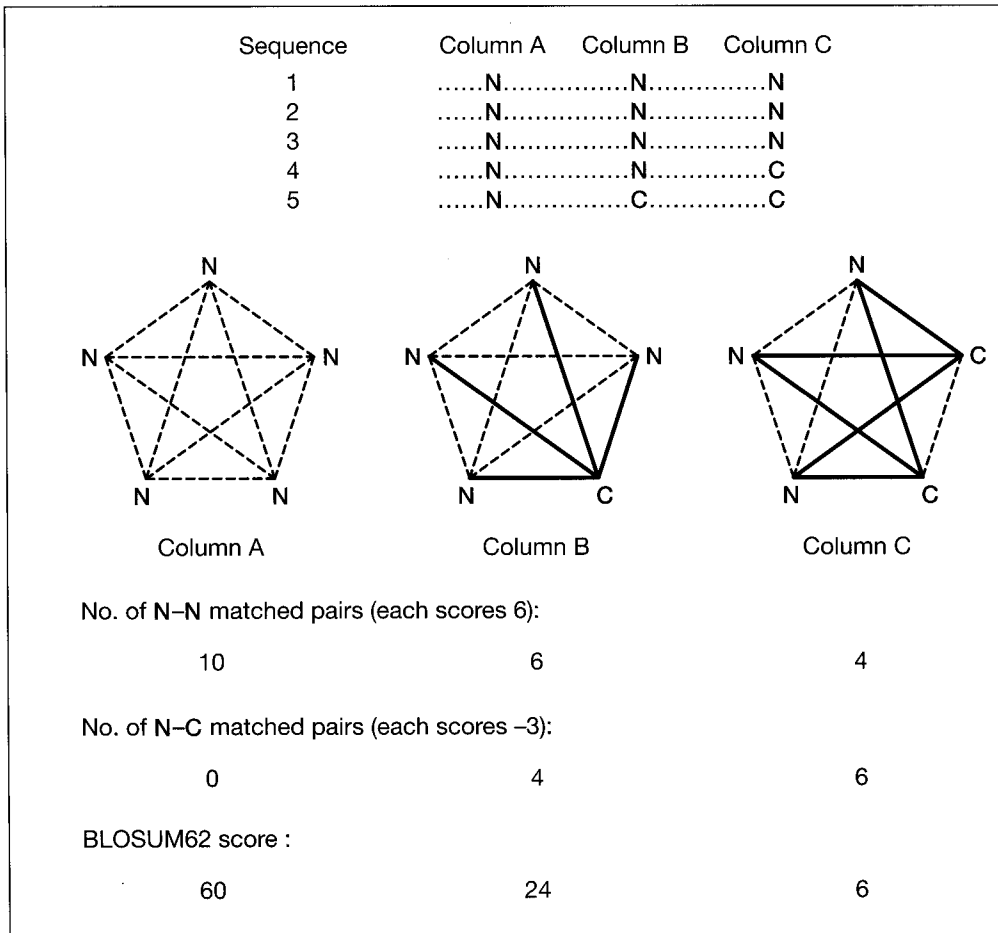

Figure 4.5. The SP model for scoring a msa. This model represents one method for optimizing the msa by maximizing the number of matched pairs (or minimizing the cost or number of mismatched pairs) summed over all columns in the msa. Shown first are three columns of a five-sequence msa with all matched (A), four matched and one mismatched (B), or three matched and two mismatched (C) sequence characters. The SP method of calculating the cumulative scores for columns of a msa is then illustrated by a graph with the five sequences as vertices and representing the ten possible sequence pair-wise sequence comparisons. Solid lines represent a matched pair and dotted lines a mismatched pair. Shown are the BLOSUM62 scores for each column calculated by the SP method. (Adapted from Altschul 1989.)

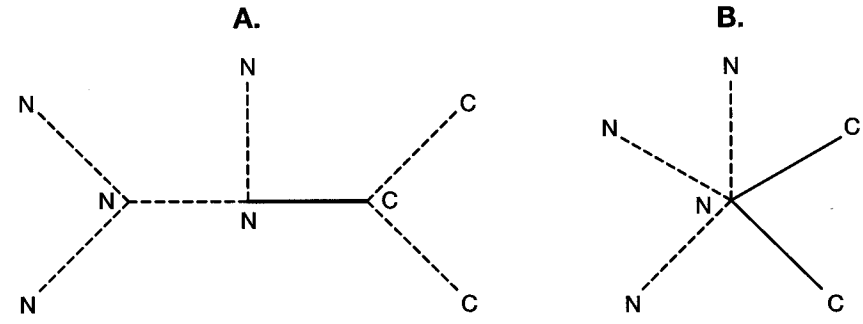

Figure 4.6. Alternative methods for scoring a column in the msa (Altschul 1989b). The variations in column C of Fig. 4.5 are shown modeled by a phylogenetic tree (*A*) and a simplified phylogenetic tree called a star phylogeny (*B*) where one of the sequences is treated as the ancestor of all the others (instead of treating them as all equally possible ancestors as in the original sum of pairs scoring method).

$n(n-1)/2$. If all are amino acid N, as in column A, then the BLOSUM62 score for the column is $6 \times n(n-1)/2$. If there is one C in the column, as in column B, then $n-1$ matched N-N pairs will be replaced by $n-1$ mismatched N-C pairs, giving a score of $9(n-1)$ less. The score for one C in the column divided by that for zero Cs is $9(n-1)/[6n(n-1)/2] = 3/n$. For three sequences, the relative difference is 1, whereas for six sequences, the relative difference is 2. As more sequences are present in the column, the relative difference increases, not in agreement with expectation. Hence, the SP method is not providing a reasonable result when this type of scoring matrix is used. Two other methods for scoring a msa (Altschul 1989) have been described and are illustrated in Figure 4.6. The first is a tree-based method. Because a phylogenetic tree describing the relationships among the sequences is found by the MSA program, the sum of the lengths of the tree branches can be calculated using the substitutions in the column of the msa. Alternatively, a simplified tree with one of the sequences as the ancestor of all of the others (a star phylogeny) can also be used (see Chapter 6). msa programs using these methods have not been implemented. Other scoring methods include information content (see p. 195) and a graph-based method called the trace method (Kececioglu 1993). A novel branch-and-cut algorithm for msa has been developed based on the trace method (Kececioglu et al. 2000). Other methods of scoring and producing an alignment guided by a tree are described below.

PROGRESSIVE METHODS OF MULTIPLE SEQUENCE ALIGNMENT

The MSA program described above for obtaining an optimal alignment of multiple sequences is limited to three sequences or to a small number (six to eight) of relatively short sequences. Progressive alignment methods use the dynamic programming method to build a msa starting with the most related sequences and then progressively adding less-related sequences or groups of sequences to the initial alignment (Waterman and Perlwitz 1984; Feng and Doolittle 1987, 1996; Thompson et al. 1994a; Higgins et al. 1996). Relationships among the sequences are modeled by an evolutionary tree in which the outer branches or leaves are the sequences (Fig. 4.7). The tree is based on pair-wise comparisons of the sequences using one of the phylogenetic methods described in Chapter 6. Progenitor sequences represented by the inner branches of the tree are derived by alignment of the outermost sequences. These inner branches will have uncertainties where positions in the

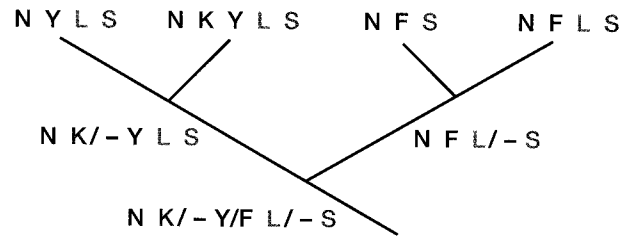

Figure 4.7. Progressive sequence alignment. Sequences are represented as the outermost branches (leaves) on an evolutionary tree. The most closely related sequences are first aligned by dynamic programming, providing a representation of ancestor sequences in deeper branches with uncertainties where amino acids have been substituted or positioned opposite a gap. These sequences are the same as those shown in EVMSA. The challenge to the msa method is to utilize an appropriate combination of sequence weighting, scoring matrix, and gap penalties so that the correct series of evolutionary changes may be found.

outermost sequences are dissimilar, as illustrated in Figure 4.7. Two examples of programs that use progressive methods are CLUSTALW and the Genetics Computer Group program PILEUP.

CLUSTALW

CLUSTAL has been around for more than 10 years, and the authors have done much to support and improve the program (Higgins and Sharp 1988; Thompson et al. 1994a; Higgins et al. 1996). CLUSTALW is a more recent version of CLUSTAL with the W standing for "weighting" to represent the ability of the program to provide weights to the sequence and program parameters, and CLUSTALX provides a graphic interface (see Table 4.1). These changes provide more realistic alignments that should reflect the evolutionary changes in the aligned sequences and the more appropriate distribution of gaps between conserved domains.

CLUSTAL performs a global-multiple sequence alignment by a different method than MSA, although the initial heuristic alignment obtained by MSA is calculated the same way. The steps include: (1) Perform pair-wise alignments of all of the sequences; (2) use the alignment scores to produce a phylogenetic tree (for an explanation of the neighbor-joining method that is used, see Chapter 6); and (3) align the sequences sequentially, guided by the phylogenetic relationships indicated by the tree. Thus, the most closely related sequences are aligned first, and then additional sequences and groups of sequences are added, guided by the initial alignments to produce a msa showing in each column the sequence variations among the sequences. The initial alignments used to produce the guide tree may be obtained by a fast *k*-tuple or pattern-finding approach similar to FASTA that is useful for many sequences, or a slower, full dynamic programming method may be used. An enhanced dynamic programming alignment algorithm (Myers and Miller 1988; see book Web site) is used to obtain optimal alignment scores. For producing a phylogenetic tree, genetic distances between the sequences are required. The genetic distance is the number of mismatched positions in an alignment divided by the total number of matched positions (positions opposite a gap are not scored).

As with MSA, sequence contributions to the msa are weighted according to their relationships on the predicted evolutionary tree. A rooted tree with known branch lengths of which the sequences are outer branches (leaves) is examined (see Chapter 6). Weights are

based on the distance of each sequence from the root, as illustrated in Figure 4.8. The alignment scores between two positions in the msa are then calculated using the resulting weights as multiplication factors.

The scoring of gaps in a msa has to be performed in a different manner from scoring gaps in a pair-wise alignment. As more sequences are added to a profile of an existing msa, gaps accumulate and influence the alignment of further sequences (Thompson et al. 1994b; Taylor 1996). CLUSTALW calculates gaps in a novel way designed to place them between conserved domains. When Pascarella and Argos (1992; see book Web site) aligned sequences of structurally related proteins, the gaps were preferentially found between secondary structural elements. These authors also prepared a table of the observed frequency

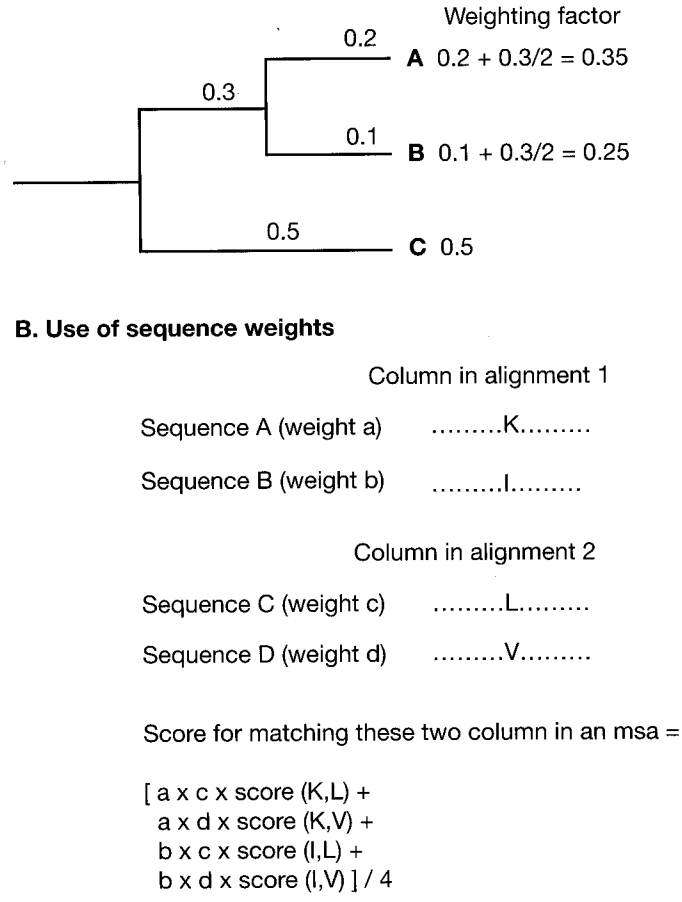

Figure 4.8. Weighting scheme used by CLUSTALW (Higgins et al. 1996). (*A*) Sequences that arise from a unique branch deep in the tree receive a weighting factor equal to the distance from the root. Other sequences that arise from branches shared with other sequences receive a weighting factor that is less than the sum of the branch lengths from the root. For example, the length of a branch common to two sequences will only contribute one-half of that length to each sequence. Once the specific weighting factors for each sequence have been calculated, they are normalized so that the largest weight is 1. As CLUSTALW aligns sequences or groups of sequences, these fractional weights are used as multiplication factors in the calculation of alignment scores. (*B*) Illustration of using sequence weights for aligning two columns in two separate alignments. Note that this sequence weighting scheme is the opposite to that used by MSA, because the more distant a sequence from the others, the higher the weight given. For a comparison of additional weighting schemes, see Vingron and Sibbald (1993).

of gaps next to each amino acid in these regions. CLUSTALW uses the information in this table and also attempts to locate what may be the corresponding domains by appropriate gap placement in the msa. Like other alignment programs, CLUSTAL uses a penalty for opening a gap in a sequence alignment and an additional penalty for extending the gap by one residue. These penalties are user-defined (defaults are available). Gaps found in the initial alignments remain fixed. New gaps introduced as more sequences are added also receive this same gap penalty, even when they occur within an existing gap, but the gap penalties for an alignment are then modified according to the average match value in the substitution matrix, the percent identity between the sequences, and the sequence lengths (Higgins et al. 1996). These changes are attempts to compensate for the scoring matrix, expected number of gaps (alignment with more identities should have fewer gaps), and differences in sequence length (should limit placement of gaps if one sequence shorter). Tables of gaps are then calculated for each group of sequences to be aligned to confine them to less conserved regions in the alignment. Gap penalties are decreased where gaps already occur (another method for achieving this same result is to enhance the scores of more closely matching regions on the alignment as described in Taylor 1996), increased in regions adjacent to already gapped regions, decreased within stretches of hydrophilic regions (amino acids DEGKNQPRS), and increased or decreased according to the table in Pascarella and Argos (1992). These rules are most useful when a correct alignment of some of the sequences is already known. The CLUSTALW algorithm and the results of using the above sequence weighting gap adjustment method are illustrated in Figure 4.9.

CLUSTALW also has options for adding one or more additional sequences with weights or an alignment to a existing alignment (Higgins et al. 1996). Once an alignment has been made, a phylogenetic tree may be made by the neighbor-joining method, with corrections for possible multiple changes at each counted position in the alignment (see Chapter 6). The predicted trees may also be displayed by various programs described in Chapter 6.

PILEUP

PILEUP is the msa program that is a part of the Genetics Computer Group package of sequence analysis programs, owned since 1997 by Oxford Communications, and is widely used due to the popularity and availability of this package. PILEUP uses a method for msa that is very similar to CLUSTALW. The sequences are aligned pair-wise using the Needleman-Wunsch dynamic programming algorithm, and the scores are used to produce a tree by the unweighted pair-group method using arithmetic averages (UPGMA; Sneath and Sokal 1973 and see Chapter 6). The resulting tree is then used to guide the alignment of the most closely related sequences and groups of sequences. The resulting alignment is a global alignment produced by the Needleman-Wunsch algorithm. Standard scoring matrices and gap opening/extension penalties are used. Unfortunately, there have not been any recent enhancements of this program such as gap modifications or sequence weighting comparable to those introduced for CLUSTALW. As with other progressive alignment msa programs, PILEUP does not guarantee an optimal alignment.

Problems with Progressive Alignment

The major problem with progressive alignment programs such as CLUSTAL and PILEUP is the dependence of the ultimate msa on the initial pair-wise sequence alignments. The very first sequences to be aligned are the most closely related on the sequence tree. If these sequences align very well, there will be few errors in the initial alignments. However, the more distantly related these sequences, the more errors will be made, and these errors will

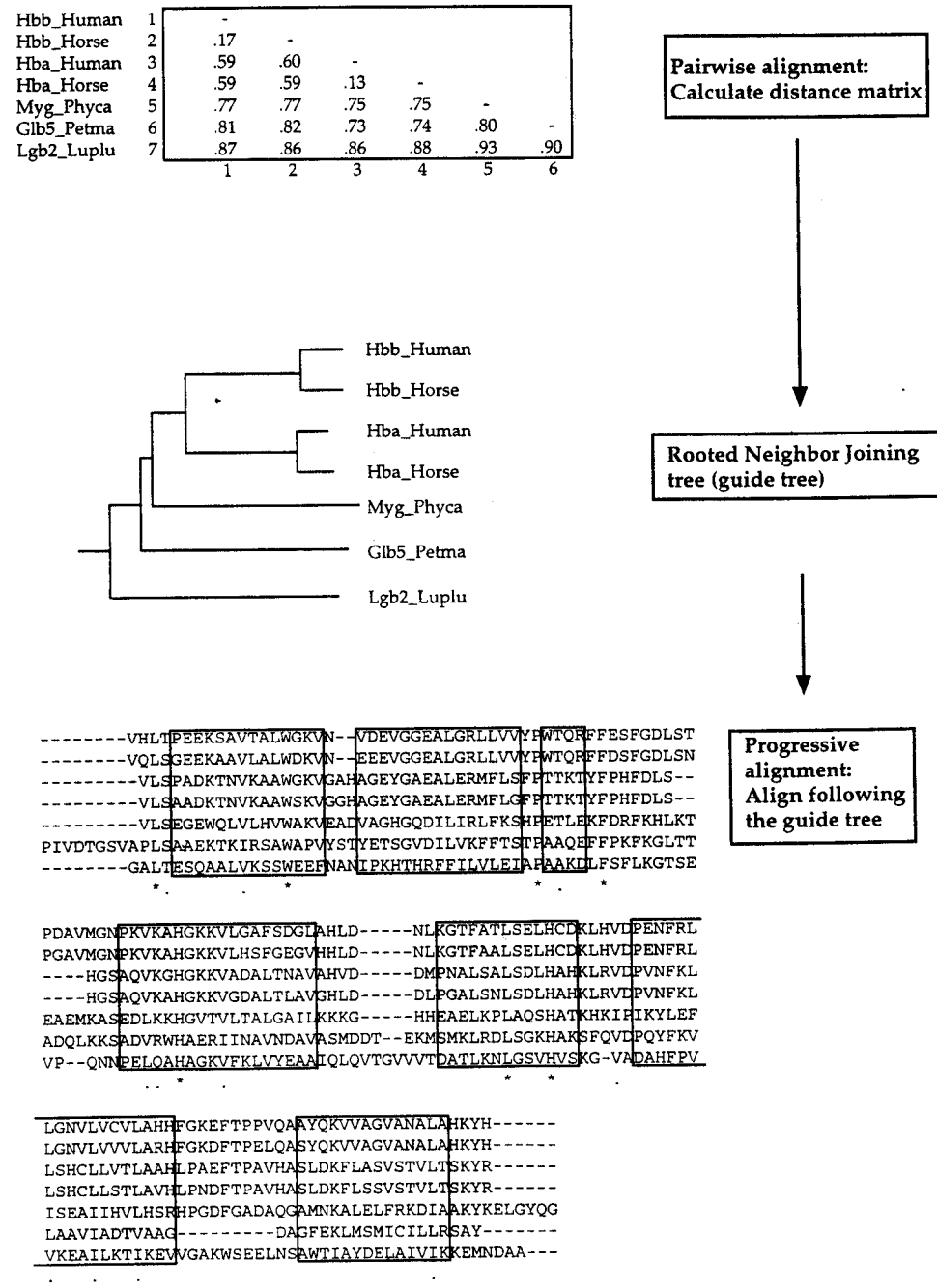

Figure 4.9. A msa of seven globins by CLUSTALW. The protein identifiers are from the SwissProt database. The amino acid subsitution matrix was the Dayhoff PAM250 matrix, and gap penalties were varied to emphasize conserved ungapped regions. The approximate and known locations of seven α-helices in the structure of this group are shown in boxes. (Reprinted, with permission, from Higgins et al. 1996 [copyright Academic Press].)

be propagated to the msa. There is no simple way to circumvent this problem. A second problem with the progressive alignment method is the choice of suitable scoring matrices and gap penalties that apply to the set of sequences (Higgins et al. 1996).

For the difficult task of aligning more distantly related sequences, using Bayesian methods such as hidden Markov models (HMMs) may be useful. For more closely related

sequences, CLUSTALW is designed to provide an adequate alignment of a large number of sequences and provide a very good indication of the domain structure of those sequences.

ITERATIVE METHODS OF MULTIPLE SEQUENCE ALIGNMENT

The major problem with the progressive alignment method described above is that errors in the initial alignments of the most closely related sequences are propagated to the msa. This problem is more acute when the starting alignments are between more distantly related sequences. Iterative methods attempt to correct for this problem by repeatedly realigning subgroups of the sequences and then by aligning these subgroups into a global alignment of all of the sequences. The objective is to improve the overall alignment score, such as a sum of pairs score. Selection of these groups may be based on the ordering of the sequences on a phylogenetic tree predicted in a manner similar to that of progressive alignment, separation of one or two of the sequences from the rest, or a random selection of the groups. These methods are compared in Hirosawa et al. (1995).

MultAlin (Corpet 1988) recalculates pair-wise scores during the production of a progressive alignment and uses these scores to recalculate the tree, which is then used to refine the alignment in an effort to improve the score. The program PRRP (Table 4.1) uses iterative methods to produce an alignment. An initial pair-wise alignment is made to predict a tree, the tree is used to produce weights for making alignments in the same manner as MSA except that the sequences are analyzed for the presence of aligned regions that include gaps rather than being globally aligned, and these regions are iteratively recalculated to improve the alignment score. The best scoring alignment is then used in a new cycle of calculations to predict a new tree, new weights, and new alignments, as illustrated in Figure 4.10. The process is repeated until there is no further increase in the alignment score (Gotoh 1994, 1995, 1996).

The program DIALIGN (see Table 4.1) finds an alignment by a different iterative method. Pairs of sequences are aligned to locate aligned regions that do not include gaps, much like continuous diagonals in a dot matrix plot. Diagonals of various lengths are identified. A consistent collection of weighted diagonals that provides an alignment which is a maximum sum of weights is then found.

Additional methods that use iterative procedures are described below.

Genetic Algorithm

The genetic algorithm is a general type of machine-learning algorithm that has no direct relationship to biology and that was invented by computer scientists. The method has been recently adapted for msa by Notredame and Higgins (1996) in a computer program package called SAGA (Sequence Alignment by Genetic Algorithm; see Table 4.1). Zhang and Wong (1997) have developed a similar program. The method is of considerable interest because the algorithm can find high-scoring alignments as good as those found by other methods. Similar genetic algorithms have been used for RNA sequence alignment (Notredame et al. 1997) and for prediction of RNA secondary structure (Shapiro and Navetta 1994). Although the method is relatively new and not used extensively, it likely represents the first of a series of sequence analysis programs that produce alignments by attempted simulation of the evolutionary changes in sequences.

The basic idea behind this method is to try to generate many different msas by rearrangements that simulate gap insertion and recombination events during replication in

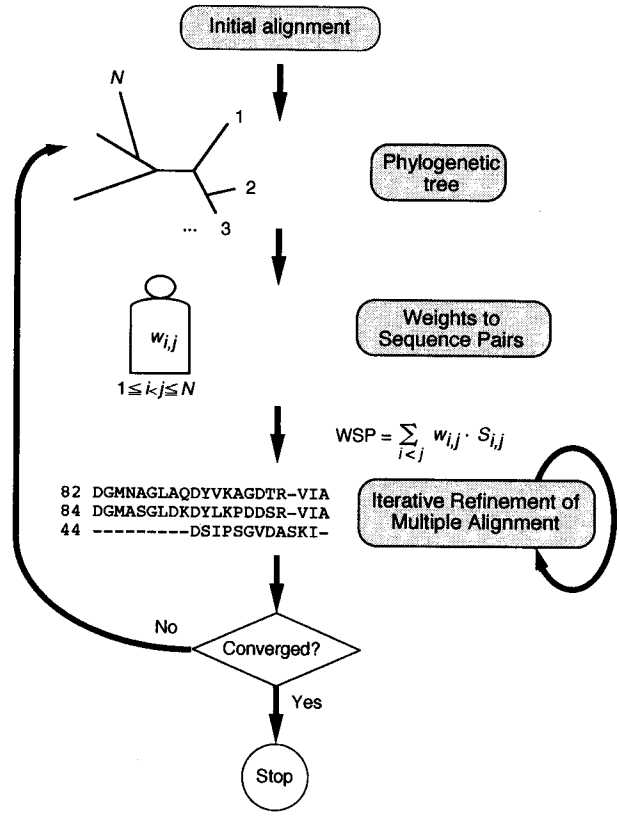

Figure 4.10. The iterative procedures used by PRRP to compute a multiple sequence alignment. (Reprinted, with permission, from Gotoh 1996 [copyright Academic Press].)

order to generate a higher and higher score for the msa. The alignments are not guaranteed to be optimal or to be the highest scoring that is achievable (optimal alignment). Although SAGA can generate alignments for many sequences, the program is slow for more than about 20 sequences.

A similar approach for obtaining a higher-scoring msa by rearranging an existing alignment uses a probability approach called simulated annealing (Kim et al. 1994). The program MSASA (Multiple Sequence Alignment by Simulated Annealing) starts with a heuristic msa and then changes the alignment by following an algorithm designed to identify changes that increase the alignment score.

The success of the genetic algorithm may be attributed to the steps used to rearrange sequences, many of which might be expected to have occurred during the evolution of the protein family. The steps in the algorithm are as follows:

1. The sequences to be aligned (up to ~20 in number) are written in rows, as on a page, except that they are made to overlap by a random amount of sequence, up to 50 residues long for sequences about 200 in length. The ends are then padded with gaps. A typical population of 100 of these msas is made, although other numbers may be set.

```
XXXXXXXXXX----
---XXXXXXXXXX
-XXXXXXXXX---
```

Shown is an initial msa for the genetic algorithm (1 of ~100 in number).

2. The 100 initial msas are scored by the sum of pairs method, except that both natural and quasi-natural gap-scoring schemes (Fig. 4.4) are used. Recall that the best SSP score for a msa is the minimum one and the one that is closest to the sum of the pair-wise sequence alignment. Standard amino acid scoring matrices and gap opening and extension penalties are used.
3. These initial msas are now replicated to give another generation of msas. The half with the lowest SSP scores are sent to the next generation unchanged. The remaining half for the next generation are selectively chosen by lot, like picking marbles from a bag, except that the chance for a particular choice is inversely proportional to the msa score (the lower the score, the better the msa, therefore gives that one a greater chance of replicating). These latter one-half of the choices for the next generation are now subject to mutation, as described in step 4 below, to produce the children of the next generation. All members of the next-generation msas undergo recombination to make new child msas derived from the two parents, as described in step 5 below. The relative probabilities of these separate events are governed by program parameters. These parameters are also adjusted dynamically as the program is running to favor those processes that have been most useful for improving msa scores.
4. In the mutation process, the sequence is not changed (else it would no longer be an alignment), but gaps are inserted and rearranged in an attempt to create a better-scoring msa. In the gap insertion process, the sequences in a given msa are divided into two groups based on an estimated phylogenetic tree, and gaps of random length are inserted into random positions in the alignment. Alternatively, in a "hill-climbing" version of the procedure, the position is so chosen as to provide the best possible score following the change.

```
XXXXXXXXXX                    XXX--XXXXXXX
XXXXXXXXXX                    XXX--XXXXXXX
XXXXXXXXXX        ----->      XXXXXXXXX--X
XXXXXXXXXX                    XXXXXXXXX--X
XXXXXXXXXX                    XXXXXXXXX--X
```

Shown above are random gap insertions into phylogenetically related sequences. The first two and last three sequences comprise the two related groups in this example. x indicates any sequence character.

Another mutational process is to move common blocks of sequence (overlapping ungapped regions) delineated by a gap, or blocks of gaps (overlapping gaps). Some of the possible moves are illustrated below. These moves may also be tailored to improve the alignment score.

```
XXX--XXXXX    XX--XXXXXX    XXX--XXXXX    XXXXX--XXX
XXXXXXXXXX    XXXXXXXXXX    XXXXXXXXXX    XXXXXXXXXX
XX--XXXXXX    X--XXXXXXX    XXX--XXXXX    XX-XX-XXXX
XXXXXXXXXX    XXXXXXXXXX    XXXXXXXXXX    XXXXXXXXXX
```

Starting block	Whole block move	Split block horizontally (guided by phylogenetic grouping)	Split block vertically

5. Recombination among next-generation parent msas is accomplished by one of t mechanisms. The first is not homology-driven. One msa is cut vertically through, a the other msa is cut in a staggered manner that does not lose any sequence after the fra ments are spliced. The higher scoring of the two reciprocal recombinants is kept. T second, illustrated below, is recombination between msas driven by conserved sequer positions. It is driven by homology expressed as a vertical column of the same resid and is very like standard homologous recombination.

```
xxGxxxxDxx     xxGxx-xDxx     xxGxx-xDxx
xxGx-xxDxx     xxGxxxxDxx     xxGxxxxDxx
xxGxx-xDxx     xxGxxxxDxx     xxGxxxxDxx
xxGxxxxDxx     xxGx-xxDxx     xxGx-xxDxx
```

Parent A alignment | **Parent B** alignment | **Child** alignment

6. The next generation, an overlapping one of the previous one-half of the best-scori parental msas and the mutated children, is now evaluated as in step 2, and the cycle steps 2–5 is typically repeated as much as 100 times, although as many as 1000 gene tions can be run. The best-scoring msa is then obtained.
7. The entire process of producing a set of msas for replication and mutation is repeat several times to obtain several possible msas, and the best scoring is chosen.

Hidden Markov Models of Multiple Sequence Alignment

The HMM is a statistical model that considers all possible combinations of matches, m matches, and gaps to generate an alignment of a set of sequences. A localized region of si ilarity, including insertions and deletions, may also be modeled by an HMM. Analysis sequences by an HMM is discussed on page 185 along with other statistical methods.

OTHER PROGRAMS AND METHODS FOR MULTIPLE SEQUENCE ALIGNMENT

The msa method often used, especially for 10 or more sequences, is to first determ sequence similarity between all pairs of sequences in the set. On the basis of these simil ities, various methods are used to cluster the sequences into the most related groups or i a phylogenetic tree.

In the group approach, a consensus is produced for each group and then used to m further alignments between groups. Two examples of programs using the group approa are the program PIMA (Smith and Smith 1992), which uses several novel alignment te niques, and the program MULTAL described by Taylor (1990, 1996; see Table 4.1).

The tree method uses the distance method of phylogenetic analysis to arrange sequences. The two closest sequences are then aligned, and the resulting consensus ali ment is aligned with the next best sequence or cluster of sequences, and so on, until alignment is obtained that includes all of the sequences. The programs PILEUP a CLUSTALW discussed above are examples. The ALIGN set of programs (Feng and Doo tle 1996) and the MS-DOS program by Corpet (1988) use this method. Additional p grams for msa are also described in Barton (1994), Kim et al. (1994), and Morgenstern al. (1996).

Another program (Vingron and Argos 1991) aligns all possible pairs of sequences to c

ate a set of dot matrices, and the matrices are then filtered sequentially to find motifs that provide a starting point for sequence alignment. A set of programs for interactive msa by dot matrix analysis and other alignment techniques has also been developed (Boguski et al. 1992).

The program TREEALIGN takes the approach that multiple sequence alignments should be done in a fashion that simultaneously minimizes the number of changes needed during evolution to generate the observed sequence variation (Hein 1990). TREEALIGN (also named ALIGN in the program versions) has a method for performing the alignment and the most parsimonious tree construction at the same time. The initial steps are similar to other multiple sequence alignment methods, except for the use of a distance scale: i.e., the sequences are aligned pair-wise and the resulting distance scores are used sequentially to produce a tree, which is rearranged as more sequences are added. The sequences are then realigned so that the same tree can be produced by maximum parsimony. Finally, the tree is rearranged to maximize parsimony. The advantage to this method is the increased use of phylogenetic analysis to improve the multiple sequence alignment.

LOCALIZED ALIGNMENTS IN SEQUENCES

Multiple sequence alignment programs based on the methods discussed above report a global alignment of the sequences, including all parts of all sequences. A portion of the alignment that is highly conserved may then be identified and a type of scoring matrix called a profile may be produced. A profile includes scores for amino acid substitutions and gaps in each column of the conserved region so that an alignment of the region to a new sequence can be determined. Alternatively, the alignment may be scanned for regions that include only substituted regions without gaps, called blocks, and these blocks may then be used in sequence alignments.

There is also a third method for finding a localized region of sequence similarity in a set of sequences without first having to produce an alignment. In this method, the sequences are analyzed by pattern-searching or statistical methods. All of these methods for finding localized sequence similarity are discussed below.

Profile Analysis

Profiles are found by performing the global msa of a group of sequences and then removing the more highly conserved regions in the alignment into a smaller msa. A scoring matrix for the msa, called a profile, is then made. The profile is composed of columns much like a mini-msa and may include matches, mismatches, insertions, and deletions. A tutorial on preparing profiles by the first method, prepared by M. Gribskov, is at Web address http://www.sdsc.edu/projects/profile/profile_tutorial.html, and the Web site at http://www.sdsc.edu/projects/profile/ will perform a motif analysis on the University of California at San Diego Supercomputer Center. The program Profilemake can be used to produce a profile from a msa (Gribskov et al. 1987, 1990; Gribskov and Veretnik 1996). A version of the Profilesearch program, which performs a database search for matches to a profile, is available at the University of Pittsburgh Supercomputer Center (http://www.psc.edu/general/software/packages/profiless/profiless.html). A special grant application may be needed to use this facility. Profile-generating programs are available by FTP from ftp.sdsc.edu/pub/sdsc/biology and are included in the Genetics Computer Group suite of programs (http://www.gcg.com/), although the more recent features (Gribskov and Veretnik 1996) are not included in GCG, v. 9.1.

Once produced, the profile is used to search a target sequence for possible matches to the profile using the scores in the table to evaluate the likelihood at each position. For example, the table value for a profile that is 25 amino acids long will have 25 rows of 20 scores, each score in a row for matching one of the amino acids at the corresponding position in the profile. If a sequence 100 amino acids in length is to be searched, each 25-amino-acid-long stretch of sequence will be examined, 1–25, 2–26, ... 76–100. The first 25-amino-acid-long stretch will be evaluated using the profile scores for the amino acids in that sequence, then the next 25-long stretch, and so on. The highest-scoring sections will be the most similar to the profile.

The disadvantage of this method of profile extraction from an msa is that the profile produced is only as representative of the variation in the family of sequences as the msa itself. If several sequences in the msa are similar, the msa and the derived profile will be biased in favor of those sequences. Methods have been devised for partially circumventing this problem with the profile (Gribskov and Veretnik 1996), but the difficulty with the msa itself is not easily reconciled, as discussed at the beginning of this section. Sequence weighting is based on the production of a simple phylogenetic tree by distance methods; more closely related sequences then receive a reduced weight in the profile. Another problem is that some amino acids may not be represented in a particular column because not enough sequences have been included. Athough absence of an amino acid may mean that the amino acid may not occur at that position in the protein family, adding counts to such positions generally increases the usefulness of the profile. This feature is built into the profile method discussed below.

An example of the generation of a profile and the matrix representation of this profile for a set of heat shock proteins is illustrated in Figure 4.11. The profile is similar to the log odds form of the amino acid substitution table, such as the PAM250 and BLOSUM62

Cons	A	B	C	D	E	F	G	H	I	K	L	M	N	P	Q	R	S	T	V	W	Y	Z	Gap	Len
I	8	3	-2	5	4	5	5	-4	24	0	15	13	1	1	1	-7	2	22	21	-18	-6	4	100	100
T	13	19	-5	24	18	-18	19	7	1	7	-7	-4	14	11	10	-1	9	29	3	-28	-14	15	100	100
L	5	5	-5	3	4	13	4	2	8	-4	14	12	8	-5	0	-10	0	10	10	-1	5	2	22	22
S	17	14	17	13	10	-12	29	-5	-5	6	-14	-9	12	10	0	-2	34	19	1	-8	-15	4	100	100
T	15	3	22	0	-1	-5	12	-2	7	-3	-8	-6	5	7	-8	-7	16	29	9	-22	6	-4	100	100
T	8	-1	12	-2	0	5	6	-4	19	-4	8	5	-1	2	-8	-8	7	22	19	-15	4	-3	100	100
C	17	0	24	-1	-3	11	8	-1	7	-10	1	-2	1	-3	-8	-14	8	5	9	-5	14	-7	100	100
V	11	0	18	-1	-2	2	14	-10	26	-4	9	7	-3	7	-7	-7	21	10	31	-19	-5	-5	100	100
C	10	-8	15	-11	-11	6	8	-7	11	-10	4	3	-7	0	-11	-4	11	5	15	-22	14	-11	100	100
V	7	7	-3	8	8	-3	11	1	20	-1	14	10	4	2	8	-5	0	5	26	-24	-6	8	100	100

Figure 4.11. Pattern identification by the profile method. A set of heat shock 70 (hsp70) proteins from a diverse group of organisms were aligned by the Genetics Computer Group msa program PILEUP. A profile was then made from one region in the alignment with the Genetics Computer Group program Profilemake. The profile represents the specific motif pattern found for the chosen location shown for this set of hsp70 proteins. The first column gives the consensus amino acid at each position in the profile. Thus, the consensus pattern is ITLSTTCVCV. This profile is used to search a target sequence for matches to the profile. The table values are a log odds score of giving the probability of finding the amino acid in the target sequence at that position in the profile divided by the probability of aligning the two amino acids by random chance. If a gap must be placed in the target sequence to align the sequence with the profile, then the penalties for opening a gap and extending the gap, respectively, are subtracted. The profile itself may include gaps, in which case the penalty is reduced, as seen for example in the row 3 of the profile table. The method of producing the substitution scores shown in the table is described in the text.

matrices used for sequence alignments. The matrix is 23 columns wide, one column for each of the 20 amino acids, plus one column for an unknown amino acid *z* and two columns for a gap opening and extension penalty. There is one row for each column in the msa. The consensus sequence, derived from the most common amino acid in each column of the msa, is listed down the left-hand column. The scores on each row reflect the number of occurrences of each amino acid in the aligned sequences. For example, in the first row, I, T, and V were found, with I being the majority amino acid. The highest positive score on each row (underlined) is in the column corresponding to the consensus amino acid, the most negative score for an amino acid not expected at that position. These values are derived from the log odds amino acid substitution matrix that was used to produce the alignment, such as the log odds form of the Dayhoff PAM250 matrix. Two methods are used to produce profile tables, the average method and the evolutionary method. The evolutionary method seems somewhat better for finding family members.

In the average method, the profile matrix values are weighted by the proportion of each amino acid in each column of the msa. For example, if column 1 in the msa has 5 Ile (I), 3 Thr (T), and 2 Val (V), then the frequency of each amino acid in this column is 0.5 I, 0.3 T, and 0.2 V. These amino acids are considered to have arisen with equal probability from any of the 20 amino acids as ancestors. In the example in Figure 4.11, the I, T, and V in column 1 could have arisen from any of the 20 amino acids by mutation. Suppose that they arose from an Ile (I). The profile values in the Ile (I) column of the corresponding row in the profile matrix would then use the amino acid scoring matrix values for I-I, I-T, and I-V, which are log odds scores of 5, 0, and 4 in the Dayhoff PAM250 matrix. Then the profile value for the I column is the frequency-weighted value, or $0.5 \times 5 + 0.3 \times 0 + 0.2 \times 4 = 3.3$.

The profile table also includes penalties for matching a gap in the target sequence, shown in the two right columns. All of these table values are multiplied by a constant for convenience so that only the value of a score with one sequence relative to the score with another sequence matters. Once a profile table has been obtained, the table may be used in database searches for additional sequences with the same pattern (program Profilesearch) or as a scoring matrix for aligning sequences (program Profilegap). If several profiles characteristic of a protein family can be identified, the chance of a positive identification of additional family members is greatly increased (Bailey and Gribskov 1998; also see http://www.sdsc.edu/MEME).

The evolutionary method for producing a profile table is based on the Dayhoff model of protein evolution (Chapter 2) (Gribskov and Veretnik 1996). The amino acids in each column of the msa are assumed to be evolving at a different rate, as reflected in the amount of amino acid variation that is observed. As with the average model, the object is to consider each of the 20 amino acids as a possible ancestor of the pattern of each column. In the evolutionary model, the evolutionary distance in PAM units that would be required to give the observed amino acid distribution in each column is determined. Recall that each PAM unit represents an overall probability of 1% change in a sequence position. For example, in the original Dayhoff PAM1 matrix for an evolutionary distance of 1 PAM unit (very roughly 10 my), the probability of an I not changing is 0.9872, and the probabilities for changing to a T or a V are 0.0011 and 0.0057, respectively. All of the probabilities of changing I to any other amino acid add up to 1.0000, for a combined probability of change of 1% for I. For an evolutionary distance of *n* PAM, the PAM1 matrix is multiplied by itself *n* times to give the expected changes at that distance. At a distance of 250 PAMs, the above three probabilities of an I not changing or of changing to a T or V are 0.10, 0.06, and 0.15, respectively, representing a much greater degree of change than for a shorter time, as might be expected (Dayhoff 1978).

Do not confuse these probabilities of one amino acid changing to another in the original Dayoff PAM250 matrix with scores from the log odds form of the PAM250 matrix, which have been used up to now. The log odds scores are derived from the original Dayhoff matrix by dividing each probability of change with the probability of a chance matching of the amino acids in a sequence alignment; i.e., that the one amino acid is not an ancestor of the other. These ratios are then converted to logarithms.

Thus, for the example of the msa column 1 with 5 Ile (I), 3 Thr (T), and 2 Val (V), the object is to find what amount of PAM distance from each of the 20 amino acids as possible ancestors will generate this much diversity. This amount can be found by a formula giving the amount of information (entropy) of the observed column variation given the expected variation in the evolutionary model,

$$H = -\sum_{\text{all } a\text{'s}} f_a \log(p_a) \tag{1}$$

where f_a is the observed proportion of each amino acid a in the msa column and p_a is the expected frequency of the amino acid when derived from a given ancestor amino acid. For a given column in the msa, H is calculated for each 20 ancestor amino acids and for a large number of evolutionary distances (PAM1, PAM2, PAM4, ...). The distance that gives the minimum value for H for each column-possible ancestor combination is the best estimate of the distance that generates the column diversity from that ancestor. This analysis provides 20 possible models (M_a for a = 1,2,3, . . . 20) as to how the amino acid frequencies in a column (F) may have originated. The next step in the evolutionary profile construction determines the extent to which each M_a predicts F by the now-familiar Bayes conditional probability analysis.

$$P(M_a|F) = P(M_a) \times P(F|M_a) / \sum_{\text{all } a\text{'s}} P(M_a) \times P(F|M_a) \tag{2}$$

where the prior distribution $P(M_a)$ is the given by the background amino acid frequencies and

$$P(F \mid M_a) = p_{aa1}^{faa1} \times p_{aa2}^{faa2} \times p_{aa3}^{faa3} \ldots\ldots\ldots p_{aa20}^{faa20} \tag{3}$$

i.e., the product of the expected amino acid frequencies in M_a raised to the power of the fraction observed for each amino acid in the msa column, as defined above. From $P(M_a \mid F)$, the weights for each of the 20 possible distributions that give rise to the msa column diversity are calculated as follows:

$$W_a = P(M_a \mid F) - P(M_{\text{random}} \mid F) \tag{4}$$

where W_a is the weight given to M_a and $P(M_{\text{random}} \mid F)$ is calculated as above using the background amino acid distribution.

The log odds scores for the profile (Profile_{ij}) are given by:

$$\text{Profile}_{ij} = \log\left[\sum_{\text{all } a\text{'s}} (W_{ai} \times p_{aij}) / p_{\text{random } j}\right] \tag{5}$$

where W_{ai} is the weight of an ancestral amino acid a at row i in the profile, p_{aij} is the frequency of amino acid j in the PAM amino acid distribution that best matches at row i, and

$p_{\text{random } j}$ is the background frequency of amino acid j. An example of a profile matrix for the ATP-dependent RNA helicase ("DEAD" box family) from the M. Gribskov laboratory is given in Figure 4.12.

The usefulness of the evolutionary profile is demonstrated by the following: A profile for the 4Fe-4S ferredoxin family was prepared from six sequences. This profile was then used to search the SwissProt database for family members. Success was measured by the so-called receiver operating characteristic test (ROC) plot. The fraction of scores equal to or greater than a certain value is plotted for the true positive matches (a correct family member identified) on the y axis and for the true negatives (unrelated sequences) on the x axis. The area under the curve and the x axis gives the probability of correct identification. The ROC_{50} is the area under the curve when it is truncated to the first 50 incorrect sequences, and can be used as a standard for success in a database search (Gribskov and Veretnik 1996). For the ferredoxin family search, the ROC_{50}, 95.6 $\pm$ 0.6% of the known family members, was identified in a search of SwissProt by an evolutionary profile, whereas 93.0 $\pm$ 2.0% was identified by the average profile method (Gribskov and Veretnik 1996). The success rate was increased 0.4–0.6% by using 12 training sequences and 2–3% by using 134 training sequences.

Block Analysis

Like profiles, blocks represent a conserved region in the msa. Blocks differ from profiles in lacking insert and delete positions in the sequences. Instead, every column includes only matches and mismatches. Like profiles, blocks may be made by searching for a section of an msa alignment that is highly conserved. However, aligned regions may also be found by searching each sequence in turn for similar patterns of the same length. These patterns may include a region with one or a few matching characters followed by a short spacer region of unmatched characters and then by another set of a few matching characters, and so on, until the sequences start to be different. These patterns are all of the same length, and when they are aligned, the matching sequence characters will appear in columns. The first alignments of this type were performed by computer programs that searched for patterns in sequences (Henikoff and Henikoff 1991; Neuwald and Green 1994). Several blocks located in different regions in a set of sequences may be used to produce a msa (Zhang et al. 1994), and blocks may be constructed from a set of aligned sequence pairs (Miller et al. 1994). Statistical and Bayesian statistical methods are also used to locate the most alike regions of sequences (Lawrence et al. 1993; Lawrence and Reilly 1990). Web sites that perform some of these types of analyses are discussed below and also given in Table 4.1. Finally, the information content of these tables can be displayed by a sequence logo (see p. 195). Note that few of these types of analyses presently provide a method for phylogenetic estimates of the sequence relationships so that sequence weighting can be used to make the changes more reflective of the phylogenetic histories among the sequences. Additionally, except where noted, these methods do not use substitution matrices such as the PAM and BLOSUM matrices to score matches. Rather, they are based on finding exact matches that have the same spacing in at least some of the input sequences, and that may be repeated in a given sequence.

Extraction of Blocks from a Global or Local Multiple Sequence Alignment

A global msa of related protein sequences usually includes regions that have been aligned without gaps in any of the sequences. These ungapped patterns may be extracted from these aligned regions and used to produce blocks. Blocks found in this manner are

A. The multiple sequence alignment.

```
rhle_ecoli  GVDVLVATPG RLLDLEHQNA ....VKLDQV EILVLDEADR MLDMGFIHDI
dbp2_schpo  GVEICIATPG RLLDMLDSNK ....TNLRRV TYLVLDEADR MLDMGFEPQI
dbp2_yeast  GSEIVIATPG RLIDMLEIGK ....TNLKRV TYLVLDEADR MLDMGFEPQI
dbpa_ecoli  APHIIVATPG RLLDHLQKGT ....VSLDAL NTLVMDEADR MLDMGFSDAI
rm62_drome  GCEIVIATPG RLIDFLSAGS ....TNLKRC TYLVLDEADR MLDMGFEPQI
 p68_human  GVEICIATPG RLIDFLECGK ....TNLRRT TYLVLDEADR MLDMGFEPQI
rhlb_ecoli  GVDILIGTTG RLIDYAKQNH ....INLGAI QVVVLDEADR MYDLGFIKDI
yn21_caeel  RPHIIVATPG RLVDHLENTK ...GFNLKAL KFLIMDEADR ILNMDFEVEL
yhm5_yeast  KPHIIIATPG RLMDHLENTK ...GFSLRKL KFLVMDEADR LLDMEFGPVL
me31_drome  KVQLIIATPG RILDLMDKKV ....ADMSHC RILVLDEADK LLSLDFQGML
drs1_yeast  RPDIVIATPG RFIDHIRNSA ...SFNVDSV EILVMDEADR MLEEGFQDEL
if4a_rabit  APHIIVGTPG RVFDMLNRRY ....LSPKYI KMFVLDEADE MLSRGFKDQI
if41_human  APHIIVGTPG RVFDMLNRRY ....LSPKYI KMFVLDEADE MLSRGFKDQI
vasa_drome  GCHVVIATPG RLLDFVDRTF ....ITFEDT RFVVLDEADR MLDMGFSEDM
srmb_ecoli  NQDIVVATTG RLLQYIKEEN ....FDCRAV ETLILDEADR MLDMGFAQDI
DEAD_ecoli  GPQIVVGTPG RLLDHLKRGT ....LDLSKL SGLVLDEADE MLRMGFIEDV
if4a_orysa  GVHVVVGTPG RVFDMLRRQS ....LRPDYI KMFVLDEADE MLSRGFKDQI
DEAD_klepn  GPQIVVGTPG RLLDHLKRGT ....LDLSKL SGLVLDEADE MLRMGFIEDV
pl10_mouse  GCHLLVATPG RLVDMMERGK ....IGLDFC KYLVLDEADR MLDMGFEPQI
 p54_human  TVHVVIATPG RILDLIKKGV ....AKVDHV QMIVLDEADK LLSQDFVQIM
if4a_drome  GCHVVVGTPG RVYDMINRKL .....RTQYI KLFVLDEADE MLSRGFKDQI
 ded1_yeast  GCDLLVATPG RLNDLLERGK ....ISLANV KYLVLDEADR MLDMGFEPQI
 ms16_yeast  RPNIVIATPG RLIDVLEKYS ...NKFFRFV DYKVLDEADR LLEIGFRDDL
 pr28_yeast  GCDILVATPG RLIDSLENHL ....LVMKQV ETLVLDEADK MYDLGFEDQV
 if4n_human  GQHVVAGTPG RVFDMIRRRS ....LRTRAI KMLVLDEADE MLNKGFKEQI
  an3_xenla  GCHLLVATPG RLVDMMERGK ....IGLDFC KYLVLDEADR MLDMGFEPQI
 dbp1_yeast  GCDLLVATPG RLNDLLERGK ....VSLANI KYLVLDEADR MLDMGFEPQI
 if4a_yeast  DAQIVVGTPG RVFDNIQRRR ....FRTDKI KMFILDEADE MLSSGFKEQI
 spb4_yeast  RPQILIGTPG RVLDFLQMPA ....VKTSAC SMVVMDEADR LLDMSFIKDT
 if4a_caeel  GIHVVVGTPG RVGDMINRNA ....LDTSRI KMFVLDEADE MLSRGFKDQI
 pr05_yeast  GTEIVVATPG RFIDILTLND .GKLLSTKRI TFVVMDEADR LFDLGFEPQI
 if42_mouse  APHIVVGTPG RVFDMLNRRY ....LSPKWI KMFVLDEADE MLSRGFKDQI
 dhh1_yeast  TVHILVGTPG RVLDLASRKV ....ADLSDC SLFIMDEADK MLSRDFKTII
 db73_drome  KADIVVTTPG RLVDHLHATK ...GFCLKSL KFLVIDEADR IMDAVFQNWL
 yk04_yeast  GCNFIIGTPG RVLDHLQNTK VIKEQLSQSL RYIVLDEGDK LMELGFDETI
 ybz2_yeast  SGQIVIATPG RFLELLEKDN .TLIKRFSKV NTLILDEADR LLQDGHFDEF
 yhw9_yeast  KPHFIIATPG RLAHHIMSSG DDTVGGLMRA KYLVLDEADI LLTSTFADHL
 glh1_caeel  GATIIVGTVG RIKHFCEEGT ....IKLDKC RFFVLDEADR MIDAMGFGTD
```

Figure 4.12. msa and the derived evolutionary profile.

B. The evolutionary profile. Note the location of red conserved regions in the alignment in the corresponding profile of these sequences.

Cons	A	B	C	D	E	F	G	H	I	K	L	M	N	P	Q	R	S	T	V	W	Y	Z	Gap	Len
G	17	18	0	19	14	-22	31	0	-9	12	-15	-5	15	10	9	6	18	14	1	-15	-22	11	100	100
P	18	0	13	0	0	-12	13	0	8	-3	-3	-1	-2	23	2	-2	12	11	17	-31	-8	1	100	100
H	5	24	-12	29	25	-20	8	32	-9	9	-10	-9	22	7	30	10	0	4	-8	-20	-7	27	100	100
I	-1	-12	6	-13	-11	33	-12	-13	63	-11	40	29	-15	-9	-14	-15	-6	7	50	-17	8	-11	100	100
V	3	-11	1	-11	-9	22	-3	-11	46	-9	37	30	-13	-3	-9	-13	-6	6	50	-19	2	-8	100	100
V	5	-9	9	-9	-9	19	-1	-13	57	-9	35	26	-13	-2	-11	-13	-4	9	58	-29	0	-9	100	100
A	54	15	12	20	17	-24	44	-6	-4	-1	-11	-5	12	19	9	-13	21	19	9	-39	-20	10	100	100
T	40	20	20	20	20	-30	40	-10	20	20	-10	0	20	30	-10	-10	30	150	20	-60	-30	10	100	100
P	31	6	7	6	6	-41	19	11	-9	6	-16	-11	0	89	17	17	24	22	9	-50	-48	12	100	100
G	70	60	20	70	50	-60	150	-20	-30	-10	-50	-30	40	30	20	-30	60	40	20	-100	-70	30	100	100
! 11																								
R	-30	10	-30	0	0	-50	-30	50	-30	80	-40	20	10	30	40	150	10	-10	-30	140	-60	20	100	100
L	-2	-17	-15	-18	-12	38	-13	-9	38	-12	49	39	-15	-9	-9	-15	-11	0	38	6	12	-10	100	100
L	0	-12	-15	-14	-9	32	-12	-7	32	-7	41	35	-11	-9	-6	-12	-9	0	29	6	9	-7	100	100
D	15	58	-27	78	54	-52	35	27	-12	16	-26	-21	38	6	41	3	9	10	-12	-57	-25	50	100	100
L	-5	-5	-7	-8	-4	24	-12	13	13	-6	25	17	-1	-7	0	-2	-8	-3	10	11	17	-2	100	100
L	3	-13	-13	-13	-8	31	-11	-8	34	-9	41	36	-12	-7	-5	-13	-8	2	31	-1	8	-6	100	100
E	6	19	-15	23	27	-21	9	15	-6	18	-8	-1	16	6	23	12	6	5	-6	-15	-16	25	100	100
K	3	14	-12	11	12	-16	2	10	-5	23	-7	4	15	6	15	22	8	3	-5	7	-15	14	100	100
G	11	17	0	16	14	-16	19	5	-6	11	-11	-5	16	9	8	4	14	15	-1	-13	-14	11	100	100
T	12	9	-1	7	7	-8	9	2	4	12	0	4	10	5	4	3	9	12	7	-8	-8	5	100	100

Figure 4.12. *Continued.*

```
! 21
 D    1    1    0    2    1   -1    1    0    1    0    0    0    1    0    1    0    0    1    2   -3   -1    1   22   22
 T    2    2    0    3    2   -2    3    0    2    0    0    0    1    1    1   -1    1    4    2   -5   -2    2   22   22
 K    0    1   -3    0    1    0    0    0    1    4    1    3    1    0    1    1    0    3    1    0   -2    1   22   22
 G    3    3    0    4    4   -1    6   -1    3    0    1    1    3    1    1   -2    4    3    5   -6   -3    2   22   22
 L    5   -6   -4   -7   -4   16   -2   -4   21   -4   23   17   -5   -4   -4   -8   -2    4   19    0    6   -4   22   22
 B    5   16   -6   15   11  -15   10    6   -3   16   -8   -1   15    4    9   10   12    7   -2   -3  -11   10  100  100
 L    1  -13  -12  -14   -9   27   -8   -7   24   -8   36   30  -10   -5   -7  -10   -4    7   23    6    9   -8  100  100
 D    7   19   -7   22   17  -22   13    7   -6   19  -11   -3   14    8   15   14   17    6   -5   -5  -18   16  100  100
 K   11   10   -3   10    9  -12    5    9   -4   16   -6    0   10    6   11   12   10    4   -4    3   -8   10  100  100
 V    7  -10   11  -11  -10   14    0   -8   31  -11   19   16  -10    0  -10  -12    2    8   34  -22    9  -10  100  100
! 31
 K    4   16  -11   16   17  -21    6    9   -7   27  -12    0   16    7   16   20   12    8   -7    0  -18   17  100  100
 F   -3  -10    3  -14  -10   29  -10   -3   20   -9   26   19   -7  -12  -13  -10   -6    5   14   10   20  -11  100  100
 L   -5  -18  -19  -21  -14   42  -16   -8   34  -12   51   40  -15  -12  -10  -15  -12   -3   32   16   17  -11  100  100
 V   10  -11   11  -11  -11   15    8  -17   66  -11   46   34  -17    4  -12  -17   -6   11   83  -43   -4  -11  100  100
 L   -4  -23  -37  -24  -14   53  -23  -11   39  -10   73   67  -19  -14   -4  -14  -19   -4   39   17   11   -9  100  100

 D   30  110  -50  150  100 -100   70   40  -20   30  -50  -40   70   10   70    0   20   20  -20 -110  -50   90  100  100
 E   30   70  -60  100  150  -70   50   40  -20   30  -30  -20   50   10   70    0   20   20  -20 -110  -50  110  100  100
 A  121   17   24   25   25  -41   58   -8    0    0   -9    0   17   41   16  -24   33   33   16  -66  -25   16  100  100
 D   30  110  -50  150  100 -100   70   40  -20   30  -50  -40   70   10   70    0   20   20  -20 -110  -50   90  100  100

 R   -7    9  -16    7   10  -23   -7   17   -9   36  -14    7    8   10   18   49    5    0  -10   35  -25   14  100  100
```

Figure 4.12. *Continued.*

```
! 41
 M   -1  -16  -28  -19  -10   33  -16  -12   31    1   60   62  -15  -10   -2   -1  -14   -1   31   -2    2   -6  100  100
 L   -6  -25  -35  -26  -16   61  -26  -10   41  -15   74   64  -20  -17   -7  -20  -20   -5   39   24   18  -12  100  100
 D   12   32   -9   41   32  -30   23   11   -7   12  -17  -12   23    7   20    3   19   10   -7  -27  -19   27  100  100
 M    5   -2  -15   -3    1    8   -3   -3   13    6   25   30   -3    0    5    6   -1    2   13   -1   -6    3  100  100
 G   26   26    4   31   23  -25   54   -5   -8   -1  -16   -9   17   11   10  -10   23   17    8  -41  -27   15  100  100
 F  -31  -44   -6  -63  -44   96  -36   -4   44  -45   77   31  -31  -45  -50  -32  -19  -19   13   82   90  -44  100  100
 E    7    8   -7   10   13   -7    5    4    7   10    3    5    6    2   10    3    6    5    5   -9   -7   12  100  100
 D   12   24  -12   31   27  -27   19   12   -6   12  -12   -8   17   12   21    4    8    9   -3  -30  -19   25  100  100
 D    8   18  -14   25   22  -18   11   13    0    9   -3   -1   13    5   24    5    3    8    0  -24  -12   24  100  100
 I    0   -8   -5   -8   -7   27  -10   -9   43   -7   36   29  -10   -8   -7  -11   -6    6   35   -9    5   -6  100  100
! 51
 E    6   15   -5   18   21  -11    7   11   -2    8   -7   -3   12    2   12    6    6    6   -3   -8   -7   16  100  100
 Z    3   17  -14   20   21  -19    5   17   -7   18   -9   -3   15    5   20   15    4    8   -7  -10  -12   21  100  100
 I    2   -9    9  -10   -9   27   -9  -13   60   -9   34   26  -13   -6  -13  -13   -3   11   49  -23    4   -9  100  100
 L    1  -10   -5  -11   -8   26   -9   -8   33   -7   34   28  -10   -7   -8   -9   -5    2   28   -2    8   -7  100  100
 K    8    9   -4    9    9  -13   11    1    0   16   -4    4    8    7    8   11   13   12    3   -2  -15    8  100  100
 L    3    4   -9    3    6    3   -2    8    9    7   10   10    5    0    8    3    0    5    7   -2    0    7  100  100
 L    1  -13  -13  -13   -9   32  -11   -7   32   -9   42   36  -12   -7   -6  -13   -9    3   33    2    8   -7  100  100
 *   99    0   25  208  120   94  137   44  181  105  256   94   41   62   64  144   59   99  162    3   35    0
```

Figure 4.12. *Continued.*

only as good as the msa from which they are derived. Using the BLOCKS (http://www.blocks.fhcrc.org/blocks/process_blocks.html), blocks of width 10–55 are extracted from a protein msa of up to 400 sequences (Henikoff and Henikoff 1991, 1992). The program accepts FASTA, CLUSTAL, or MSF formats, or manually reformatted msas. Several types of analyses may be performed with such extracted blocks. The BLOCKS server primarily generates blocks from unaligned sequences. The eMOTIFs server at http://dna.stanford.edu/emotif/ (Nevill-Manning et al. 1998) similarly extracts motifs from msas in several msa formats and provides a formatter for additional msa formats. These types of analyses are discussed below in greater detail.

Pattern Searching

This type of analysis was performed on groups of related proteins, and the amino acid patterns that were located may be found in the Prosite catalog (Bairoch 1991). This catalog groups proteins that have similar biochemical functions on the basis of amino acid patterns such as those in the active site. Subsequently, these families were searched for amino acid patterns by the MOTIF program (Smith et al. 1990), which finds patterns of the type aa1 d1 aa2 d2 aa3, where aa1 and aa2 are conserved amino acids and d1 and d2 are stretches of intervening sequence up to 24 amino acids long. These initial patterns are then organized into blocks between 3 and 60 amino acids long by the Henikoff PROTOMAT program (Henikoff and Henikoff 1991, 1992). The BLOCKS database can be accessed at http://www.blocks.fhcrc.org/, and the server may also be used to produce new blocks by the original pattern-finding method or other methods described below.

Although used successfully for making the BLOCKS database, the MOTIF program is limited in the pattern sizes that can be found. The MOTIF program distinguishes true motifs from random background patterns by requiring that motifs occur in a number of the input sequences and tend not to be internally repeated in any one sequence. As the length of the motif increases, there are many possible combinations of patterns of a given length where only a few characters match, e.g., $>10^9$ possible patterns for a 15-amino-acid-long pattern with only five matches. The MOTIF program always provides a motif, even for random sequences, thus making it difficult to decide how significant the found motif really is. This problem has been circumvented by combining the analysis performed by MOTIF with that of the Gibbs sampler (discussed on p. 177), which is based on sound statistical principles. A rigorous searching algorithm called Aligned Segment Statistical Evaluation Tool (ASSET) has been devised (Neuwald and Green 1994) that can find patterns in sequence up to 50 amino acids long, group them, and provide a measure of the statistical significance of the patterns. These patterns may also include certain pairs, the 26 positive scoring pairs in the BLOSUM62 scoring matrix. Consideration of all BLOSUM pairs is not possible because this would greatly increase the complexity of the analysis.

The efficiency of ASSET is achieved by a combination of an efficient pattern search strategy called the depth-first method, which assures searching for the same patterns only once, and the use of formulas for efficiently organizing the patterns. Low-complexity regions with high proportions of the same residue and use of sequences, some of which are more similar than the others, can interfere with the ability of the method to find a range of patterns. ASSET removes low-complexity regions and redundant sequences from consideration. The program was easily able to find subtle motifs in the DNA methylase, reverse transcriptase, and tRNA ligase families, and previously identified by the MOTIF program. In addition, however, ASSET gave these motifs an expect score, the probability that these are random matches of unrelated sequences, of <0.001. The program also found motifs in

families with only a fraction of the sequences sharing a motif (the acyltransferase family) and in a set of distantly related sequences sharing the helix-turn-helix motif. Finally, the program found several repeat sequences in a prenyltransferase and ankyrin-like repeats in an *E. coli* protein. This source code of the program is available by anonymous FTP from ncbi.nlm.nih.gov/pub/neuwald/asset. The European Bioinformatics Institute has a Web page for another complex pattern-finding program (PRATT) at http://www2.ebi.ac.uk/pratt/ (Jonassen et al. 1995).

Blocks Produced by the BLOCKS Server from Unaligned Sequences

As described above, the BLOCKS server can extract a conserved, ungapped region from a msa to produce a sequence block. This same server can also find blocks in a set of unaligned, input sequences and maintains a large database of blocks based on an analysis of proteins in the Prosite catalog. Blocks are found by the Protomat program (Henikoff and Henikoff 1991). Blocks are found in two steps: First, the program MOTIF (Smith et al. 1990) described on the previous page is used to locate spaced patterns. The second step takes the best and most consistent patterns found in step 1 and uses the program MOTOMAT to merge overlapping triplets and extend them, orders the resulting blocks, and chooses those that are in the largest subset of sequences. Since 1993, the Gibbs sampler (see below) has been used as an additional tool for finding the initial set of short patterns also by specifying that the sampler search for short motifs. This program is based on a statistical analysis of the sequences and can identify the most significant common patterns in a set of sequences.

An example of BlockMaker output using an example from Lawrence et al. (1993) is shown below. The program first searches for blocks using either the MOTIFS or Gibbs sampler program to identify patterns, then the Protomat program to consolidate the patterns into meaningful blocks. The results of both types of analyses are reported.

```
A.  Motif analysis

              LipocalA, width = 15          LipocalB, width = 11
 BBP_PIEBR    16 NFDWSNYHGKWWEVA (  70)    101 VLSTDNKNYII
ICYA_MANSE    17 DFDLSAFAGAWHEIA (  73)    105 VLATDYKNYAI
LACB_BOVIN    25 GLDIQKVAGTWYSLA (  70)    110 VLDTDYKKYLL
MUP2_MOUSE    27 NFNVEKINGEWHTII ( 101)    143 DLSSDIKERFA
RETB_BOVIN    14 NFDKARFAGTWYAMA (  77)    106 IIDTDYETFAV


B.  Gibbs sampler analysis

              LipocalA, width = 15          LipocalB, width = 11
 BBP_PIEBR    16 NFDWSNYHGKWWEVA (  70)    101 VLSTDNKNYII
ICYA_MANSE    17 DFDLSAFAGAWHEIA (  73)    105 VLATDYKNYAI
LACB_BOVIN    25 GLDIQKVAGTWYSLA (  70)    110 VLDTDYKKYLL
MUP2_MOUSE    27 NFNVEKINGEWHTII (  68)    110 IPKTDYDNFLM
RETB_BOVIN    14 NFDKARFAGTWYAMA (  77)    106 IIDTDYETFAV
```

In the above example, two blocks identified as Lipocal A and B are reported using bot
the MOTIF and Gibbs sampler programs for step 1, the initial pattern-finding step. Th
MOTIF program is based on a heuristic method that will always find motifs, even in ran
dom sequences, whereas the Gibbs sampler discriminates found motifs based on soun
statistical methods. These blocks are identical to those determined from analysis of three
dimensional structures. Note that MOTIF aligned MUP2_MOUSE incorrectly in the

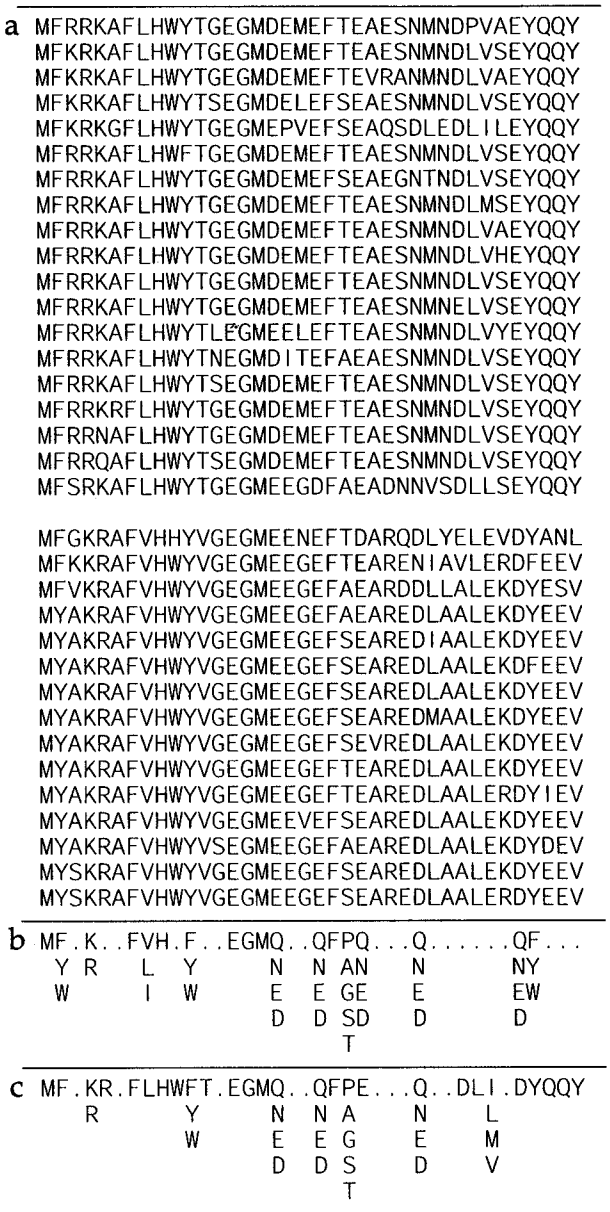

Figure 4.13. Aligned block of 34 tubulin proteins. (*a*) The sequences are divided into two groups based on the occurrence of R or L in the fourth position and Y in the last position. (*b*) Specific substitution groups found in the columns of the block. If a group cannot be found, then the position is ambiguous and a dot is printed at the position. (*c*) If only the first group of sequences is used, a more specific motif may be found because sequences in this group are more closely related to each other. (Reprinted, with permission, from Nevill-Manning et al. 1998 [copyright National Academy of Sciences].)

block. The Gibbs sampler results may differ when the same sequences are submitted repeatedly with a different initial alignment (see below).

The eMOTIF Method of Motif Analysis

Another somewhat different but extemely useful method of identifying motifs in protein sequences has been described (Nevill-Manning et al. 1998). From the BLOCKS database (derived from msa of proteins in the Prosite catalog) and the HSSP database (derived from msa of proteins based on predicted structural similarities), a set of amino acid substitution groups characteristic of each column in all of the alignments was found. These patterns reflect the higher log odds scores in the amino acid substitution matrices. A statistical analysis was performed to identify amino acids that are found together in the same msa column as opposed to amino acids that are found in different columns at the 0.01 level of significance. Thirty and 51 substitution groups that met this criterion were found in the BLOCKS and HSSP msas, respectively. For example, the chemically aromatic group of amino acids F, W, and Y were found to define a group often located in the same column of the msa.

From the msa for a particular group of proteins, each column is examined to see whether these groups are represented in the column, as illustrated in Figure 4.13. In column 1, M is always present, and because M is one group, M is used in column 1 of the motif, as shown in part *b*. Similarly for column 2, Y and F, which are members of the group FYW, are found, and hence this group is used as column 2 in the motif. The final motif shown in *b* describes the variation in all the sequences. Instead, a motif may be made for only the first group of 19 sequences, and is shown in *c*. This second motif (*c*) has less variability and greater specificity for the first 19 sequences and thus would be more likely to find those sequences in a database search (i.e., it is a more sensitive motif for those sequences) than motif *b*.

The probability of each motif is estimated from the frequencies of the individual amino acids in the SwissProt database. The probability of the motif *b* above is given by the product of the probability sums in each column, or $p(\text{Motif}) = p(M) \times 1 \times [p(F)+p(W)+p(y)] \times [p(Y)+p(R)]$ x . . . This value has been found to provide a good estimate of false positives, or of the selectivity of the motif, in a database search. Both the sensitivity and selectivity of a given motif must be taken into account in using the motif for a database search. Ideally, a motif can find all of the sequences used to generate the motif but none other. In practice, eMOTIF produces a large set of motifs, some more and some less sensitive for the set of aligned sequences. The more sensitive ones, which are also the most selective based on the value of $p(\text{Motif})$, are then chosen. Some are useful for specifying subfamilies of a protein superfamily. A database of such motifs called Identify is a useful resource for discovering the function of a gene (Nevill-Manning et al. 1998; http://dna.stanford.edu/emotif/).

STATISTICAL METHODS FOR AIDING ALIGNMENT

Expectation Maximization Algorithm

This algorithm has been used to identify both conserved domains in unaligned proteins and protein-binding sites in unaligned DNA sequences (Lawrence and Reilly 1990), including sites that may include gaps (Cardon and Stormo 1992). Given are a set of sequences that are expected to have a common sequence pattern and may not be easily recognizable by eye. An initial guess is made as to the location and size of the site of interest

in each of the sequences, and these parts of the sequence are aligned. The alignment provides an estimate of the base or amino acid composition of each column in the site. The EM algorithm then consists of two steps, which are repeated consecutively. In step 1, the expectation step, the column-by-column composition of the site already available is used to estimate the probability of finding the site at any position in each of the sequences. These probabilities are used in turn to provide new information as to the expected base or amino acid distribution for each column in the site. In step 2, the maximization step, the new counts of bases or amino acids for each position in the site found in step 1 are substituted for the previous set. Step 1 is then repeated using these new counts. The cycle is repeated until the algorithm converges on a solution and does not change with further cycles. At that time, the best location of the site in each sequence and the best estimate of the residue composition of each column in the site will be available.

As an example, suppose that there are 10 DNA sequences having very little similarity with each other, each about 100 nucleotides long and thought to contain a binding site near the middle 20 residues, based on biochemical and genetic evidence. As we will later see when examining the EM program MEME, the size and number of binding sites, the location in each sequence, and whether or not the site is present in each sequence do not necessarily have to be known. For the present example, the following steps would be used by the EM algorithm to find the most probable location of the binding sites in each of the 10 sequences.

The Initial Setup of the Algorithm

The 20-residue-long binding motif patterns in each sequence are aligned as an initial guess of the motif. The base composition of each column in the aligned patterns is then determined. The composition of the flanking sequence on each side of the site provides the surrounding base or amino acid composition for comparison, as illustrated below. For illustration purposes, each sequence is assumed to be the same length and to be aligned by the ends, and each character in the alignment represents five sequence positions (o, not in motif; x, in motif).

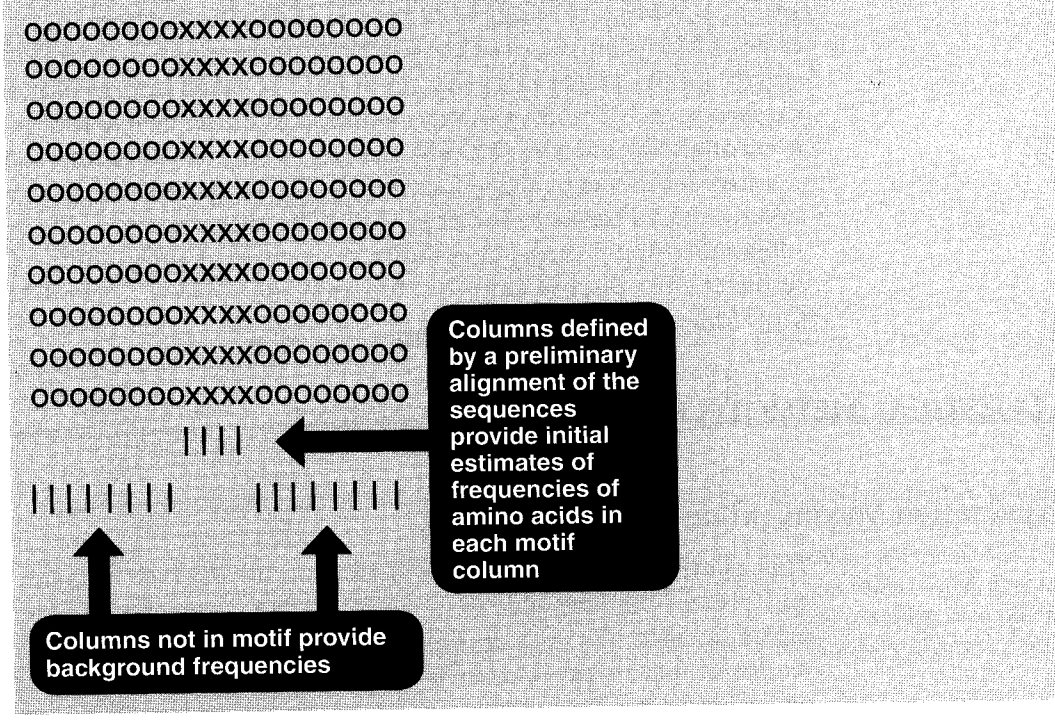

The number of each base in each column is determined and then converted to fractions. Suppose, for example, that there are four Gs in the first column of the 10 sequences, then the frequency of G in the first column of the site, $fs_G = 4/10 = 0.4$. This procedure is repeated for each base and each column. For the rest of the sequences not included in the sites, the background frequency of each base is calculated. For example, let one of these four values for the background frequency, the frequency of G, be $fb_G = 224/800 = 0.28$. These values are now placed in a 5×20 matrix of values, the first column for the background frequencies, and the next 20 columns for the base frequencies in each successive column in the sites. Thus, the counts in the first three columns of the matrix may appear as shown in Table 4.2.

The following calculations are performed in the expectation step of the EM algorithm:

1. The above estimates provide an initial estimate of the composition of the site and the location in each sequence. The object of this step is to improve this estimate by discriminating to the greatest possible extent between sequence within and sequence not within the site. Using the above estimates of base frequencies for (1) background sequences that are not within the site and (2) each column within the site, each sequence is scanned for all possible locations for the site to find the most probable location of the site. For the 10-residue DNA sequence example, there are $100 - 20 + 1$ possible starting sites for a 20-residue-long site, the first one being at position 1 in the sequence ending at 20 and the last beginnning at position 81 and ending at 100 (there is not enough sequence for a 20-residue-long site beyond position 81).

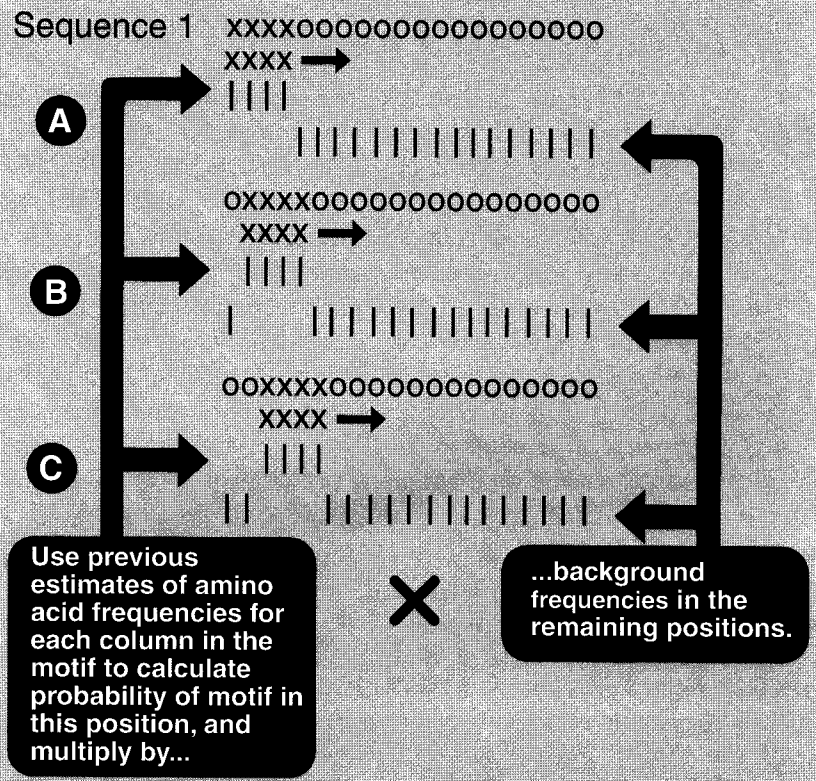

The resulting score gives the likelihood that the motif matches positions (a) 1-20, (b) 6-25, or (c) 11-30 in sequence 1. Repeat for all other positions and find most likely locator. Then repeat for the remaining sequences.

Table 4.2. *Column frequencies of each base in the example given*

	Background	Site column 1	Site column 2	...
G	0.27	0.4	0.1	...
C	0.25	0.4	0.1	...
A	0.25	0.2	0.1	...
T	0.23	0.2	0.7	...
	1.00	1.0	1.0	

The first column gives the background frequencies in the flanking sequence. Subsequent columns give base frequencies within the site given in the above example.

For each possible site location, the probability that the site starts is just the product of the probabilities given by Table 4.2. For example, suppose that the site starts in column 1 and that the first two positions in sequence 1 are A and T, respectively. The site will then end at position 20 and the first two nonsites, flanking background sequence positions, are 21 and 22. Suppose that these positions have an A and a T, respectively. Then the probability of this location of the site in sequence 1 is given by $P_{\text{site1,sequence1}} = 0.2$ (for A in position 1) $\times$ 0.7 (for T in position 2) $\times$ *Ps* for next 18 positions in site $\times$ 0.25 (for A in first flanking position) $\times$ 0.23 (for T in second flanking position) $\times$ *Ps* for next 78 flanking positions. Similar probabilities for $P_{\text{site2, sequence1}}$ to $P_{\text{site78, sequence1}}$ are then calculated, thus providing a comparative set of probabilities for the site location. The probability of this best location in sequence 1, say at site k, is the ratio of the site probability at k divided by the sum of all the other site probabilities $P(\text{site } k \text{ in sequence 1}) = P_{\text{site } k, \text{ sequence 1}} / (P_{\text{site 1, sequence 1}} + P_{\text{site 2, sequence 1}} + \ldots\ldots + P_{\text{site 78, sequence 1}})$. The probability of the site location in each sequence is then calculated in this manner.

2. The above site probabilities for each sequence are then used to provide a new table of expected values for base counts for each of the site positions using the site probabilities as weights. For example, suppose that P (site 1 in sequence 1) = 0.01 and that P (site 2 in sequence 1) = 0.02. In the above example, the first base in site 1 is an A and the first base for site 2 is a T. Then 0.01 As and 0.02 Ts are added to the accumulated list of bases at site column 1. This procedure is repeated for every other 76 possible first columns in sequence 1. Similarly, site column 2 in the new table of expected values is augmented by counts from the 78 possible column 2 positions in sequence 1, the first, for example, being 0.01 Ts. The weighted sequence data from the remaining sequences are also added to the new table, resulting finally in a new estimate of the expected number of each base at each site position and providing a new version of Table 4.2.

   In this maximization step, the base frequencies found in the expectation step are used as an updated estimate of the site residue composition. In this case, the data are more complete than the initial estimate because all possible sites in each of the sequences have been evaluated. The expectation and maximization steps are repeated until the estimates of the base frequencies do not change.

An Alternative Method of Calculating Site Probabilities by the EM Algorithm

The example shown above uses the frequencies of each base in the trial alignment and background base frequencies to calculate the probabilities of each possible location in each sequence. An alternative method is to produce an odds scoring matrix calculated

by dividing each base frequency by the background frequency of that base. The probability of each location is then found by multiplying the odds scores from each column. An even simpler method is to use log odds scores in the matrix. The column scores are then simply added. In this case, the log odds scores must be converted to odds scores before position probabilities are calculated.

Multiple EM for Motif Elicitation (MEME)

A Web resource for performing local msas by the above expectation maximization method is the program Multiple EM for Motif Elicitation (MEME) developed at the University of California at San Diego Supercomputing Center. The Web page for two versions of MEME, ParaMEME, a Web program that searches for blocks by an EM algorithm (described below), and a similar program MetaMEME (which searches for profiles using HMMs, described below) is found at http://www.sdsc.edu/MEME/meme/website/meme.html. The Motif Alignment and Search Tool (MAST) for searching through databases for matches to motifs may also be found at http://www.sdsc.edu/MEME/meme/website/mast.html.

MEME will locate one or more ungapped patterns in a single DNA or protein sequence or in a series of DNA or protein sequences. A search is conducted for a range of possible motif widths, and the most likely width for each profile is chosen on the basis of the log-likelihood score after one iteration of the EM algorithm. The EM algorithm then iterates to find the best EM estimate for that width. Three types of possible motif models may be chosen. The OOPS model is for one expected occurrence of a motif per sequence, the ZOOPS model is for zero or one occurrence per sequence, and the TCM model is for a motif to appear any number of times in a sequence. These models are reflected in the choices on the Web page (Fig. 4.14). The current version of MEME can use prior knowledge about a motif being present in all or only some of the sequences, the length of the motif and whether it is a palindrome (DNA sequences), and the expected patterns in individual motif positions (Dirichlet mixtures, see section on HMMs, p. 189) that provide information as to which amino acids are likely to be interchangeable in a motif (Bailey and Elkan 1995). Once a motif has been found, the motif and its position are effectively erased to prevent finding the same one twice. An example of the output from a ParaMEME analysis is given in Figure 4.15.

The Gibbs Sampler

Another statistical method for finding motifs in sequences is the Gibbs sampler. The method is similar in principle to the EM method described above, but the algorithm is different. Like the EM method, given a set of sequences, the Gibbs sampler searches for the statistically most probable motifs and can find the optimal width and number of these motifs in each sequence (Lawrence et al. 1993; Liu et al. 1995; Neuwald et al. 1995). The source code of the program code is available by anonymous FTP from ncbi.nlm.nih.gov/pub/neuwald/gibbs9-95. A combinatorial approach of the Gibbs sampler and MOTIF may be used to make blocks at the BLOCKS Web site (http://www.blocks.fhcrc.org/). The expected number of blocks in the search is one block for approximately each 40 residues of sequence. The Gibbs sampler is also an option of the msa block-alignment and editing program MACAW (Schuler et al. 1991), which runs on MS-DOS, Macintosh, and other computer platforms and is available by anonymous FTP from ncbi.nlm.nih.gov/pub/schuler/macaw.

MEME -- Multiple EM for Motif Elicitation: Version 2.2

Motif discovery tool

Data Submission Form - Advanced Version

Basic MEME

Your data will be processed on the Cray-T3E supercomputer at the **San Diego Supercomputer Center** and the results will be sent to you by e-mail.

Please enter the **e-mail** address where you would like your results sent:

[Optional] Please enter a brief **description** of your sequences.

Please enter the **sequences** which you believe share one or more motifs. The sequences may contain no more than **100,000 characters** total in any of a large number of **formats**. Please enter either:

1. the **name of a file** containing the sequences here:
2. or the **actual sequences** here:

How do you think the occurrences of a single motif are **distributed** among the sequences?

- **One** per sequence
- **Zero or one** per sequence
- **Any number** of repetitions

How many different motifs would you like to look for?

3

MEME can choose the **width** of each motif favoring **short** or **wide** motifs. **Wide** is recommended if there are fewer than 10 occurrences of any motif in your sequences. Choosing a number will cause all motifs reported to have that width. Select the width you want with the select button below, or enter a width in the text window. Legal choices are "short", "wide" or any number from 2 to 300. (If you enter something in the text window, it will override what is shown on the select button.)

short **or**

Brief output format:

ADVANCED OPTIONS

Shuffle letters in input sequences:

DNA-ONLY OPTIONS

DNA **palindromes:**	**ignore allow force**
Additional **strands/directions** to search:	**complementary strand, 5' to 3' (inverse complement)**
	main strand, 3' to 5'
	complementary strand, 3' to 5'
Strength of the prior (enter a positive number):	

Click here for **more information** on MEME.
Return to **MEME SYSTEM introduction**.

You might be interested in trying other motif-making programs such as BLOCK MAKER at the Fred Hutchinson Cancer Research Center .

Please send comments and questions to: *tbailey@sdsc.edu* .

Figure 4.14. The MEME Web page. The MEME program finds ungapped motifs (blocks) in unaligned protein or DNA sequences. As indicated, the program can be directed to search for the size and expected number of motifs or can predict motifs based on a statistical analysis based on the EM algorithm described in the text.

A. Summary line

MOTIF 1 width = 9 sites = 29.5

B. Letter-probability matrix

Simplified motif letter-probability matrix

```
A ::1::::8:
C :::::::::
D :8:::::::
E :::::::::
F :::::::::
G ::1:::::9
H :::::::::
I 2:212::::
K :::::::::
L 3:18:::::
M :::::::::
N :::::89::
P :::::::::
Q :::::::::
R :::::::::
S :::::::::
T :::::::::
V 3:3:7::::
W :::::::::
Y :::::::::
```

C. Information content of the profile

Information content (22.0 bits)

```
bits 6.2
     5.6
     5.0
     4.4
     3.7
     3.1  *    **
     2.5  *    **  *
     1.9  *  ******
     1.2 **  ******
     0.6 *********
     0.0 ---------
```

D. The multilevel consensus sequence

Multilevel consensus sequence

VDVLVNNAG
L

Figure 4.15. Results produced by a MEME analysis of sequences for motifs. The output diagrams are discussed in the text. (*A*) Summary line giving the number of the next motif found in order of statistical significance, width, and expected number of occurrences in the given sequences. (*B*) Simplified motif letter-probability matrix showing the frequency of each amino acid in each column of the matrix. The columns are the columns of the motif. For easier reading, the numbers shown are frequencies rounded to the nearest one-tenth and multiplied by 10, and zeros are shown as colons. (*C*) The information content of the profile is given in a diagram. Basically, the diagram shows the degree of amino acid variation in each column of the profile: the lower the value, the greater the variation. The scale is logarithmic to the base 2 (bits). The total of all columns is also shown. The subject of information content is discussed in greater detail below under position-specific scoring matrices. (*D*) The multilevel consensus sequence shows all letters in each column of the motif that occur with a frequency of >0.2. *Continued.*

E. The next motif

Motif 1 in BLOCKS format

```
BL MOTIF 1; width = 9;  seqs = 33
2BHD_STREX      (  81)  VDGLVNNAG  1
3BHD_COMTE      (  81)  LNVLVNNAG  1
ADH_DROME       (  86)  VDVLINGAG  1
AP27_MOUSE      (  77)  VDLLVNNAA  1
BA72_EUBSP      (  86)  LDVMINNAG  1
BDH_HUMAN       ( 138)  MWGLVNNAG  1
BPHB_PSEPS      (  79)  IDTLIPNAG  1
BUCD_KLETE      (  80)  FNVIVNNAG  1
DHES_HUMAN      (  84)  VDVLVCNAG  1
DHGB_BACME      (  87)  LDVMINNAG  1
DHMA_FLAS1      ( 198)  VDVTGNNTG  1
ENTA_ECOLI      (  73)  LDALVNAAG  1
FIXR_BRAJA      ( 112)  LHALVNNAG  1
GUTD_ECOLI      (  82)  VDLLVYSAG  1
HDE_CANTR       ( 396)  IDILVNNAG  1
HDHA_ECOLI      (  89)  VDILVNNAG  1
NODG_RHIME      (  81)  VDILVNNAG  1
RIDH_KLEAE      (  89)  LDIFHANAG  1
YINL_LISMO      (  83)  VDAIFLNAG  1
YRTP_BACSU      (  84)  IDILINNAG  1
CSGA_MTXXA      (  13)  VDVLINNAG  1
DHB2_HUMAN      ( 161)  LWAVINNAG  1
DHB3_HUMAN      ( 125)  IGILVNNVG  1
DHCA_HUMAN      (  83)  LDVLVNNAG  1
FVT1_HUMAN      ( 115)  VDMLVNCAG  1
HMTR_LEIMA      ( 103)  CDVLVNNAS  1
MAS1_AGRRA      ( 320)  IDGLVNNAG  1
PCR_PEA         ( 165)  LDVLINNAA  1
YURA_MYXXA      (  90)  LDLVVANAG  1
//
```

Figure 4.15. *Continued.* (*E*) Possible examples of the motif in the training set are shown. This list is based on using a position-dependent scoring matrix (log-odds matrix) to search each sequence. The threshold score for displaying a site is chosen such that the expected number of incorrect assignments will equal the expected number of missed but correct assignments. Positions before and after the motif are also shown. *Continued.*

F. Possible examples of motif 1 in the training set

Sequence name	Start	Score	Site		
2BHD_STREX	81	28.80	VAYAREEFGS	VDGLVNNAG	ISTGMFLETE
3BHD_COMTE	81	25.99	MAAVQRRLGT	LNVLVNNAG	ILLPGDMETG
ADH_DROME	86	22.33	LKTIFAQLKT	VDVLINGAG	ILDDHQIERT
AP27_MOUSE	77	24.36	TEKALGGIGP	VDLLVNNAA	LVIMQPFLEV
BA72_EUBSP	86	26.39	VGQVAQKYGR	LDVMINNAG	ITSNNVFSRV
BDH_HUMAN	138	23.46	PFEPEGPEKG	MWGLVNNAG	ISTFGEVEFT
BPHB_PSEPS	79	18.60	ASRCVARFGK	IDTLIPNAG	IWDYSTALVD
BUDC_KLETE	80	20.97	VEQARKALGG	FNVIVNNAG	IAPSTPIESI
DHES_HUMAN	84	25.67	AARERVTEGR	VDVLVCNAG	LGLLGPLEAL
DHGB_BACME	87	26.39	VQSAIKEFGK	LDVMINNAG	MENPVSSHEM
DHMA_FLAS1	198	16.36	ILVNMIAPGP	VDVTGNNTG	YSEPRLAEQV
ENTA_ECOLI	73	21.90	CQRLLAETER	LDALVNAAG	ILRMGATDQL
FIXR_BRAJA	112	23.67	EVKKRLAGAP	LHALVNNAG	VSPKTPTGDR
GUTD_ECOLI	82	17.17	SRGVDEIFGR	VDLLVYSAG	IAKAAFISDF
HDE_CANTR	92	20.90	VETAVKNFGT	VHVIINNAG	ILRDASMKKM
HDE_CANTR	396	29.32	IKNVIDKYGT	IDILVNNAG	ILRDRSFAKN
HDHA_ECOLI	89	30.18	ADFAISKLGK	VDILVNNAG	GGGPKPFDMP
NODG_RHIME	81	30.18	GQRAEADLEG	VDILVNNAG	ITKDGLFLHM
RIDH_KLEAE	89	16.02	LQGILQLTGR	LDIFHANAG	AYIGGPVAEG
YINL_LISMO	83	14.65	VELAIERYGK	VDAIFLNAG	IMPNSPLSAL
YRTP_BACSU	84	27.41	VAQVKEQLGD	IDILINNAG	ISKFGGFLDL
CSGA_MYXXA	13	28.94	AFATNVCTGP	VDVLINNAG	VSGLWCALGD
DHB2_HUMAN	161	19.62	KVAAMLQDRG	LWAVINNAG	VLGFPTDGEL
DHB3_HUMAN	125	18.63	HIKEKLAGLE	IGILVNNVG	MLPNLLPSHF
DHCA_HUMAN	83	30.23	RDFLRKEYGG	LDVLVNNAG	IAFKVADPTP
FVT1_HUMAN	115	24.21	IKQAQEKLGP	VDMLVNCAG	MAVSGKFEDL
HMTR_LEIMA	103	24.02	VAACYTHWGR	CDVLVNNAS	SFYPTPLLRN
MAS1_AGRRA	320	27.93	VTAAVEKFGR	IDGLVNNAG	YGEPVNLDKH
PCR_PEA	165	23.97	VDNFRRSEMP	LDVLINNAA	VYFPTAKEPS
YURA_MYXXA	90	18.59	IRALDAEAGG	LDLVVANAG	VGGTTNAKRL

Figure 4.15. *Continued.* (*F*) The next motif is given in the format used for the BLOCKS database (http://www.blocks.fhcrc.org/blocks). The predicted locations of this motif in each sequence and the probability that the motif starts at that location are shown. The sites reported depend on the motif search model used: (1) OOPS, the most probable location in each sequence is given; (2) ZOOPS, the most probable location in each sequence is reported but only probabilities greater than 0.5 (a significant level for Bayesian statistics); TCM, all positions in each sequence with probabilities > 0.5 are shown. *Continued.*

G. Position-specific scoring matrix

Log-odds matrix: alength = 20 w = 9 n = 9732 bayes = 8.36118

-2.725	0.818	-5.204	-4.539	-0.082	-4.432	-3.515	1.560	-4.218	1.814	0.701	-4.126	-3.146	-3.848	.
-3.441	-3.841	-4.023	-1.204	-4.313	-2.395	-0.889	-4.226	-4.009	-4.571	-3.882	-0.220	-4.682	-3.547	.
-0.768	-2.342	-4.756	-4.189	-2.319	0.376	-3.154	1.757	-3.870	0.288	0.918	-3.149	-4.229	-3.492	.
-3.379	-2.600	-5.066	-4.331	-0.586	-5.089	-3.668	-0.081	-4.098	3.045	1.107	-4.393	-4.287	-3.383	.
-1.373	-1.895	-3.823	-3.574	-1.086	-1.952	-0.466	1.480	-3.565	-2.234	-1.834	-3.701	-3.612	-3.536	.
-1.879	-0.980	-2.231	-4.187	-3.807	-3.562	-0.892	-3.306	-3.238	-2.753	-3.337	4.193	-2.276	-2.750	.
-2.460	-0.912	-2.252	-4.176	-3.833	-2.391	-0.968	-3.339	-3.262	-4.256	-3.364	4.217	-4.026	-2.768	.
-3.475	-1.137	-3.874	-3.535	-3.304	-2.080	-2.080	-2.826	-3.544	-3.127	-2.263	-3.592	-4.599	-3.533	.
-0.693	-3.833	-3.137	-3.879	-4.963	3.663	-3.647	-3.364	-3.716	-5.287	-4.212	-2.849	-4.518	-4.155	.

H. Motif letter-frequency matrix

Letter-probability matrix: alength = 20 w = 9 n = 9732

0.011063	0.032022	0.001403	0.002682	0.038055	0.003212	0.001962	0.165990	0.003143	0.322510	0.037503	0.011063
0.006738	0.001268	0.841023	0.027061	0.002026	0.013178	0.012108	0.003008	0.003632	0.003860	0.001564	0.011063
0.124630	0.003583	0.001915	0.003418	0.008070	0.089951	0.002520	0.190255	0.004000	0.112000	0.043590	0.011063
0.007032	0.002996	0.001544	0.003098	0.026845	0.002037	0.001765	0.053213	0.003415	0.756853	0.049683	0.011063
0.028238	0.004883	0.003655	0.005236	0.018977	0.017917	0.016240	0.156947	0.004942	0.019499	0.006470	0.011063
0.019895	0.009211	0.011023	0.003422	0.002878	0.005871	0.012089	0.005691	0.006199	0.013606	0.002282	0.011063
0.013301	0.009656	0.010865	0.003449	0.002827	0.013217	0.011467	0.005564	0.006098	0.004800	0.002240	0.011063
0.813801	0.008259	0.003529	0.005378	0.004079	0.016396	0.005304	0.007937	0.005014	0.010499	0.004806	0.011063
0.045249	0.001275	0.005879	0.004237	0.001291	0.878064	0.001790	0.005467	0.004450	0.002354	0.001244	0.011063

Figure 4.15. *Continued.* (*G*) Position-specific scoring matrix. This matrix is a log-odds matrix calculated by taking the log (base 2) of the ratio of the observed to expected counts for each amino acid in each column of the profile. Columns and rows in the matrix correspond to the amino acids in each column and positions of the motif, respectively. The counts for each column may have additional pseudocounts added to compensate for zero occurrences of an amino acid in a column or for a small number of sequences, as discussed below for this type of matrix. (*H*) Motif letter-frequency matrix is given, showing the frequency of amino acid found in each column of the profile. Columns and rows correspond to the amino acids in each column and rows to columns in the motif, respectively. Shown also are the numbers of types of residues, the width of the motif, and number of characters in the sequences. Only portions of the output are shown.

To understand the algorithm, consider a simple example using the Gibbs sampler algorithm to locate a single 20-residue-long motif in 10 sequences, each 200 residues long, as was done above to illustrate the EM algorithm. The method iterates through two steps. In the first step, the predictive update step, a random start position for the motif is chosen for all sequences but for one that is chosen at random or in a specified order. So let us choose sequence 1 as the outlier and use the other 9 to find an initial guess of the motif. These other 9 sequences are aligned with random overlaps. The following figure illustrates how this initial motif is located (an x equals 20 sequence positions, M indicates the random location of the motif chosen for each sequence, and – the 20 initially aligned motif positions).

The objective is to find the most probable pattern common to all of the sequences by sliding them back and forth until the ratio of the motif probability to the background probability is a maximum. This is accomplished by first using the initial alignment shown above to estimate the residue frequencies in each column of the motif, and the sequence residues

Steps of the Gibbs sampler algorithm.

A. Estimate the amino acid frequencies in the motif columns of all but 1 sequence. Also obtain background

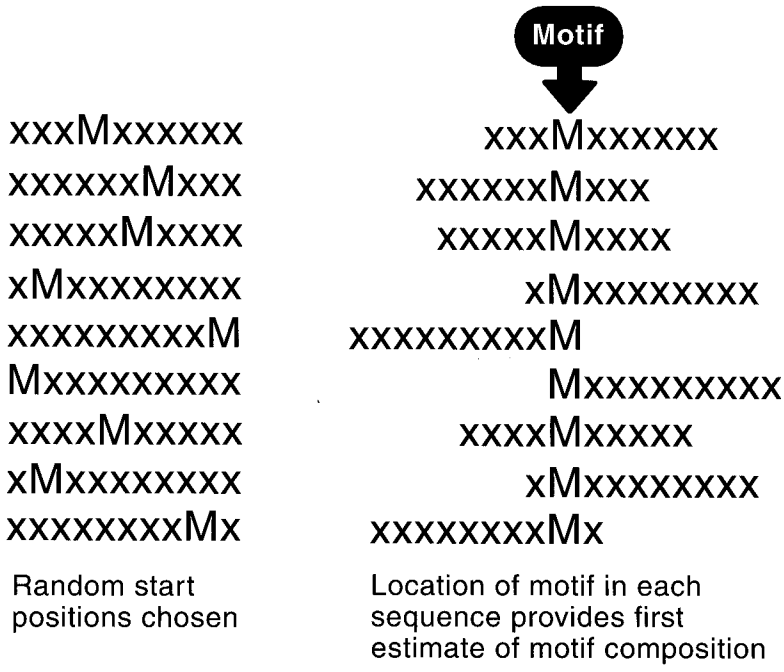

B. Use the estimates from A to calculate the ratio of probability of motif to background score at each position in the left out sequence. This ratio for each possible location in the sequence is the weight of the position.

```
xxxxxxxxxxx   xxxxxxxxxxx   xxxxxxxxxxx   xxxxxxxxxxx   xxxxxxxxxxx
M ->          M ->          M ->          M ->          M ->
```

C. choose a new location for the motif in the left out sequence by a random selection using the weights to bias the choice.

```
xxxxxxxxMxx   Estimated location of the motif in left out sequence
```

D. Repeat steps A to C >100 times.

that are not included in the motif to estimate the background residue frequencies. For example, if these sequences are DNA sequences and the first column of the estimated motif in the 10 sequences includes 3 Gs, then the value for $f_{g,\,\text{column1}} = 3/9 = 0.33$. Similarly, let $f_{t,\,\text{column2}} = 1/9 = 0.11$ for illustration. These frequencies are determined for each of the 20 columns in our example. Similarly, if there are 240 Gs among the $10 \times 80 = 800$ sequence positions not within the estimated motif, then $f_{g,\,\text{background}} = 240/800 = 0.30$. Also let $f_{t,\,\text{background}} = 180/800 = 0.225$. If the first two positions in sequence 1 are G and T in that order, then the probability of the motif starting at position 1, Q_1, is calculated as $0.33 \times 0.11 \times \ldots\ldots x\, f_{\text{last base, column20}}$. The background probability of this first possible motif, P_1, is also calculated as $0.30 \times 0.225 \times \ldots\ldots x\, f_{\text{last base, background}}$.

Note the difference between the Gibbs sampler method and the EM method, which calculates the probability of the entire sequence using the motif column frequencies within the motif and the background frequencies elsewhere.

The ratio Q_1/P_1 is designated as weight A_1 for motif position 1 in sequence 1. A_1s are then calculated for all other $100 - 20 + 1 = 81$ possible locations of the 20-residue-long motif in sequence 1. These weights are then normalized by dividing each weight by their sum to give a probability for each motif position. From this probability distribution, a random start position is chosen for position 1. In so doing, the chance of choosing a particular position is proportional to the weight of that position so that a higher scoring position is more likely to be chosen. (You can think of a bag with 81 kinds of balls, with the number of each ball proportional to the weight or probability of that kind. Drawing a random ball will favor the more prevalent ones.) This position in the left-out sequence is then used as an estimate of the location for the motif in sequence 1. The procedure is then repeated. Select the next sequence to be scanned, align the motifs in the other 9 sequences with sequence 1 now using the estimated location found above, and so on. This process is repeated until the residue frequencies in each column of the motif do not change. For different starting alignments, the number of iterations needed may range from several hundred to several thousand.

As the above cycles are repeated, the more accurate the initial estimate of the motif in the aligned sequences, the more accurate the pattern location in the outlier sequence. The second step in the algorithm tends to move the sequence alignments in a direction that favors a better score but also has a random element to search for other possible better locations. When correct start positions have been selected in several sequences by chance, the compositions of the motif columns begin to reflect a pattern that the algorithm can search for in the other sequences, and the method converges on the optimal motif and the probability distribution of the motif location in each sequence.

Several additional procedures are used to improve the performance of the algorithm.

1. For a correct Bayesian statistical analysis, the amino acid counts in the motif and the background in the outlier sequence are estimated and added to the counts in the remaining aligned sequences. This step is the equivalent of combining prior and updated information to improve the estimation of the motif. These counts may be estimated by Dirichlet mixtures (see discussion of HMMs, p. 189), which give frequencies expected based on prior information from amino acid distributions (Liu et al. 1995). The missing background counts for each residue b_i are estimated by the formula $b_i = f_i\, x,\, B$ where B is chosen based on experience with the method as $\sqrt{N}$, the number of sequences in the motif, and f_i is the frequency of residue i in the sequences (Lawrence et al. 1993).
2. Another feature is a procedure to prevent the algorithm from getting locked in a suboptimal solution. In the HMM method (see below), noise is introduced for this purpose. In the Gibbs sampler, after a certain number of iterations, the current alignments are shifted a certain number of positions to the right and left, and the scores from these shifted positions are found. A probability distribution of these scores is then used as a basis for choosing a new random alignment.
3. The results of a range of motif widths can be investigated. The major difficulty in exploring motif width is to arrive at a criterion for comparing the resulting scores. One suitable measure is to optimize the average information (see below) per free parameter in the motif, a value that can be calculated (Lawrence et al. 1993; Liu et al. 1995). The number of free parameters for proteins is $20 - 1 = 19$, and for DNA, $4 - 1 = 3$, times the model width.
4. The method can be readily extended to search for multiple motifs in the same set of sequences.
5. The method has been extended to seek a pattern in only a fraction of the input sequences.

The Gibbs sampler was used to align 30 helix-turn-helix DNA-binding domains showing very little sequence similarity. The information per parameter criterion was used to find the best motif width. Multiple motifs were found in lipocalins, a family with quite dissimilar motif sequences separated by variable spacer regions, and also in protein isoprenyltransferase subunits, which have very large numbers of repeats of several kinds (Lawrence et al. 1993). Thus, the method is widely applicable for discovering complex and variable motifs in proteins.

Hidden Markov Models

The HMM is a statistical model that considers all possible combinations of matches, mismatches, and gaps to generate an alignment of a set of sequences (Fig. 4.16). A model of a sequence family is first produced and initialized with prior information about the sequences. A set of 20–100 sequences or more is then used as data to train the model. The trained model may then be used to produce the most probable msa as posterior information. Alternatively, the model may be used to search sequence databases to identify additional members of a sequence family. A different HMM is produced for each set of sequences. HMMs have been previously used very successfully for speech recognition, and an excellent review of the methodology is available (Rabiner 1989). In addition to their use in producing multiple sequence alignments (Baldi et al. 1994; Krogh et al. 1994; Eddy 1995, 1996), HMMs have also been used in sequence analysis to produce an HMM that represents a sequence profile (a profile HMM), to analyze sequence composition and patterns (Churchill 1989), to locate genes by predicting open reading frames (Chapter 8), and to produce protein structure predictions (Chapter 9). Pfam, a database of profiles that represent protein families, is based on profile HMMs (Sonhammer et al. 1997).

HMMs often provide a msa as good as, if not better than, other methods. The approach also has a number of other strong features: It is well grounded in probability theory, no sequence ordering is required, insertion/deletion penalties are not needed, and experimentally derived information can be used. Two disadvantages to using HMMs are that at least 20 sequences and sometimes many more are required to accommodate the evolutionary history (see Mitchison and Durbin 1995). The HMM can be used to improve an existing heuristic alignment. The two HMM programs in common use are Sequence Alignment and Modeling Software System, or SAM (Krogh et al. 1994; Hughey and Krogh 1996), and HMMER (see Eddy 1998). The software is available at http://www.cse.ucsd.edu/research/compbio/sam.html and http://hmmer.wustl.edu/. The algorithms used for producing HMMs are extensively discussed in Durbin et al. (1998). A comparison of HMMs with other methods is given at the end of this section.

The HMM representation of a section of multiple sequence alignment that includes deletions and insertions was devised by Krogh et al. (1994) and is shown in Figure 4.6. This HMM generates sequences with various combinations of matches, mismatches, insertions, and deletions, and gives these a probability, depending on the values of the various parameters in the model. The object is to adjust the parameters so that the model represents the observed variation in a group of related protein sequences. A model trained in this manner will provide a statistically probable msa of the sequences.

As illustrated in Figure 4.6, the object is to calculate the best HMM for a group of sequences by optimizing the transition probabilities between states and the amino acid compositions of each match state in the model. The sequences do not have to be aligned to use the method. Once a reasonable model length reflecting the expected length of the sequence alignment is chosen, the model is adjusted incrementally to predict the sequences. Several methods for training the model in this fashion have been described (Baldi et al. 1994; Krogh et al. 1994; Eddy et al. 1995; Eddy 1996; Hughey and Krogh 1996;

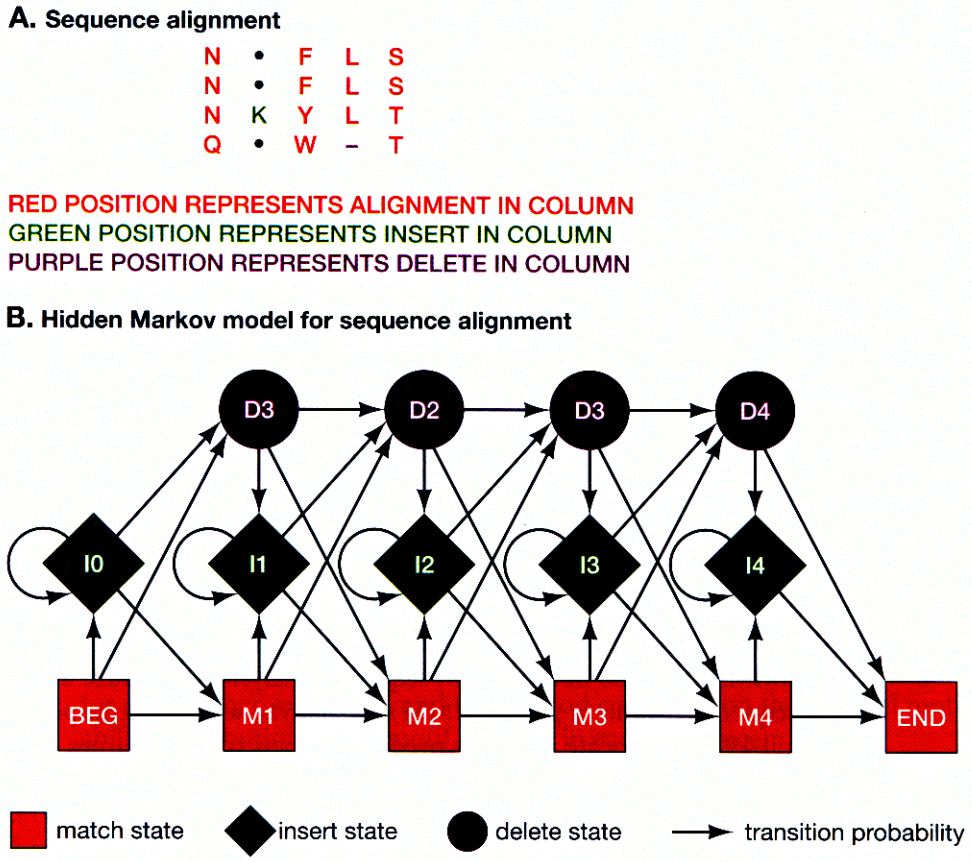

Figure 4.16. Relationship between the sequence alignment and the hidden Markov model of the alignment (Krogh et al. 1994). This particular form for the HMM was chosen to represent the sequence, structural, and functional variation expected in proteins. The model accommodates the identities, mismatches, insertions, and deletions expected in a group of related proteins. (*A*) A section of a multiple sequences alignment. The illustration shows the columns generated in a multiple sequence alignment. Each column may include matches and mismatches (*red* positions), insertions (*green* positions), and deletions (*purple* position). (*B*) The HMM. Each column in the model represents the possibility of a match, insert, or delete in each column of the alignment in *A*. The HMM is a probabilistic representation of a section of a msa. Sequences can be generated from the HMM by starting at the beginning state labeled BEG and then by following any one of many pathways from one type of sequence variation to another (states) along the state transition arrows and terminating in the ending state labeled END. Any sequence can be generated by the model and each pathway has a probability associated with it. Each square match state stores an amino acid distribution such that the probability of finding an amino acid depends on the frequency of that amino acid within that match state. Each diamond-shaped insert state produces random amino acid letters for insertions between aligned columns and each circular delete state produces a deletion in the alignment with probability 1. For example, one of many ways of generating the sequence **N K Y L T** in the above profile is by the sequence BEG→M1→I1→M2→M3→M4→END. Each transition has an associated probability, and the sum of the probabilities of transitions leaving each state is 1. The average value of a transition would thus be 0.33, since there are three transitions from most states (there are only two from M4 and D4, hence the average from them is 0.5). For example, if a match state contains a uniform distribution across the 20 amino acids, the probability of any amino acid is 0.05. Using these average values of 0.33 or 0.5 for the transition values and 0.05 for the probability of each amino acid in each state, the probability of the above sequence **N K Y L T** is the product of all of the transition probabilities in the path BEG→M1→I1→M2→M3→M4→END, and the probability that each state will produce the corresponding amino acid in the sequences, or $0.33 \times 0.05 \times 0.33 \times 0.05 \times 0.33 \times 0.05 \times 0.33 \times 0.05 \times 0.33 \times 0.05 \times 0.5 = 6.1 \times 10^{-10}$. Since these probabilities are very small numbers, amino acid distributions and transition probabilities are converted to log odds scores, as done in other statistical methods (see pp. 176–177), and the logarithms are added to give the overall probability score. The secret of the HMM is to adjust the transition values and the distributions in each state by training the model with the sequences. The training involves finding every possible pathway through the model that can produce the sequences, counting the number of times each transition is used

Continued.

Durbin et al. 1998). For example, an EM algorithm from speech recognition methods known as the Baum-Welch algorithm is used as follows:

1. The model is initialized with estimates of transition probabilities and amino acid composition for each match and insert date. If an initial alignment of the sequences is known, or some other kinds of data suggest which sequence positions are the same, then these data may be used in the model. For other cases, the initial distribution of amino acids to be used in each state is described below. The initial transition probabilities generally favor transitions from one match state to the next rather than favoring insert and delete states, which build more uncertainty into a sequence motif.
2. All possible paths through the model for generating each sequence in turn are examined. There are many possible such paths for each sequence. This procedure would normally require a huge amount of time computationally. Fortunately, an algorithm, the forward-backward algorithm, reduces the number of computations to the number of steps in the model times the total length of the training sequences. This calculation provides a probability of the sequence, given all possible paths through the model, and, from this value, the probability of any particular path may be found. Another algorithm, the Baum-Welch algorithm, then counts the number of times a particular state-to-state transition is used and a particular amino acid is required by a particular match state to generate the corresponding sequence position.
3. A new version of the HMM is produced that uses the results found in step 2 to generate new transition probabilities and match-insert state compositions.
4. Steps 3 and 4 are repeated up to 10 more times until the parameters do not change significantly.
5. The trained model is used to provide the most likely path for each sequence, as described in Figure 4.16. The algorithm used for this purpose, the Viterbi algorithm, does not have to go through all of the possible alignments of a given sequence to the HMM to find the most probable alignment, but instead can find the alignment by a dynamic programming technique very much like that used for the alignment of two sequences, discussed in Chapter 3. The collection of paths for the sequences provides a msa of the sequences with the corresponding match, insert, and delete states for each sequence. The columns in the msa are defined by the match states in the HMM such that amino acids from a particular match state are placed in the same column. For columns that do not correspond to a match state, a gap is added.
6. The HMM may be used to search a sequence database for additional sequences that share the same sequence variation. In this case, the sum of the probabilities of all possible sequence alignments to the model is obtained. This probability is calculated by the forward component of the forward-backward algorithm described above. This analysis

and which amino acids were required by each match and insert state to produce the sequences. This training procedure leaves a memory of the sequences in the model. As a consequence, the model will be able to give a better prediction of the sequences. Once the model has been adequately trained, of all the possible paths through the model that can generate the sequence **N K Y L T**, the most probable should be the match-insert-3 match combination (as opposed to any other combination of matches, inserts, and deletions). Likewise, the other sequences in the alignment would also be predicted with highest probability as they appear in the alignment; i.e., the last sequence would be predicted with highest probability by the path match-match-delete-match. In this fashion, the trained HMM provides a multiple sequence alignment, such as shown in *A*. For each sequence, the objective is to infer the sequence of states in the model that generate the sequences. The generated sequence is a Markov chain because the next state is dependent on the current one. Because the actual sequence information is hidden within the model, the model is described as a hidden Markov model.

gives a type of distance score of the sequence from the model, thus providing an indication of how well a new sequence fits the model and whether the sequence may be related to the sequences used to train the model. In later derivations of HMMs, the score was divided by the length of the sequence because it was found to be length-dependent. A z score giving the number of standard deviations of the sequence length-corrected score from the mean length-corrected score is therefore used (Durbin et al. 1998).

Recall that for the Bayes block aligner, the initial or prior conditions were amino acid substitution matrices, block numbers, and alignments of the sequences. The sequences were then used as new data to examine the model by producing scores for every possible combination of prior conditions. By using Bayes' rule, these data provided posterior probability distributions for all combinations of prior information. Similarly, the prior conditions of the HMM are the initial values given to the transition values and amino acid compositions. The sequences then provide new data for improving the model. Finally, the model provides a posterior probability distribution for the sequences and the maximum posterior probability for each sequence represented by a particular path through the model. This path provides the alignment of the sequence in the msa; i.e., the sequence plus matches, inserts, and deletes, as described in Figure 4.16.

The success of the HMM method depends on having appropriate initial or prior conditions, i.e., a good prior model for the sequences and a sufficient number of sequences to train the model. The prior model should attempt to capture, for example, the expected amino acid frequencies found in various types of structural and functional domains in proteins. As the distributions are modified by adding amino acid counts from the training sequences, new distributions should begin to reflect common patterns as one moves through the model and along the sequences. It is important that the model reflect not only the patterns in the training sequences, but also pattern variations that might be present in other members of the same protein family. Otherwise, the model will only recognize the training sequences but not other family members. Thus, some smoothing of the amino acid frequencies is desirable, but not to the extent of suppressing highly conserved pattern information from the training sequences. Such problems are avoided by using a method called regularization to avoid overfitting the data to the model. Basically, the method involves using a carefully designed amino acid distribution as the prior condition and then modifying this distribution in a manner that uses training information in a complementary manner.

Rather than using simple amino acid composition as a prior condition for the match states in the HMM, amino acid patterns that capture some of the important features of protein structure and function have been used with considerable success (Sjölander et al. 1996). Other prior conditions include using Dayhoff PAM or BLOSUM amino acid substitution matrices modified by adding additional counts (pseudocounts) to smooth the distributions (Tatusov et al. 1994; Eddy 1996; Henikoff and Henikoff 1996; Sonnhammer et al. 1997; and see Chapter 2). Sjölander et al. (1996) have prepared particularly useful amino acid distributions called Dirichlet mixtures to use as prior information in the match states of the HMM. These mixtures provide amino acid compositions that have proven to be useful for the detection of weak but significant sequence similarity. As an example, the amino acid frequencies that are characteristic of a particular set of nine blocks in the BLOCKS database have been determined. These blocks represent amino acid frequencies that are favored in certain chemical environments such as aromatic, neutral, and polar residues and are useful for detecting such environments in test sequences. The nine-component system has been used successfully for producing an HMM for globin sequences (Hughey and Krogh 1996). To use these frequencies as prior information, they are treated

as possible posterior distributions that could have generated the given amino acid frequencies as posterior probabilities. The probability of a particular amino acid distribution given a known frequency distribution, i.e., 100 A, 67 G, 5 C, etc., where pA is the probability of A given by the frequency of A, pG the probability of G, etc., and n is the total number of amino acids given by the multinomial distribution

$$P(100\text{A}, 67\text{G}, 5\text{C} \ldots) = n!\, p\text{A}^{100} p\text{G}^{67}\, p\text{C}^{5} \ldots / 100!\, 67!\, 5! \ldots \quad (6)$$

The prior distribution for the multinomial distribution is the Dirichlet distribution (Carlin and Louis 1996), whose formulation is similar to that given in Equation 6 with a similar set of parameters but with factorial and powers reduced by 1. The idea behind using this particular distribution is that if additional sequence data with a related pattern are added, then by the Bayesian procedure of multiplying prior probabilities with the likelihood of the new data to obtain the posterior distribution, the probability of finding the correct frequency of amino acids is favored statistically. Because the amino acid frequencies in the test sequences could be any one of several alternatives, a prior distribution that reflects these several choices is necessary. There is a method for weighting the prior distributions expected for several different multinomial distributions into a combined frequency distribution, the Dirichlet mixture. Calculation of these mixtures is a complex mathematical procedure (Sjölander et al. 1996). Dirichlet mixtures recommended for use in aligning proteins by the HMM method have been described previously (Karplus 1995) and are available from http://www.cse.ucsc.edu/research/compbio/. After the prior amino acid frequencies are in place in the match states of the model, these are modified by training the HMM with the sequences, as described in steps 2 and 3 above. For each match state in the model, a new frequency for each amino acid is calculated by dividing the sum of all new and prior counts for that amino acid by the new total of all amino acids. In this fashion, the new HMM (step 4 above) reflects a combination of expected distributions averaged over patterns in the Dirichlet mixture and patterns exhibited in the training sequences. A similar method is used to refashion the transition probabilities in the HMM during training following manual insertion of initial values.

Another consideration in using HMMs is the number of sequences. If a good prior model such as the above Dirichlet distribution is used, it should be possible to train the HMM with as few as 20 sequences (SAM manual; Eddy 1996; Hughey and Krogh 1996). In general, the smaller the sequence number, the more important the prior conditions. If the number of sequences is >50, the initial conditions play a lesser role because the training step is more effective. As with any msa method, the more sequence diversity, the more challenging the task of aligning sequences with HMMs. HMMs are also more effective if methods to inject statistical noise into the model are used during the training procedure. As the model is refashioned to fit the sequence data, it sometimes goes into a form that provides locally optimal instead of globally optimal alignments of the sequences. One of several noise injection methods (Baldi et al. 1994; Krogh et al. 1994; Eddy et al. 1995; Eddy 1996; Hughey and Krogh 1996) may be used in the training procedure. One method called simulated annealing is used by SAM (Hughey and Krogh 1996). A user-defined number of sequences are generated from the model at each cycle and the counts so generated are added to those from the training sequences. The noise generated in this way is reduced as the cycle number is increased. Finally, the HMM program SAM has a built-in feature of model surgery during training. If a match state is used by fewer than half of the sequences, it is deleted. These same sequences then have to use an insert state in the revised model. Similarly, if an insert state is used by more than half of the sequences, a number of addi-

tional match states equal to the average number of insertions is added, and the model has to be revised accordingly. These fractions may be varied in SAM to test the effect on the type of HMM model produced (Hughey and Krogh 1996).

In trying to produce an HMM for a set of related sequences, the recommended procedure is to produce several models by varying the prior conditions. Using regularization by adding prior Dirichlet mixtures to the match states produces models that are more representative of the protein family from which the training sequences are derived. Varying the noise and model surgery levels is another way to vary the training procedure and the HMM model. The best HMM model is the one that predicts a family of related sequences with the lowest and most narrow distribution of NLL scores. An example of a portion of an HMM trained on a set of globin sequences is shown in Figure 4.17.

Motif-based Hidden Markov Models

The program Meta-MEME uses the HMM method to find motifs (conserved sequence domains) in a set of related protein sequences and the spacer regions between them (Grundy et al. 1997) and is built in part on the HMM program HMMER (Eddy et al. 1995). A similar method was originally used to analyze prokaryotic promoters with two conserved patterns separated by a variable spacer region (Cardon and Stormo 1992). A Meta-MEME analysis may be performed at http://www.sdsc.edu/MEME using the University of California at San Diego Supercomputing Center. The use of hidden Markov models for producing a global msa is described in the above section. A problem with HMMs is that the training set has to be quite large (50 or more sequences) to produce a useful model for the sequences. For a smaller number of sequences, it is possible to obtain a model if suitable prior data are used, and an amino acid frequency that is a mixture of frequencies characteristic of certain structural domains (the Dirichlet mixture) is used as prior information of the match states of the model. This mixture is a reasonable guess of combinations of amino acid patterns that are likely to be found. A difficulty in training the HMM residues is that many different parameters must be found (the amino acid distributions, the number and positions of insert and delete states, and the state transition frequencies add up to thousands of parameters) to obtain a suitable model, and the purpose of the prior and training data is to find a suitable estimate for all of these parameters. When trying to make an alignment of short sequence fragments to produce a profile HMM, this problem is worsened because the amount of data for training the model is even further reduced.

Two methods are used by Meta-MEME to circumvent this problem. First, another pattern-finding algorithm, the EM algorithm (discussed on p. 173), is used to locate ungapped regions that match in the majority of the sequences. Second, a simplified HMM with a much reduced number of parameters is produced. The model includes a series of match states that model the patterns located by MEME with transition probabilities of 1 between them and a single insert state between each of these patterns, as illustrated in Figure 4.18. As a result, fewer parameters need to be used, mostly for the amino acid frequencies in the match states.

The most probable order and spacing of the patterns is next found. Another program (Motif Alignment and Search Tool, or MAST; Bailey and Gribskov 1997) is used for this purpose. MAST searches a sequence database for the patterns and reports the database sequences that have the statistically most significant matches. The order and spacing of the patterns found in the highest-scoring database sequences are then used by Meta-MEME as a basis for designing the number of match and insert states and the transition probabilities for the insert states. The match states are filled with modified Dirichlet mixtures (Baylor

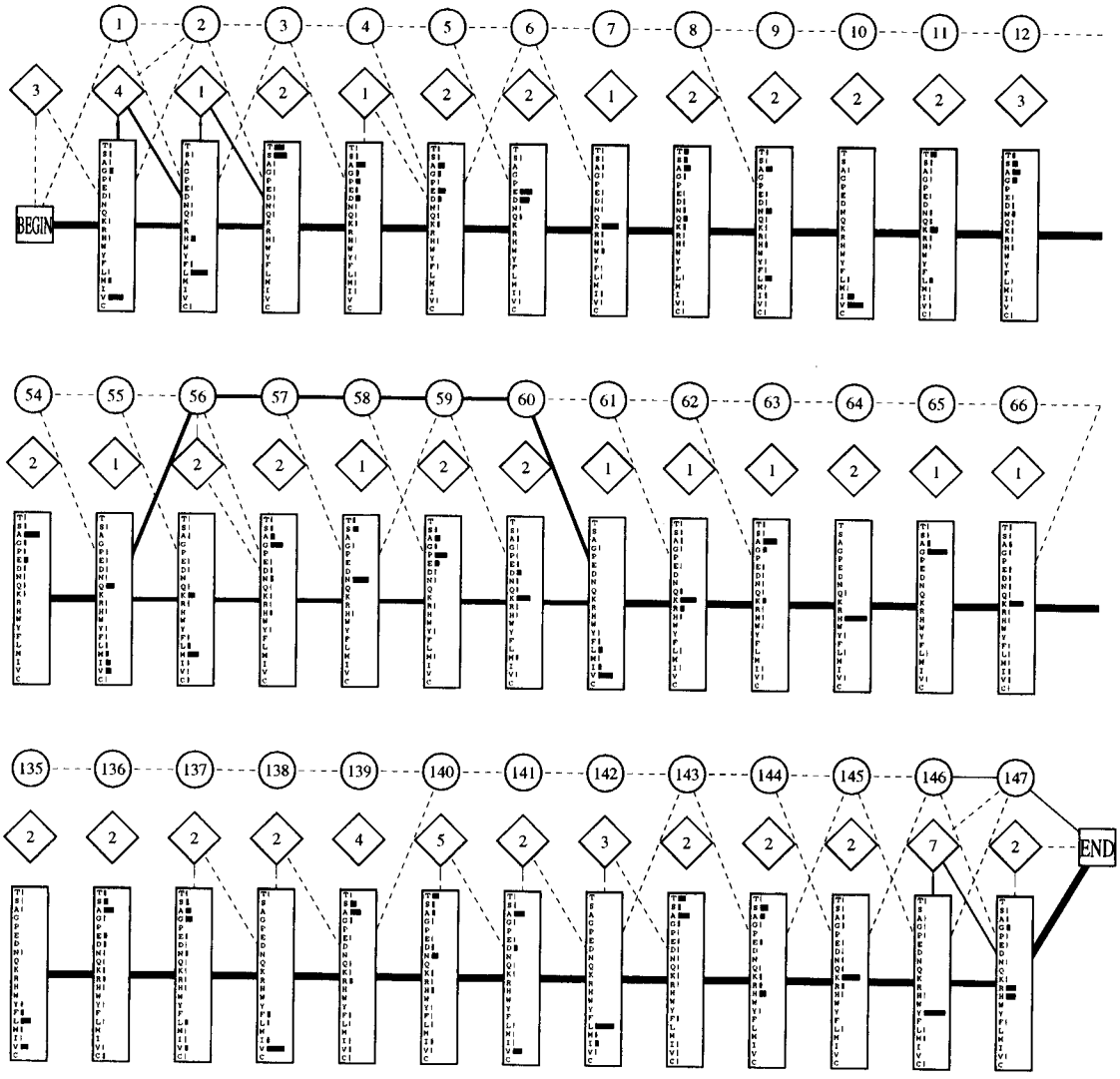

Figure 4.17. HMM trained for recognition of globin sequences. Circles in the top row are delete states that include the position in the alignment; the diamonds in the second row are insert states showing the average length of the insertion, and the rectangles in the bottom row show the amino acid distribution in the match states: V is common at match position 1, L at 2, and so on. The width of each transition line joining these various states indicates the extent of use of that path in the training procedure, and dotted lines indicate a rarely used path. The most used paths are between the match states, but about one-half of the sequences use the delete states at model positions 56–60. Thus, for most of the sequences, the msa or profile will show the first two columns aligned with a V followed by an L, but at 56–60, about one-half of the sequences will have a 5-amino-acid deletion. (Reprinted, with permission, from Krogh et al. 1994 [copyright Academic Press].)

and Gribskov 1996), and the model is trained by the motif models found by MEME. For the 4Fe-4S ferredoxins, a measure of the success of the HMM for database search, the ROC_{50} score (see p. 165), was approximately 0.6–0.8 for 4 to 8 training sequences, compared to 0.95–0.96 using an evolutionary profile of 6 to 12 sequences. However, this family was one of the most difficult ones to model, and other families produced an ROC_{50} of 0.9 or better when trained by 20 or more sequences.

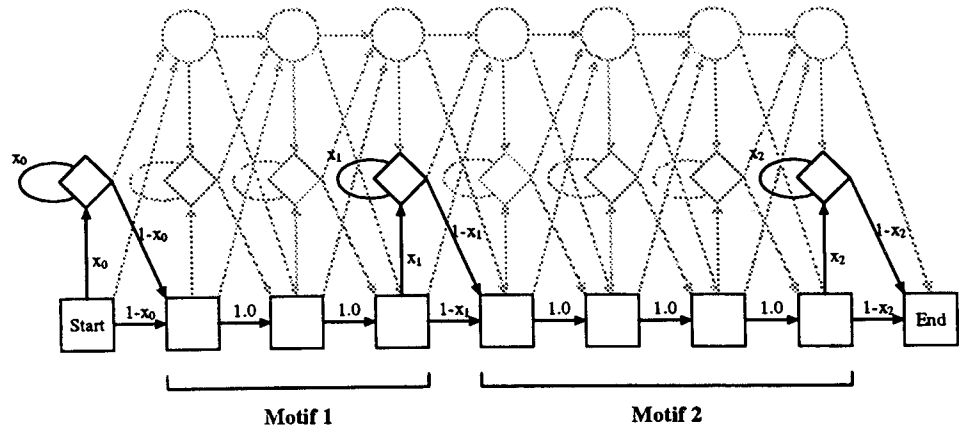

Figure 4.18. The HMM used by Meta-MEME to estimate motifs in sequences. (Reprinted, with permission of Oxford University Press, from Grundy et al. 1997.)

POSITION-SPECIFIC SCORING MATRICES

Analysis of msas for conserved blocks of sequence leads to production of the position-specific scoring matrix, or PSSM. An example of a PSSM produced by the MEME Web site is shown in Figure 4.15G. The PSSM may be used to search a sequence to obtain the most probable location or locations of the motif represented by the PSSM. Alternatively, the PSSM may be used to search an entire database to identify additional sequences that also have the same motif. Consequently, it is important to make the PSSM as representative of the expected sites as possible. The quality and quantity of information provided by the PSSM also varies for each column in the motif, and this variation profoundly influences the matches found with sequences. This situation can be accurately described by information theory, and the results can be displayed by a colored graph called a sequence logo (see Fig. 4.19).

The PSSM is constructed by a simple logarithmic transformation of a matrix giving the frequency of each amino acid in the motif. Two considerations arise in trying to tune the PSSM so that it adequately represents the training sequences. First, if the number of sequences with the found motif is large and reasonably diverse, the sequences represent a good statistical sampling of all sequences that are ever likely to be found with that same motif. If a given column in 20 sequences has only isoleucine, it is not very likely that a different amino acid will be found in other sequences with that motif because the residue is probably important for function. In contrast, another column in the motif from the 20 sequences may have several amino acids, and some amino acids may not be represented at all. Even more variation may be expected at that position in other sequences, although the more abundant amino acids already found in that column would probably be favored. Thus, if a good sampling of sequences is available, the number of sequences is sufficiently large, and the motif structure is not too complex, it should, in principle, be possible to obtain frequencies highly representative of the same motif in other sequences also (Henikoff and Henikoff 1996; Sjölander et al. 1996).

However, the number of sequences for producing the motif may be small, highly diverse, or complex, giving rise to a second level of consideration. If the data set is small, then unless the motif has almost identical amino acids in each column, the column frequencies in the motif may not be highly representative of all other occurrences of the motif. In such cases,

it is desirable to improve the estimates of the amino acid frequencies by adding extra amino acid counts, called pseudocounts, to obtain a more reasonable distribution of amino acid frequencies in the column. Knowing how many counts to add is a difficult but fortunately solvable problem. On the one hand, if too many pseudocounts are added in comparison to real sequence counts, the pseudocounts will become the dominant influence in the amino acid frequencies, and searches using the motif will not work. On the other hand, if there are relatively few real counts, many amino acid variations may not be present because of the small sample of sequences. The resulting matrix would then only be useful for finding the sequences used to produce the motif. In such a case, the pseudocounts will broaden the evolutionary reach of the profile to variations in other sequences. Even in this case, the pseudocounts should not drown out but serve to augment the influence of the real counts. In summary, relatively few pseudocounts should be added when there is a good sampling of sequences, and more should be added when the data are more sparse.

The goal of adding pseudocounts is to obtain an improved estimate of the probability p_{ca} that amino acid a is in column c in all occurrences of the blocks, and not just the ones in the present sample. The current estimate of p_{ca} is f_{ca}, the frequency of counts in the data. A simplified Bayesian prediction improves the estimate of p_{ca} by adding prior information in the form of pseudocounts (Henikoff and Henikoff 1996):

$$p_{ca} = (n_{ca} + b_{ca}) / (N_c + B_c) \tag{7}$$

where n_{ca} and b_{ca} are the real counts and pseudocounts, respectively, of amino acid a in column c, N_c and B_c are the total number of real counts and pseudocounts, respectively, in the column, and $f_{ca} = n_{ca} / N_c$. It is obvious that as b_{ca} becomes larger, the pseudocounts will have a greater infuence on p_{ca}. Furthermore, not only the types of pseudocounts but also the total number added to the column (B_c) will influence p_{ca}. Finally, fractions such as p_{ca} are used to produce the log odds form of the motif matrix, the PSSM, which is the most suitable representation of the data for sequence comparisons. A count and probability of zero for an amino acid a in a given column, which is quite common in blocks, may not be converted to logarithms. Addition of a small number of b_{ca} will correct this problem without producing a major change in the PSSM values. An equation similar to Equation 7 is used in the Gibbs sampler (p. 177), except that the number of sequences is $N - 1$.

Pseudocounts are added based on simple formulas or on the previous variations seen in aligned sequences. The amino acid substitution matrices, including the Dayhoff PAM and BLOSUM matrices, provide one source of information on amino acid variation. Another source is the Dirichlet mixtures derived as a posterior probability distribution from the amino acid substitutions observed in the BLOCKS database (see HMMs; Sjölander et al. 1996).

One simple formula that has worked well in some studies is to make B in Equation 7 equal to $\sqrt{N}$, where N is the number of sequences, and to allot these counts to the amino acids in proportion to their frequencies in the sequences (Lawrence et al. 1993; Tatusov et al. 1997). As N increases, the influence of pseudocounts will decrease because $\sqrt{N}$ will increase more slowly. The main difficulties with this method are that it does not take into account known substitutions of amino acids in alignments and the observed amino acid variations from one column in the motif to the next, and it does not add enough pseudocounts when the number of sequences is small.

The information in scoring matrices may be used to produce an average sequence profile, as illustrated in Figure 4.12. Rather than count amino acids, the scoring table values are averaged between each possible 20 amino acids and those amino acids found in the col-

umn of the scoring matrix. Zero counts in a column are not a problem because amino acids not present are not used in the calculations. Because these averaging methods do not take into account the number of sequences in the block, they do not have the desirable effect of a reduced influence when there is a large number of sequences.

Another method of using the information from amino acid substitution matrices is to base pseudocounts on these matrices. Recall the log odds form of the matrices is derived by taking the logarithm of the frequency of substitution q_{ia} of amino acid i for amino acid a divided by the frequency of occurrence of amino acid a, p_a. Then, b_{ca} may be estimated from the total number of pseudocounts in the column by (Henikoff and Henikoff 1996),

$$b_{ca} = B_c Q_i \text{ where } Q_i = \sum_{\text{all } i} q_{ia} \tag{8}$$

b_{ca} in column c can also be made to depend on the observed data in that column (Tatusov et al. 1997), which is given by multiplying B_c by the following conditional probabilities.

$$\begin{aligned} b_{ca} &= B_c \sum_{\text{all } i} \text{prob (amino acid } i|\text{column } c) \times \text{prob (amino acid } a|i) \\ &= B_c \sum_{\text{all } i} (n_{ci}/N_c \times q_{ia}/Q_i) \end{aligned} \tag{9}$$

where n_{ci} is the real count of amino acid i in column c.

The total number of pseudocounts in each column needs also to be estimated. As described above, one estimate is to make B_c for each column equal to $\sqrt{N}$, where N is the number of sequences, but this method does not take into account the differences between columns and, for a small number of sequences, the total number of pseudocounts is not sufficient. Allowing B_c to be a constant that can exceed N_c overcomes this limitation but still does not take into account variations in amino acid frequencies between columns, such that a column with conserved amino acids should receive fewer pseudocounts. Using the number of different amino acids in column c, R_c , as an indicator, B_c has been estimated by the formula (Henikoff and Henikoff 1996)

$$B_c = m \times R_c \tag{10}$$

where m is a positive number derived from trial database searches and $m \leq m \times B_c \leq \min(m \times N_c, m/20)$ (the latter term meaning the minimum of the two given values). By this formula and a given value of m, when $N_c \leq m \times 20$, the total number of pseudocounts B_c is greater, and when $N_c > m \times 20$, B_c is smaller than the total number of real counts, N_c, regardless of the value of R_c. The number of pseudocounts is also reduced when $R_c = 1$. In a test search of the SwissProt and Prosite catalogs with various values of m, a value of 5–6 for m produced the most efficient PSSMs for finding known family members. Of the several methods for making PSSMs discussed above, the one with pseudocounts derived by Equations 9 and 10 was most successful. This search was performed with PSSMs derived from blocks with amino acid counts also weighted to account for redundancy (Henikoff and Henikoff 1996). However, pseudocounts added from Dirichlet mixtures, which also

vary in each column of the scoring matrix, are also very effective (Henikoff and Henikoff 1996; Tatusov et al. 1997).

Once pseudocounts have been added to real counts of amino acids in each column of the motif, the PSSM may be calculated. The PSSM has one column (or row) for each position in the motif and one row (or column) for each amino acid, and the entries are log odds entries. Each entry is derived by taking the logarithm to the base 2 (bit units, but sometimes also natural logarithms in nat units are used) of the total of the real counts plus pseudocounts for each amino acid, divided by the probability of that amino acid (b_{ca} / N_c). An example of a PSSM produced by MEME is shown in Figure 4.15G.

As a sequence is searched with the PSSM, the value of the first amino acid in the sequence is looked up in the first column of the PSSM, then the value of the second amino acid in the matrix, and so on, until the length scanned is the same as the motif width represented by the matrix. All the log odds scores are added to produce a summed score for start position 1 in the sequence. The process is repeated starting at the second position in the sequence, and so on, until there is not enough sequence left. The highest log odds scoring sequence positions have the closest match statistically to the PSSM. Adding logarithms in this manner is the equivalent of mutiplying the probabilities of the amino acids at each sequence position. To convert each summed log odds score (S) to a likelihood or odds score of the sequence matching the PSSM, use the formula odds score = 2^S. These odds scores may be summed and each individual score divided by the sum to normalize them and to thereby produce a probability of the motif at each sequence location.

The above description and example are of using a PSSM to define motifs in protein families. PSSM are also used to define DNA sequence patterns that define regulatory sites, such as promoters or exon–intron junctions in genomic sequences. These topics are discussed in Chapter 8.

Information Content of the PSSM

The usefulness of a PSSM in distinguishing real sequence patterns from background may be measured. The unit of measure is the information content in bits. The PSSM described above gives the log odds score for finding a particular matching amino acid in a target sequence corresponding to each motif position. Variations in the scores found in each column of the table are an indication of the amino acid variation in the original training sequences that were used to produce the motif. In some columns, only one amino acid may have been present, whereas in others several may have been present. The columns with highly conserved positions have more information than do the variable columns and will be more definitive for locating matches in target sequences. There is a formal method known as information theory for describing the amount of information in each column that is useful for evaluating each PSSM. The information content of a given amino acid substitution matrix was previously introduced (p. 83) and is discussed in greater detail here. T. Schneider has prepared a Web site that gives excellent tutorials and a review on the topic of information theory, along with methods to produce sequence logos (Schneider and Stephens 1990) at http://www-lmmb.ncifcrf.gov/~toms/sequencelogo. html.

To illustrate the concepts of information and uncertainty (see above Web site), consider 64 cups in a row with an object hidden under one of them. The goal is to find the object with as few questions as possible. The solution is quite simple. First, ask whether the object is hidden under the first or second half of the cups. If the answer is the first 32, then ask which half of that 32, the first 16 or the second 16, and so on. The sequential questions reduce the possibilities from 64-32-16-8-4-2-1, and six questions will therefore suffice to locate the object. This number is also a measure of the amount of uncertainty in the data

because this number of questions must be asked to find the object. After the first question has been asked, uncertainty has been reduced by 1, so that only five questions then need to be asked to find the object. The uncertainty is zero when the object is found.

A method to calculate uncertainty (the number of questions to be asked) may be derived from the probability of finding the object under a given cup [p(object) = 1/64]. Uncertainty is found by taking the negative logarithm to the base 2 of 1/64 [$-\log_2(1/64) = 6$ bits]. A situation similar to the hidden object example is found with amino acids in the columns of a PSSM. Here, the interest is to find which amino acid belongs at a particular column in the motif. When we have no information at all, since there are 20 possible choices in all, the amount of uncertainty is $\log_2 20 = 4.32$.

The data from the PSSM provide information that reduces this uncertainty. If only one amino acid is observed in a column of the PSSM, the uncertainty is zero because there are no other possibilities. If two amino acids are observed with equal frequency, there is still uncertainty as to which one it is, and one question must be asked to find the answer, or uncertainty = 1. The formula for finding the uncertainty in this example is the sum of the fractional information provided by each amino acid, or $-[0.5 \times \log_2 0.5 + 0.5 \times \log_2 0.5] = 1$. In general, the average amount of uncertainty (H_c) in bits per symbol for column c of the PSSM is given by

$$H_c = -\sum_{\text{all } i} p_{ic} \log_2(p_{ic}) \tag{11}$$

where p_{ic} is the frequency of amino acid i in column c and is estimated by the frequency of occurrence of each amino acid (b_{ca}/N_c) and $\log_2(p_{ic})$ is the log odds score for each amino acid in column c. Uncertainty for the entire PSSM may then be calculated as

$$H = \sum_{\text{all columns}} H_c \tag{12}$$

H is also known as the entropy of the PSSM position in information theory because the higher the value, the greater the uncertainty. The lower the value of the uncertainty H for the PSSM, the greater the ability of the PSSM to distinguish real occurrences of the motif from random matches. Conversely, the higher the information content, calculated as shown below, the more useful the PSSM.

Sequence Logos

Sequence logos are graphs that illustrate the amount of information in each column of a motif. The logo is derived from sequence information in the PSSM described above. Conserved patterns in both protein and DNA sequences can be represented by sequence logos. A program for producing logos, along with several examples, is available from http://www-lmmb.ncifcrf.gov/~toms/sequencelogo.html. The Web site of S.E. Brenner at http://www.bio.cam.ac.uk/seqlogo/ will produce sequence logos from an input alignment using the Gibbs sampler method, and an implementation of an extension of the logo method for structural RNA alignment (Gorodkin et al. 1997) is at http://www.cbs.dtu.dk/gorodkin/appl/plogo.html. A logo representation for the BLOCKS database has been implemented (Henikoff et al. 1995) and may be viewed when the information on a partic-

ular block is retrieved from the BLOCKS Web server (http://www.blocks.fhcrc.org/). An example of a Block logo is shown in Figure 4.19. Another example of a simple graph of information content is given in Figure 4.15C. In this case, the information for the entire motif has been calculated by the MEME server by summing the values in each column to a total value of 22 bits. Although logos are primarily used with ungapped motifs and sequence patterns, logos of alignments that include gaps in some sequence positions may also be made. If such is the case, then the height of the column with gaps is reduced by the proportion of sequence positions that are not gaps.

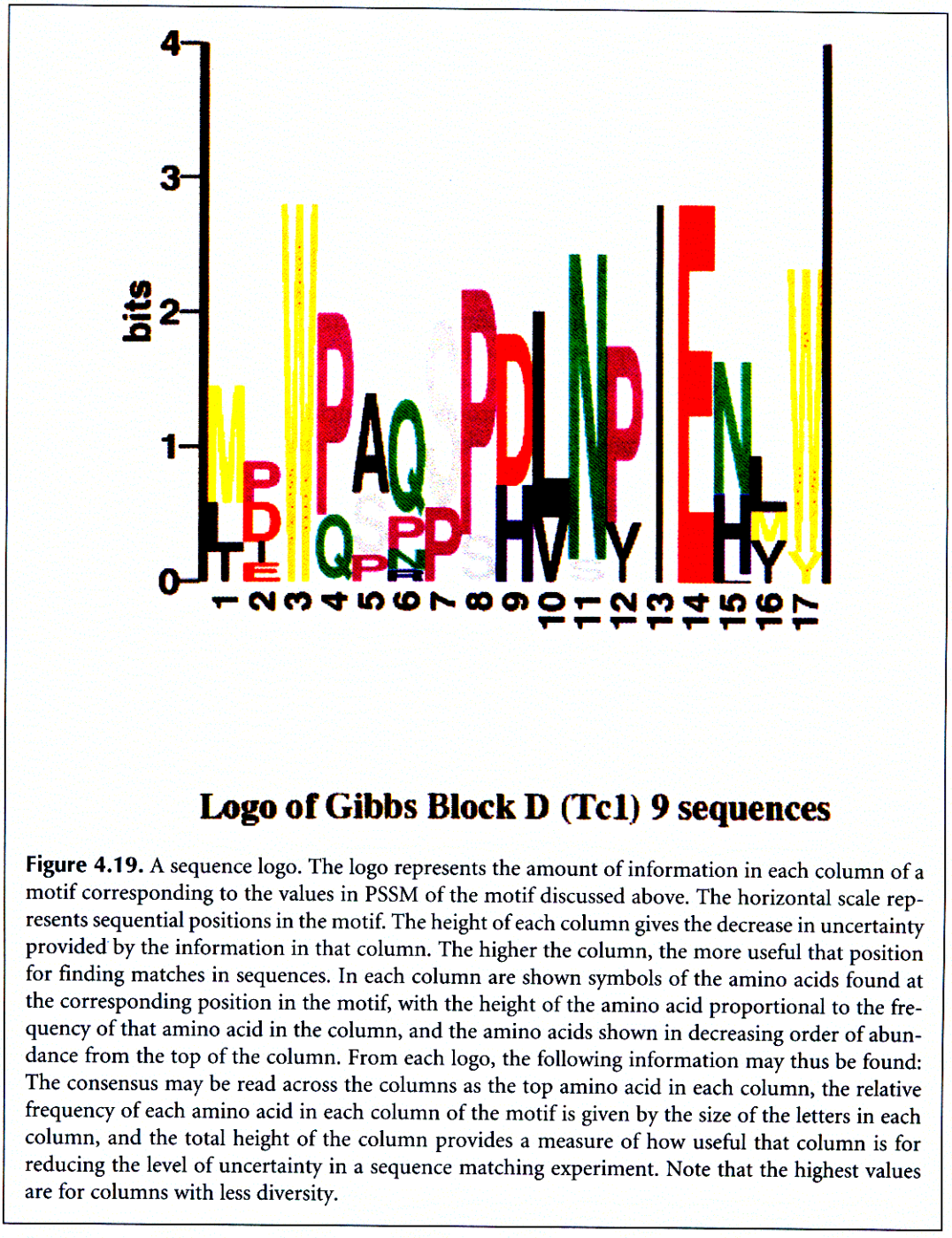

Figure 4.19. A sequence logo. The logo represents the amount of information in each column of a motif corresponding to the values in PSSM of the motif discussed above. The horizontal scale represents sequential positions in the motif. The height of each column gives the decrease in uncertainty provided by the information in that column. The higher the column, the more useful that position for finding matches in sequences. In each column are shown symbols of the amino acids found at the corresponding position in the motif, with the height of the amino acid proportional to the frequency of that amino acid in the column, and the amino acids shown in decreasing order of abundance from the top of the column. From each logo, the following information may thus be found: The consensus may be read across the columns as the top amino acid in each column, the relative frequency of each amino acid in each column of the motif is given by the size of the letters in each column, and the total height of the column provides a measure of how useful that column is for reducing the level of uncertainty in a sequence matching experiment. Note that the highest values are for columns with less diversity.

The height of each logo position is calculated as the amount by which uncertainty has been decreased by the available data; in this case, the amino acid frequencies in each column of the motif. The relative heights of each amino acid within each column are calculated by determining how much each amino acid has contributed to that decrease. The uncertainty at column c is given by Equation 11. Because the maximum uncertainty at a position/column when no information is available is $\log_2 20 = 4.32$, as more information about the motif is obtained by new data, the decrease in uncertainty (or increase in the amount of information) R_c is

$$R_c = \log_2 20 - (H_c + \epsilon_n) \tag{13}$$

where H_c is given by Equation 11 and ϵ_n is a correction factor for a small sequence number n. R_c is used as the total height of the logo column. The height of amino acid a at position c in the motif logo is then given by $f_{ac} \times R_c$.

The above description applies to protein sequences. Sequence logos are also produced for DNA sequences. The methodology is very similar to the above except that there are only four possible choices for each logo location. Hence, the maximum amount of uncertainty is $\log_2 4 = 2$. The above method assumes that the sequence pattern is less random than the background or expected sequence variation, and this assumption limits the ability of the method to locate subtle patterns in sequences.

An improved method for finding more subtle patterns in sequences is called the relative entropy method (Durbin et al. 1998). In this case, differences between the observed frequencies and background frequencies are used (Gorodkin et al. 1997), and the decrease in uncertainty from background to observed (or amount of information) in bits is given by

$$R_c = \sum_{\text{all } i} p_{ic} \log_2 (p_{ic}/b_i) \tag{14}$$

where b_i is the background frequency of residue i in the organism and the maximum uncertainty in column c is given by $-\Sigma_{\text{all } i} [p_{ic} \log_2 (1/b_i)]$. When background frequencies are taken into account, and the column frequency is less than the background frequency, it is possible for the information given by a particular residue in a logo column to be negative. To accommodate this change, the corresponding sequence character is inverted in the logo to indicate a less than expected frequency. There are also two ways used to illustrate the contribution of each character through the height of the symbol. The first method is described above. The second method is to display symbol heights in proportion to the ratio of the observed to the expected frequency, i.e., by the fraction $(p_{ic}/b_i) / (\Sigma_{\text{all } i} p_{ic}/b_i)$ for each symbol i. Gaps are included in the analysis by using $p_{\text{gap}} = 1$ and, as a result, will always give a negative contribution to the information (Gorodkin et al. 1997).

MULTIPLE SEQUENCE ALIGNMENT EDITORS AND FORMATTERS

Once a multiple sequence alignment has been obtained by the global msa program, it may be necessary to edit the sequence manually to obtain a more reasonable or expected alignment. Several considerations must be kept in mind when choosing a sequence editor, which should include as many of the following features as possible: (1) provision for displaying the sequence on a color monitor with residue colors to aid in a clear visual repre-

sentation of the alignment, (2) recognition of the multiple sequence format that was output by the msa program and maintenance of the alignment in a suitable format when the editing is completed, (3) provision of a suitable windows interface, allowing use of the mouse to add, delete, or move sequence followed by an updated display of the alignment. In addition, there are other types of editing that are commonly performed on msas such as, for example, shading conserved residues in the alignment.

The large number of multiple sequence alignment formats that are in use were discussed in Chapter 2. Two commonly encountered examples are the Genetics Computer Group's MSF format and the CLUSTALW ALN format. Because these formats follow a precise outline, one may be readily converted to another by computer programs. READSEQ by D.G. Gilbert at Indiana University at Bloomington is one such program. This program will run on almost any computer platform and may be obtained by anonymous FTP from ftp.bio.indiana.edu/molbio/readseq. There is also a Web-based interface for READSEQ from Baylor College of Medicine at http://dot.imgen.bcm.tmc.edu:9331/seq-util/seq-util.html/. A software package SEQIO, which provides C program modules for conversion of sequence files from one format to another, is available by anonymous FTP from ftp.pasteur.fr/pub/GenSoft/unix/programming/seqio-1.2.tar.gz; documentation is available at http://bioweb.pasteur.fr/docs/doc-gensoft/seqio/.

A short list of the many available programs that have or exceed the above-listed features is discussed below. For a more comprehensive list, visit the catalog of software page at Web address http://www.ebi.ac.uk/biocat/.

Sequence Editors

1. CINEMA (Colour Interactive Editor for Multiple Alignments) at http://www.biochem.ucl.ac.uk/bsm/dbbrowser/CINEMA2.02/kit.html is a broadly functional program for sequence editing and analysis, including dot matrix analysis. It features drag-and-drop editing, sequence shifting to left or right, viewing of different parts of an alignment using the split-screen option, multiple motif selection and manipulation, and a number of added features such as viewing of protein structures. CINEMA was developed by A.W.R. Payne, D.J. Parry-Smith, A.D. Michie, and T.K. Attwood. CINEMA is an applet that runs under a Web browser and therefore will run on almost any computer platform.
2. GDE (Genetic Data Environment) provides a general interface on UNIX machines for sequence analysis, sequence alignment editing, and display (Smith et al. 1994) and is available from several anonymous FTP sites including ftp.ebi.ac.uk/pub/software/unix. GDE is described at http://bimas.dcrt.nih.gov/gde_sw.html, and http://www.tigr.org/~jeisen/GDE/GDE.html. GDE features are incorporated into the Seqlab interface for the GCG software, vers. 9. This interface requires communication with a host UNIX machine running the Genetics Computer Group software. Interface with MS-DOS or Macintosh is possible if the computer is equipped with the appropriate X-Windows client software.
3. GeneDoc is an alignment editing and display editor by K. Nicholas and H. Nicholas of the Pittsburgh Supercomputing Center for MSF-formatted msas. It can also import files in other formats. GeneDoc can move residues by inserting or deleting gap, and features drag-and-drop editing. As the alignment is edited, a new alignment score is calculated by sum of pairs method or based on a phylogenetic tree. GeneDoc is available from http://www.psc.edu/biomed/genedoc/ and runs under MS Windows.
4. MACAW is both a local multiple sequence alignment program and a sequence editing tool (Schuler et al. 1991). Given a set of sequences, the program finds ungapped blocks in the sequences and gives their statistical significance. Later versions of the program

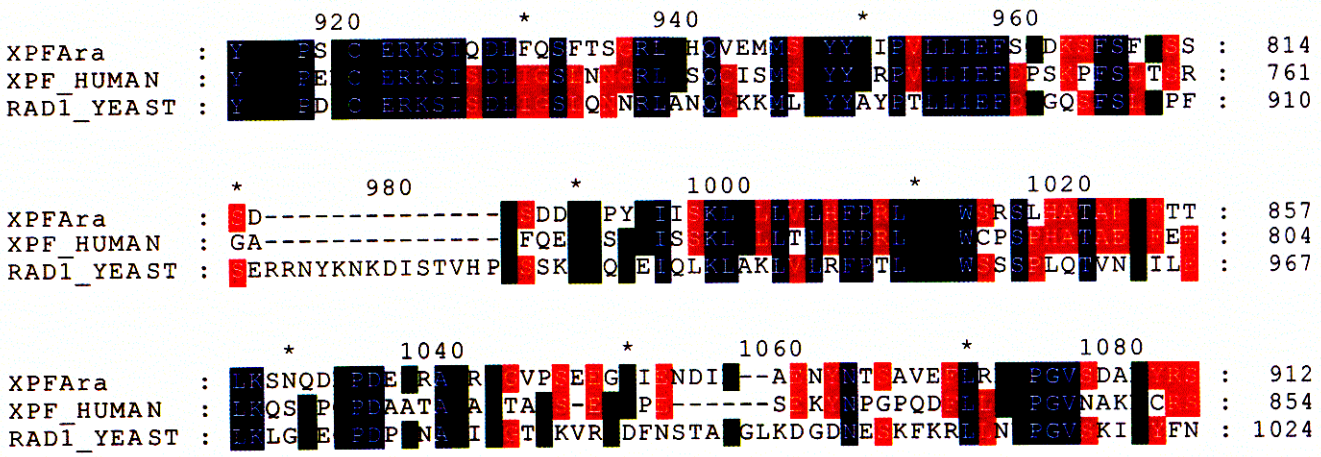

Figure 4.20. GeneDoc, a multiple sequence alignment editor with many useful features. Shown is an illustrative multiple sequence alignment of three DNA repair genes similar to the *S. cerevisiae Rad1* gene. The sequences were aligned with *CLUSTALW*, and the FASTA-formatted alignment (Chapter 2) was imported into GeneDoc on a PC.

find blocks by one of three user-chosen methods: by searching for maximum segment pairs or common patterns present in the sequences scored by a scoring matrix such as PAM250 or BLOSUM matrices (the methods used by the BLAST algorithm), by using the Gibbs sampling strategy, a statistical method, or by searching for user-provided patterns provided in a particular format called a regular expression. Executable programs that run under MS-DOS Windows, Macintosh, and other computer platforms are available by anonymous FTP from ncbi.nlm.nih.gov/pub/schuler/macaw.

Sequence Formatters

1. Boxshade is a formatting program by K. Hofmann for marking identical or similar residues in msas with shaded boxes, and is available by anonymous FTP from http://www.isrec.isb-sib.ch/sib-isrec/boxshade. The Web server at http://www.ch.embnet.org/software/BOX_form.html takes a multiple-alignment file in either the Genetics Computer Group MSF format or CLUSTAL ALN format and can output a file in many forms including Postscript/EPS and PICT for editing on Macintosh and MS-DOS machines.
2. CLUSTALX is a sequence formatting tool that provides a Windows interface for a CLUSTALW msa and is available for many computer platforms, including MS-DOS and Macintosh machines by anonymous FTP from ftp-igbmc.u-strasbg.fr/pub/ClustalX/ (Thompson et al. 1997).

REFERENCES

Altschul S.F. 1989. Gap costs for multiple sequence alignment. *J. Theor. Biol.* **138:** 297–309.

Altschul S.F., Carroll R.J., and Lipman D.J. 1989. Weights for data related by a tree. *J. Mol. Biol.* **207:** 647–653.

Bailey T.L. and Elkan C. 1995. The value of prior knowledge in discovering motifs with MEME. In *Pro-*

ceedings of the 3rd International Conference on Intelligent Systems for Molecular Biology (ed. C. Rawlings et al.), pp. 21–29. AAAI Press, Menlo Park, California.

Bailey T.L. and Gribskov M. 1997. Score distributions for simultaneous matching to multiple motifs. *J. Comput. Biol.* **4:** 45–59.

———. 1998. Methods and statistics for combining motif match searches. *J. Comput. Biol.* **5:** 211–221.

Bairoch A. 1991. PROSITE: A dictionary of sites and patterns in proteins. *Nucleic Acids Res.* (suppl.) **19:** 2241–2245.

Baldi P., Chauvin Y., Hunkapillar T., and McClure M.A. 1994. Hidden Markov models of biological primary sequence information. *Proc. Natl. Acad. Sci.* **91:** 1059-1063.

Barton G.J. 1994. The AMPS package for multiple protein sequence alignment. Computer analysis of sequence data, part II. *Methods Mol. Biol.* **25:** 327–347.

Baylor T.L. and Gribskov M. 1996. The megaprior heuristic for discovering protein sequence patterns. In *Proceedings of the 4th International Conference on Intelligent Systems for Molecular Biology* (ed. D.J. States et al.), pp. 15–24. AAAI Press, Menlo Park, California.

Boguski M., Hardison R.C., Schwartz S., and Miller W. 1992. Analysis of conserved domains and sequence motifs in cellular regulatory proteins and locus control regions using software tools for multiple alignment and visualization. *New Biol.* **4:** 247–260.

Briffeuil P., Baudoux G., Reginster I., Debolle X., Depiereux E., and Feytmans E. 1998. Comparative analysis of seven multiple protein sequence alignment servers: Clues to enhance reliability of predictions. *Bioinformatics* **14:** 357–366.

Cardon L.R. and Stormo G.D. 1992. Expectation maximization algorithm for identifying protein-binding sites with variable lengths from unaligned DNA fragments. *J. Mol. Biol.* **223:** 159–170.

Carlin B.P. and Louis T.A. 1996. *Bayes and empirical Bayes methods for data analysis* (*Monographs on statistics and applied probability* [ed. D.R. Cox et al.]). Chapman and Hall, New York.

Carrillo H. and Lipman D. 1988. The multiple sequence alignment problem in biology. *SIAM J. Appl. Math.* **48:** 197–209.

Churchill G.A. 1989. Stochastic models for heterogeneous DNA sequences. *Bull. Math. Biol.* **51:** 79–94.

Corpet F. 1988. Multiple sequence alignment with hierarchical clustering. *Nucleic Acids Res.* **16:** 10881–10890.

Dayhoff M.O. 1978. Survey of new data and computer methods of analysis. In *Atlas of protein sequence and structure,* vol. 5, suppl. 3. National Biomedical Research Foundation, Georgetown University, Washington, D.C.

Durbin R., Eddy S., Krogh A., and Mitchison G. 1998. *Biological sequence analysis: Probabilistic models of proteins and nucleic acids.* Cambridge University Press, United Kingdom.

Eddy S.R. 1995. Multiple alignment using hidden Markov models. *Ismb* **3:** 114–120.

———. 1996. Hidden Markov models. *Curr. Opin. Struct. Biol.* **6:** 361–365.

———. 1998. Profile hidden Markov models. *Bioinformatics* **14:** 755–763.

Eddy S.R., Mitchison G., Durbin R. 1995. Maximum discrimination hidden Markov models of sequence consensus. *J. Comput. Biol.* **2:** 9–23.

Feng D.F. and Doolittle R.F. 1987. Progressive sequence alignment as a prerequisite to correct phylogenetic trees. *J. Mol. Evol.* **25:** 351–360.

———. 1996. Progressive alignment of amino acid sequences and construction of phylogenetic trees from them. *Methods Enzymol.* **266:** 368–382.

Gorodkin J., Heyer L.J., Brunak S., and Stormo G.D. 1997. Displaying the information contents of structural RNA alignments: The structure logos. *Comput. Appl. Biosci.* **13:** 583–586.

Gotoh O. 1994. Further improvement in methods of group-to-group sequence alignment with generalized profile operations. *Comput. Appl. Biosci.* **10:** 379–387.

———. 1995. A weighting system and algorithm for aligning many phylogenetically related sequences. *Comput. Appl. Biosci.* **11:** 543–551.

———. 1996. Significant improvement in accuracy of multiple protein sequence alignments by iterative refinement as assessed by reference to structural alignments. *J. Mol. Biol.* **264:** 823–838.

———. 1999. Multiple sequence alignment: Algorithms and applications. *Adv. Biophys.* **36:** 159–206.

Gribskov M. and Veretnik S. 1996. Identification of sequence patterns with profile analysis. *Methods Enzymol.* **266:** 198–212.

Gribskov M., Luethy R., and Eisenberg D. 1990. Profile analysis. *Methods Enzymol.* **183:** 146–159.

Gribskov M., McLachlan A.D., and Eisenberg D. 1987. Profile analysis: Detection of distantly related proteins. *Proc. Natl. Acad. Sci.* **84:** 4355–4358.

Grundy W.N., Bailey T.L., and Elkan C.P. 1996. Para-MEME: A parallel implementation and a web interface for a DNA and protein motif discovery tool. *Comput. Appl. Biosci.* **12:** 303–310.

Grundy W.N., Bailey T.L., Elkan C.P., and Baker M.E. 1997. Meta-MEME: Motif-based hidden Markov models of protein families. *Comput. Appl. Biosci.* **13:** 397–406.

Gupta S.K., Kececioglu J.D., and Schaffer A.A. 1995. Improving the practical space and time efficiency of the shortest-paths approach to sum-of-pairs multiple sequence alignment. *J. Comput. Biol.* **2:** 459–472.

Hein J. 1990. Unified approach to alignment and phylogenies. *Methods Enzymol.* **183:** 626–645.

Henikoff J.G. and Henikoff S. 1996. Using substitution probabilities to improve position-specific scoring matrices. *Comput. Appl. Biosci.* **12:** 135–143.

Henikoff S. and Henikoff J.G. 1991. Automated assembly of protein blocks for database searching. *Nucleic Acids Res.* **19:** 6565–6572.

———. 1992. Amino acid substitution matrices from protein blocks. *Proc. Natl. Acad. Sci.* **89:** 10915–10919.

Henikoff S., Henikoff J.G., Alford W.J., and Pietrokovski S. 1995. Automated construction and graphical presentation of protein blocks from unaligned sequences. *Gene* **163:** GC17–GC26.

Heringa J. 1999. Two strategies for sequence comparison: Profile-preprocessed and secondary structure-induced multiple alignment. *Comput. Chem.* **23:** 341–364.

Higgins D.G. and Sharp P.M. 1988. CLUSTAL: A package for performing multiple sequence alignment on a microcomputer. *Gene* **73:** 237–244.

Higgins D.G., Thompson J.D., and Gibson T.J. 1996. Using CLUSTAL for multiple sequence alignments. *Methods Enzymol.* **266:** 383–402.

Hirosawa M., Totoki Y., Hoshida M., and Ishikawa M. 1995. Comprehensive study on iterative algorithms of multiple sequence alignment. *Comput. Appl. Biosci.* **11:** 13–18.

Hughey R. and Krogh A. 1996. Hidden Markov models for sequence analysis: Extension and analysis of the basic method. *Comput. Appl. Biosci.* **12:** 95–107.

Jonassen I., Collins J.F., and Higgins D. 1995. Finding flexible patterns in unaligned protein sequences. *Protein Sci.* **4:** 1587–1595.

Karplus K. 1995. Regularizers for estimating the distributions of amino acids from small samples. In *UCSC Technical Report* (UCSC-CRL-95-11). University of California, Santa Cruz.

Kececioglu J. 1993. The maximum weight trace problem in multiple sequence alignment. In *Proceedings of the 4th Symposium on Combinatorial Pattern Matching: Lecture notes in computer science*, no. 684, pp. 106–119. Springer Verlag, New York.

Kececioglu J., Lehof H.-P., Mehlhorn K., Mutzel P., Reinert K., and Vingron M. 2000. A polyhedral approach to sequence alignment problems. *Discrete Appl. Math.* **104:** 143–186.

Kim J., Pramanik S., and Chung M.J. 1994. Multiple sequence alignment by simulated annealing. *Comput. Appl. Biosci.* **10:** 419–426.

Krogh A., Brown M., Mian I.S., Sjölander K., and Haussler D. 1994. Hidden Markov models in computational biology. Applications to protein modeling. *J. Mol. Biol.* **235:** 1501–1531.

Lawrence C.E. and Reilly A.A. 1990. An expectation maximization (EM) algorithm for the identification and characterization of common sites in unaligned biopolymer sequences. *Proteins Struct. Funct. Genet.* **7:** 41–51.

Lawrence C.E., Altschul S.F., Boguski M.S., Liu J.S., Neuwald A.F., and Wootton J.C. 1993. Detecting subtle sequence signals: A Gibbs sampling strategy for multiple alignment. *Science* **262:** 208–214.

Lipman D.J., Altschul S.F., and Kececioglu J.D. 1989. A tool for multiple sequence alignment. *Proc. Natl. Acad. Sci.* **86:** 4412–4415.

Liu J.S., Neuwald A.F., and Lawrence C.E. 1995. Alignment and Gibbs sampling strategies. *J. Am. Stat. Assoc.* **90:** 1156–1170.

McClure M.A., Vasi T.K., and Fitch W.M. 1994. Comparative analysis of multiple protein-sequence alignment methods. *Mol. Biol. Evol.* **11:** 571-592.

Miller M.J. and Powell J.I. 1994. A quantitative comparison of DNA sequence assembly programs. *J. Comput. Biol.* **1:** 257–269.

Miller W., Boguski M., Raghavachari B., Zhang Z., and Hardison R.C. 1994. Constructing aligned sequence blocks. *J. Comput. Biol.* **1:** 51–64.

Mitchison G.J. and Durbin R.M. 1995. Tree-based maximal likelihood substitution matrices and hidden Markov models. *J. Mol. Evol.* **41:** 1139–1151.

Morgenstern B., Dress A., and Werner T. 1996. Multiple DNA and protein sequence alignment based on segment-to-segment comparison. *Proc. Natl. Acad. Sci.* **93:** 12098–12103.

Morgenstern B., Frech K., Dress A., and Werner T. 1998. DIALIGN: Finding local similarities by multiple sequence alignment. *Bioinformatics* **14:** 290–294.

Myers E.W. 1995. Toward simplifying and accurately formulating fragment assembly. *J. Comput. Biol.* **2:** 275–290.

Myers E.W. and Miller W. 1988. Optimal alignments in linear space. *Comput. Appl. Biosci.* **4:** 11–17.

Neuwald A.F. and Green P. 1994. Detecting patterns in protein sequences. *J. Mol. Biol.* **239:** 698–712.

Neuwald A.F., Liu J.S., and Lawrence C.E. 1995. Gibbs motif sampling: Detection of bacterial outer membrane protein repeats. *Protein Sci.* **4:** 1618–1632.

Nevill-Manning C.G., Wu T.D., and Brutlag D.L. 1998. Highly specific protein sequence motifs for genome analysis. *Proc. Natl. Acad. Sci.* **95:** 5865–5871.

Notredame C. and Higgins D.G. 1996. SAGA: Sequence alignment by genetic algorithm. *Nucleic Acids Res.* **24:** 1515–1524.

Notredame C., Holme L., and Higgins D.G. 1998. COFFEE: A new objective function for multiple sequence alignment. *Bioinformatics* **14:** 407–422.

Notredame C., O'Brien E.A., and Higgins D.G. 1997. RAGA: RNA sequence alignment by genetic algorithm. *Nucleic Acids Res.* **25:** 4570–4580.

Pascarella S. and Argos P. 1992. Analysis of insertions/deletions in protein sequences. *J. Mol. Biol.* **224:** 461–471.

Rabiner L.R. 1989. A tutorial on hidden Markov models and selected applications in speech recognition. *Proc. IEEE* **77:** 257–1531.

Ravi R. and Kececioglu J. 1998. Approximation algorithms for multiple sequence alignment under a fixed evolutionary tree. *Discrete Appl. Math.* **88:** 355–366.

Saitou N. and Nei M. 1987. The neighbor-joining method: A new method for reconstructing phylogenetic trees. *Mol. Biol. Evol.* **4:** 406–425.

Sankoff D. 1975. Minimal mutation trees of sequences. *SIAM J. Appl. Math.* **78:** 35–42.

Schneider T.D. and Stephens R.M. 1990. Sequence logos: A new way to display consensus sequences. *Nucleic Acids Res.* **18:** 6097–6100.

Schuler G.D., Altschul S.F., and Lipman D.J. 1991. A workbench for multiple alignment construction and analysis. *Proteins* **9:** 180–190.

Shapiro B. and Navetta J. 1994. A massively parallel genetic algorithm for RNA secondary structure prediction. *J. Supercomput.* **8:** 195–207.

Sjölander K., Karplus K., Brown M., Hughey R., Krogh A., Mian I.S., and Haussler D. 1996. Dirichlet mixtures: A method for improved detection of weak but significant protein sequence homology. *Comput. Appl. Biosci.* **12:** 327–345.

Smith H.O., Annau T.M., and Chandrasegaran S. 1990. Finding sequence motifs in groups of functionally related proteins. *Proc. Natl. Acad. Sci.* **87:** 826–830.

Smith R.F. and Smith T.F. 1992. Pattern-induced multi-sequence alignment (PIMA) algorithm employing secondary structure-dependent gap penalties for use in comparative protein modelling. *Protein Eng.* **5:** 35–41.

Smith S.W., Overbeek R., Woese C.R., Gilbert W., and Gillevet P.M. 1994. The genetic data environment and expandable GUI for multiple sequence analysis. *Comput. Appl. Biosci.* **10:** 671–675.

Sneath P.H.A. and Sokal R.R. 1973. *Numerical taxonomy.* W.H. Freeman, San Francisco, California.

Sonnhammer E.L., Eddy S.R., and Durbin R. 1997. Pfam: A comprehensive database of protein domain families based on seed alignments. *Proteins* **28:** 405–420.

Tatusov R.L., Altschul S.F., and Koonin E.V. 1994. Detection of conserved segments in proteins: Iterative scanning of sequence databases with alignment blocks. *Proc. Natl. Acad. Sci.* **91:** 12091–12095.

Tatusov R.L., Koonin E.V., and Lipman D.J. 1997. A genomic perspective on protein families. *Science* **278:** 631–637.

Taylor W.R. 1990. Hierarchical method to align large numbers of biological sequences. *Methods Enzymol.* **183:** 456–474.

———. 1996. Multiple protein sequence alignment: Algorithms and gap insertion. *Methods Enzymol.* **266:** 343–367.

Thompson J.D., Higgins D.G., and Gibson T.J. 1994a. CLUSTAL W: Improving the sensitivity of pro-

gressive multiple sequence alignment through sequence weighting, position-specific gap penalties and weight matrix choice. *Nucleic Acids Res.* **22:** 4673–4680.

———. 1994b. Improved sensitivity of profile searches through the use of sequence weights and gap excision. *Comput. Appl. Biosci.* **10:** 19–29.

Thompson J.D., Plewniak F., and Poch O. 1999. A comprehensive comparison of multiple sequence alignment programs. *Nucleic Acids Res.* **27:** 2682–2690.

Thompson J.D., Gibson T.J., Plewniak F., Jeanmougin F., and Higgins D.G. 1997. The CLUSTAL X windows interface: Flexible strategies for multiple sequence alignment aided by quality analysis tools. *Nucleic Acids Res.* **25:** 4876–4882.

Vingron M. and Argos P. 1991. Motif recognition and alignment for many sequences by comparison of dot matrices. *J. Mol. Biol.* **218:** 33–43.

Vingron M. and Sibbald P.R. 1993. Weighting in sequence space: A comparison of methods in terms of generalized sequences. *Proc. Natl. Acad. Sci.* **90:** 8777–8781.

Waterman M. and Perlwitz M.D. 1984. Line geometries for sequence comparisons. *Bull. Math. Biol.* **46:** 567–577.

Weber J.L. and Myers E.W. 1997. Human whole-genome shotgun sequencing. *Genome Res.* **7:** 401–409.

Zhang C. and Wong A.K. 1997. A genetic algorithm for multiple molecular sequence alignment. *Comput. Appl. Biosci.* **13:** 565–581.

Zhang Z., Raghavachari B., Hardison R.C., and Miller W. 1994. Chaining multiple-alignment blocks. *J. Comput. Biol.* **1:** 217–226.

CHAPTER 5

Prediction of RNA Secondary Structure

THE PREVIOUS TWO CHAPTERS DISCUSS the alignment of protein and nucleic acid sequences. The methods used either align entire sequences or search for common patterns in the sequences. In either case, the objective is to locate a set of sequence characters in the same order in the sequences. Nucleic acid sequences that specify RNA molecules have to be compared differently. Sequence variations in RNA sequences maintain base-pairing patterns that give rise to double-stranded regions (secondary structure) in the molecule. Thus, alignments of two sequences that specify the same RNA molecules will show covariation at interacting base-pair positions, as illustrated in Figure 5.1. In addition to these covariable positions, sequences of RNA-specifying genes may also have rows of similar sequence characters that reflect the common ancestry of the genes.

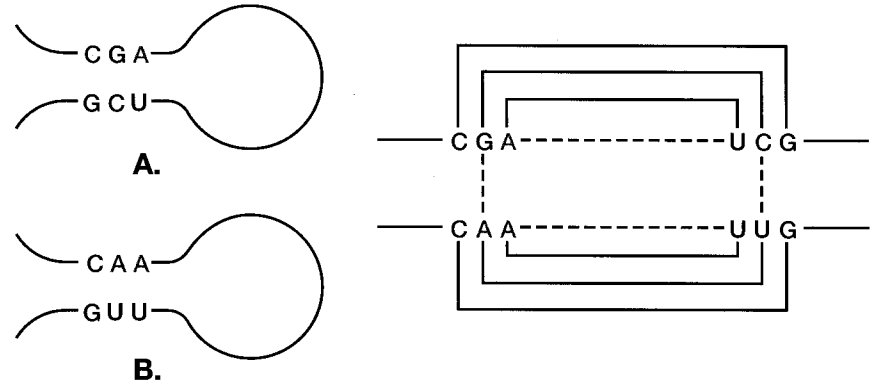

Figure 5.1. Complementary sequences in RNA molecules maintain RNA secondary structure. Shown is a simple stem-and-loop structure formed by the RNA strand folding back on itself. Molecule *A* depends on the presence of two complementary sequences CGA and UCG that are base-paired in the structure. In *B*, two sequence changes, G → A and C → U, which maintain the same structure, are present. Aligning RNA sequences required locating such regions of sequence covariation that are capable of maintaining base-pairing in the corresponding structure.

INTRODUCTION

As genomic sequences of organisms become available, it is important to be able to identify the various classes of genes, including the major class of genes that encodes RNA molecules. There are a large number of Web sites listed in Table 5.1 that provide programs

Table 5.1. *RNA databases and RNA analysis Web sites*

Site or resource	Web address	Reference
5S Ribosomal RNA data bank	http://rose.man.poznan.pl/5SData/ and mirrored at http://userpage.chemie.fu-berlin.de/fb_chemie/ibc/agerdmann/5S_rRNA.html	Szymanski et al. (1999)
5S rRNA database	http://www.bchs.uh.edu/~nzhou/temp/5snew.html	Shumyatsky and Reddy (1993)
Comparative RNA Web site	http://www.rna.icmb.utexas. edu/	see Web site
GenLang linguistic sequence analyzer	http://www.cbil.upenn.edu/	Dong and Searls (1994)
Gobase for mitochondrial sequences	http://alice.bch.umontreal.ca/genera/gobase/gobase.html	Korab-Laskowska et al. (1998)

Site or resource	Web address	Reference
Intron analysis—*Saccharomyces cerevisiae*	http://www.cse.ucsc.edu/research/compbio/yeast_introns.html	Spingola et al. (1999)
tRNA genes, higher plant mitochondria	ftp://ftp.ebi.ac.uk/pub/databases/plmitrna/	Ceci et al. (1999)
MFOLD minimum energy RNA configuration	http://bioinfo.math.rpi.edu/~zukerm/rna/	Zuker et al. (1991)
Nucleic acid database and structure resource	http://ndbserver.rutgers.edu/	Berman et al. (1998)
Pseudobase–pseudoknot database maintained by E. van Batenburg, Leiden University	http://wwwbio.leidenuniv.nl/~batenburg/pkb.html	see Web page
Ribonuclease P database Web site	http://jwbrown.mbio.ncsu.edu/RNaseP/home.html	Brown (1999)
Ribosomal RNA database project (RDP II)	http://www.cme.msu.edu/RDP/	Maidak et al. (1999)
Ribosomal RNA mutation databases	http://www.fandm.edu/Departments/Biology/Databases/RNA.html	Triman and Adams (1997)
RiboWeb Project–3D models of *E. coli* 30S ribosomal subunit and 16s rRNA	http://www-smi.stanford.edu/projects/helix/ribo3dmodels/index.html	Chen et al. (1997)
RNA aptamer sequence database (University of Texas)	http://speak.icmb.utexas.edu/ellington/aptamers.html	see Web site
RNA editing Web site, UCLA	http://www.lifesci.ucla.edu/RNA/index.html	Simpson et al. (1998)
RNA editing, uridine insertion/deletion	http://www.lifesci.ucla.edu/RNA/trypanosome/	Simpson et al. (1998)
RNA modification database	http://medlib.med.utah.edu/RNAmods/	Limbach et al. (1994); Rozenski et al. (1999)
RNA secondary structures, Group I introns, 16S rRNA, 23S rRNA	http://www.rna.icmb.utexas.edu	Gutell (1994); Schnare et al. (1996 and references therein)
RNA structure database	http://www.rnabase.org/	see Web page
RNA world at IMB Jena	http://www.imb-jena.de/RNA.html	Sühnel (1997)
rRNA–Database of ribosomal subunit sequences	http://rrna.uia.ac.be/	De Rijk et al. (1992, 1999)
Signal recognition particle database	http://psyche.uthct.edu/dbs/SRPDB/SRPDB.html	Samuelsson and Zwieb (2000)
Small RNA database	http://mbcr.bcm.tmc.edu/smallRNA/smallrna.html	see Web page
snoRNA database for *S. cerevisiae*	http://rna.wustl.edu/snoRNAdb/	Lowe and Eddy (1999)
tmRNA[a] database	http://psyche.uthct.edu/dbs/tmRDB/tmRDB.html	Wower and Zwieb (1999)
tmRNA[a] Web site	http://www.indiana.edu/~tmrna/	Williams (1999)
tRNAscan-SE search server	http://www.genetics.wustl.edu/eddy/tRNAscan-SE/	Lowe and Eddy (1997)
tRNA and tRNA gene sequences	http://www.uni-bayreuth.de/departments/biochemie/sprinzl/trna/	Sprinzl et al. (1998)
u RNA database	http://psyche.uthct.edu/dbs/uRNADB/uRNADB.html	Zwieb (1997)
Vienna RNA package for RNA secondary structure prediction and comparison	http://www.tbi.univie.ac.at/~ivo/RNA/	Hofacker et al. (1998); Wuchty et al. (1999)
Viroid and viroid-like RNA sequences	http://www.callisto.si.usherb.ca/~jpperra	Lafontaine et al. (1999)

[a] tmRNA adds a carboxy-terminal peptide tag to the incomplete protein product from a broken mRNA molecule and thereby targets the protein for proteolysis.

A list of RNA Web sites and databases is available at http://bioinfo.math.rpi.edu/~zukerm/ and at http://pundit.colorado.edu:8080/.

and guest sites for RNA analysis or for access to databases of RNA molecules and sequences. These molecules perform a variety of important biochemical functions, including translation; RNA splicing, processing, and editing; and cellular localization. As with proteins, RNA-specifying genes may be identified by using the unknown gene as a query sequence for DNA sequence similarity searches, as described in Chapter 7. If a significant match to the sequence of an RNA molecule of known structure and function is found, then the query molecule should have a similar role. For some small molecules, the amount of sequence variation necessitates the use of more complex search methods, described later in this chapter.

RNA STRUCTURE PREDICTION BASICS

A computational method for predicting the most likely regions of base-pairing in an RNA molecule has been designed, just given the sequence, thus providing an ab initio prediction of secondary structure. From the many possible choices of complementary sequences that can potentially base-pair, the compatible sets that provide the most energetically stable molecules are chosen. Structures with energies almost as stable as the most stable one may also be produced, and regions whose predictions are the most reliable can be identified from such an analysis. Sequence variations found in related sequences may also be used to predict which base pairs are likely to be found in each of the molecules. One variation of RNA structure prediction methods will predict a set of sequences that are able to form a particular structure. Methods for predicting three-dimensional structures from sequence are also being developed (see http://bioinfo.math.rpi.edu/~zuker/rna/).

Another type of RNA secondary structure prediction method takes into account conserved patterns of base-pairing that are conserved during evolution of a given class of RNA molecules. Sequence positions that base-pair are found to vary at the same time during evolution of RNA molecules so that structural integrity is maintained. For example, if two positions G and C form a base pair in a given type of molecule, then sequences that have C and G reversed, or A and U or U and A at the corresponding positions, would be considered reasonable matches. These patterns of covariation in RNA molecules are a manifestation of secondary structure that lead to a structural prediction. The computational challenge is to discover these covariable positions against the background of other sequence changes.

FEATURES OF RNA SECONDARY STRUCTURE

Like protein secondary structure, RNA secondary structure can be conveniently viewed as an intermediate step in the formation of a three-dimensional structure. RNA secondary structure is composed primarily of double-stranded RNA regions formed by folding the single-stranded molecule back on itself. To produce such double-stranded regions, a run of bases downstream in the RNA sequence must be complementary to another upstream run so that Watson–Crick base-pairing between the complementary nucleotides G/C and A/U (analogous to the G/C and A/T base pairs in DNA) can occur. In addition, however, G/U wobble pairs may be produced in these double-stranded regions. As in DNA, the G/C base pairs contribute the greatest energetic stability to the molecule, with A/U base pairs contributing less stability than G/C, and G/U wobble base pairs contributing the least. From the RNA structures that have been solved, these base pairs and a number of addi-

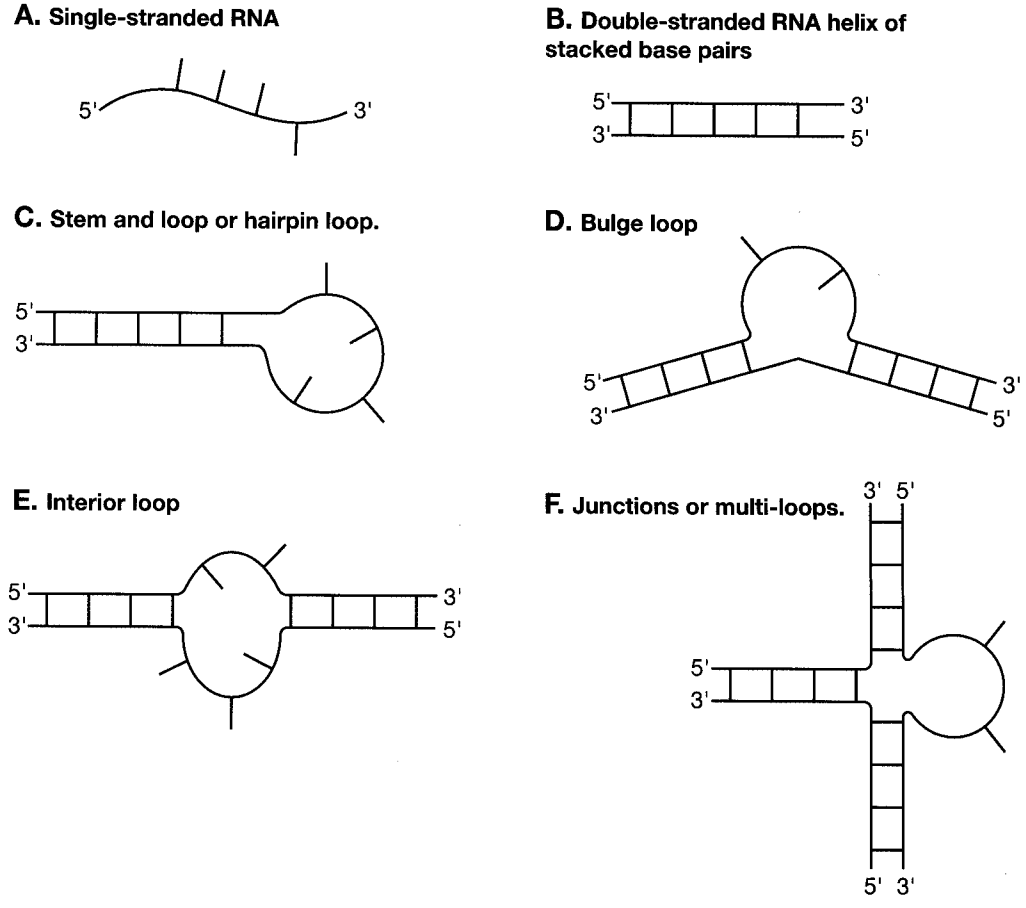

Figure 5.2. Types of single- and double-stranded regions in RNA secondary structures. Single-stranded RNA molecules fold back on themselves and produce double-stranded helices where complementary sequences are present. A particular base may either not be paired, as in *A*, or paired with another base, as in *B*. The double-stranded regions will most likely form where a series of bases in the sequence can pair with a complementary set elsewhere in the sequence. The stacking energy of the base pairs provides increased energetic stability. Combinations of double-stranded and single-stranded regions produce the types of structures shown in *C–F*, with the single-stranded regions destabilizing neighboring double-stranded regions. The loop of the stem and loop in *C* must generally be at least four bases long to avoid steric hindrance with base-pairing in the stem part of the structure. The stem and loop reverses the chemical direction of the RNA molecule. Interior loops, as in *D*, form when the bases in a double-stranded region cannot form base pairs, and may be asymmetric with a different number of base pairs on each side of the loop, as shown in *E*, or symmetric with the same number on each side. Junctions, as in *F*, may include two or more double-stranded regions converging to form a closed structure. The RNA backbone is red, and both unpaired and paired bases are blue. The types of loop structures can be represented mathematically, thereby aiding in the prediction of secondary structure (Sankoff et al. 1983; Zuker and Sankoff 1984). (Adapted from Burkhard et al. 1999b.)

tional ones (see Burkhard et al. 1999a,b) have been identified. RNA structure predictions comprise base-paired and non-base-paired regions in various types of loop and junction arrangements, as shown in Figure 5.2.

In addition to secondary structural interactions in RNA, there are also tertiary interactions, illustrated by the examples in Figure 5.3. These kinds of structures are not predictable by secondary structure prediction programs. They can be found by careful covariance analysis.

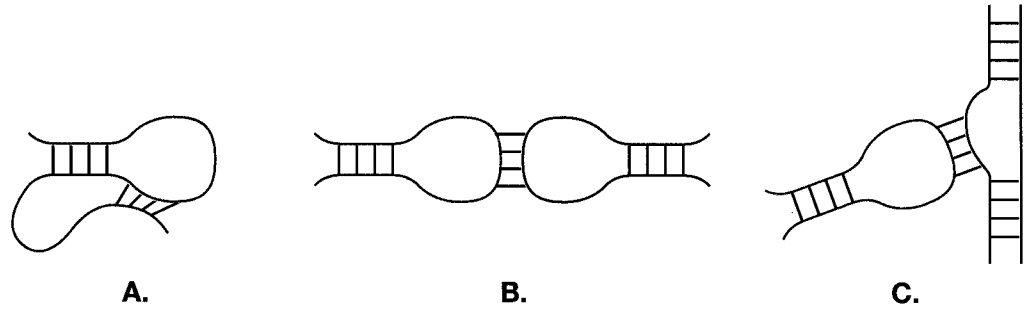

Figure 5.3. Examples of known interactions of RNA secondary structural elements. (*A*) Pseudoknot. (*B*) Kissing hairpins. (*C*) Hairpin-bulge contact. (Adapted from Burkhard et al. 1999b.)

LIMITATIONS OF PREDICTION

In predicting RNA secondary structure, some simplifying assumptions are usually made. First, the most likely structure is similar to the energetically most stable structure. Second, the energy associated with any position in the structure is only influenced by local sequence and structure. Thus, the energy associated with a particular base pair in a double-stranded region is assumed to be influenced only by the previous base pair and not by the base pairs farther down the double-stranded region or anywhere else in the structure. These energies can be reliably estimated by experimentation with small, synthetic RNA oligonucleotides (Tinoco et al. 1971, 1973; Freier et al. 1986; Turner and Sugimoto 1988; SantaLucia 1998) recently improved to include sequence dependence (Mathews et al. 1999). They are most reliable when used for standard Watson–Crick base pairs and single G-U pairs surrounded

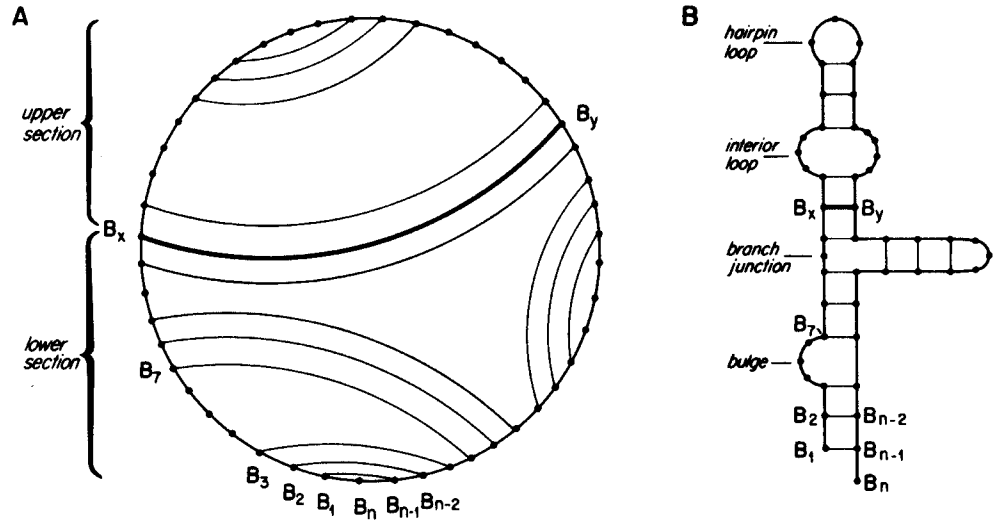

Figure 5.4. Display of base pairs in an RNA secondary structure by a circle plot. The predicted minimum free-energy structure shown in *B* is represented by a plot of the predicted base pairs as arcs connecting the bases in the sequence, which is drawn around the circumference of a circle, as shown in *A* (see Nussinov and Jacobson 1980). Note that none of the lines cross, a representation that the structure does not include any knots. (Reprinted from Nussinov and Jacobson 1980.)

by Watson–Crick pairs. Finally, the structure is assumed to be formed by folding of the chain back on itself in a manner that does not produce any knots. The best way of representing this requirement is to draw the sequence in a circular form. The paired bases are then joined by arcs. If the total structure with all predicted base pairs is to be free of knots, none of the arcs must cross (Fig. 5.4). Note, however, that if a pseudoknot (Fig. 5.3) is represented on such a diagram, the lines will cross.

DEVELOPMENT OF RNA PREDICTION METHODS

The development of methods for predicting RNA secondary structure has been reviewed by von Heijne (1987). Tinoco et al. (1971) first estimated the energy associated with regions of secondary structure by extrapolation from studies with small molecules and then attempted to predict which configurations of larger molecules were the most energetically stable. Energy estimates included the stabilizing energy associated with stacking base pairs in a double-stranded region and the destabilizing influence of regions that were not paired. Pipas and McMahon (1975) developed computer programs that listed all possible helical regions in tRNA sequences; using modified Watson–Crick base-pairing rules, they created all possible secondary structures by forming permutations of compatible helical regions, and evaluated each possible structure for total free energy. Studnicka et al. (1978) designed a method for adding compatible double-stranded regions together to produce the energetically most favorable structure. Martinez (1984) made a list of possible double-stranded regions, and these regions were then given weights in proportion to their equilibrium constants, calculated by the Boltzmann function [$\exp(-\Delta G/RT)$], where $-\Delta G$ is the free energy of the regions, R is the gas constant, and T is the temperature. The RNA molecule is folded by a Monte Carlo method in which one initial region is chosen at random from a weighted pool, similar to the method used in Gibbs sampling (see p. 177).

In the Monte Carlo method, a random drawing is made from a pool of all possible double-stranded regions, with the number of each type weighted in proportion to energetic stability.

Imagine each possible double-stranded region being represented by a marble in a bag. The number of each type of marble is weighted by the Boltzmann probability so that marbles corresponding to more energetically stable regions are more likely to be chosen. Additional compatible regions are then added sequentially by further selections from the weighted pool until no more can be added. This method generates a set of possible structures weighted by energy, but it does not take into account the destabilizing effect of unpaired regions. The Boltzmann probability function is used in more recent applications (described below) to find the most probable secondary structures (Hofacker et al. 1998; Wuchty et al. 1999).

Nussinov and Jacobson (1980) were the first to design a precise and efficient algorithm for predicting secondary structure. The algorithm generates two scoring matrices—one $M(i,j)$ to keep track of the maximum number of base pairs that can be formed in any interval i to j in the sequence and a second $K(i,j)$ to keep track of the base position k that is paired with j. From these matrices, a structure with the maximum possible number of base pairs could be deduced by a trace-back procedure similar to that used in performing sequence alignments by dynamic programming. Zuker and Stiegler (1981) used the dynamic programming algorithm and energy rules for producing the most energetically favorable structure. Their method assumes that the most energetic, and usually longest, predicted dsRNA regions are present in the molecule. Because many double-stranded regions are predictable for most RNA sequences, the number of predictions is reduced by including known biochemical or structural information to indicate which bases should be paired or not paired, by enforcing topological restraints and by requiring that the structure be in an energetically stable configuration.

MFOLD, written by Dr. Michael Zuker and colleagues, is commonly used to predict the energetically most stable structures of an RNA molecule (Jaeger et al. 1989, 1990; Zuker 1989, 1994). MFOLD provides a set of possible structures within a given energy range and provides an indication of their reliability. The program also uses covariance information from phylogenetically related sequences (Zuker et al. 1991). MFOLD includes methods for graphic display of the predicted molecules. This program is one of the most demanding on computer resources that is currently used because the algorithm is of N^3 complexity, where N is the sequence length. For each doubling of sequence length, the time taken to compute a structure increases eightfold. The program also requires a large amount of memory for storing intermediate calculations of structure energies in multiple scoring matrices. As a result, MFOLD is most often used to predict the structure of sequences less than 1000 nucleotides in length. This method is most reliable for small molecules and becomes less reliable as the length of the molecule increases.

MFOLD and many other types of useful information on RNA are found at the Web site of Dr. Michael Zuker, at http://bioinfo.math.rpi.edu/~zuker/rna/. Details of running MFOLD are not given here because the user manual for MFOLD is widely available (Jaeger et al. 1990). Recently, a new method called the partition function method for finding the most probable secondary structural configuration of an RNA molecule and the most probable base pairs has been reported by the Vienna RNA group (Wuchty et al. 1999) and is discussed below (p. 219).

One advance in the prediction of RNA structure has come from the recognition that certain RNA sequences form specific structures and that the presence of these sequences is strongly predictive of such a structure. For example, the hairpin CUUCGG occurs in different genetic contexts and forms a very stable structure (Tuerk et al. 1988). Databases of such RNA structures and RNA sequences can greatly assist in RNA structure prediction (Table 5.1).

The genetic algorithm (see Chapter 4, p. 157) has also been used to predict secondary structure (Shapiro and Navetta 1994); for aligning RNA sequences, taking into account both sequence and secondary structure and including pseudoknots (Notredame et al. 1997); and for simulation of RNA-folding pathways (Gultyaev et al. 1995). The program FOLDALIGN uses a dynamic programming algorithm to align RNAs based on sequence and secondary structure and locates the most significant motifs (Gorodkin et al. 1997). Chan et al. (1991) have described another algorithm for the same purpose, and Chetouani et al. (1997) have developed ESSA, a method for viewing and analyzing RNA secondary structure.

METHODS

SELF-COMPLEMENTARY REGIONS IN RNA SEQUENCES PREDICT SECONDARY STRUCTURE

One of the simplest types of analyses that can be performed to find stretches of sequence in RNA that are self-complementary is a dot matrix sequence comparison for self-complementary regions. For single-stranded RNA molecules, these repeats represent regions that can potentially self-hybridize to form RNA double strands (von Heijne 1987; Rice et al. 1991). All types of RNA secondary structure analysis begin by the identification of these regions, and, once identified, the compatible regions may be used to predict a minimum free-energy structure. A more advanced type of dot matrix can be used to show the most energetic parts of the molecule (see Fig. 5.8, below).

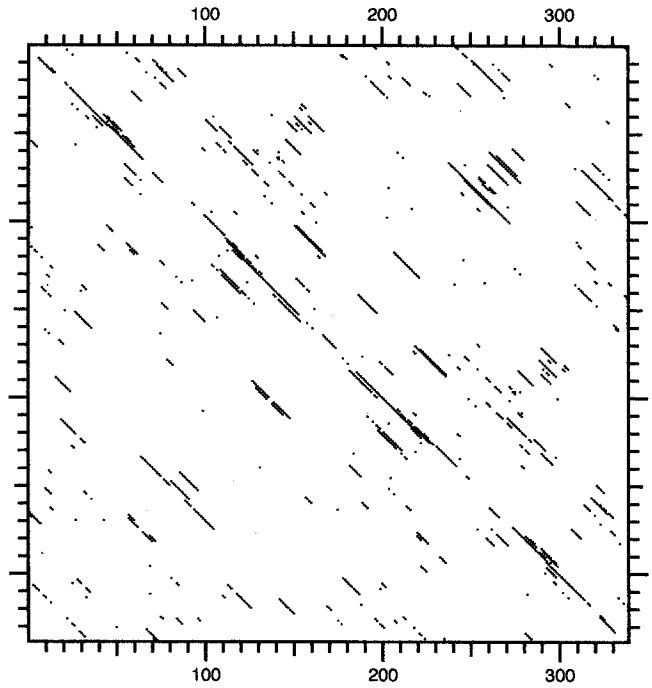

Figure 5.5. Dot matrix analysis of the potato tuber spindle viroid for RNA secondary structure using the MATRIX function of DNA Strider v. 1.2 on a Macintosh computer.

Self-complementary regions in RNA may be found by performing a dot matrix analysis with the sequence to be analyzed listed in both the horizontal and vertical axes. In one method for finding such regions, the sequence is listed in the 5′→3′ direction across the top of the page and the sequence of the complementary strand is listed down the side of the page, also in the 5′→3′ direction. The matrix is then scored for identities. Self-complementary regions appear as rows of dots going from upper left to lower right. For RNA, these regions represent sequences that can potentially form A/U and G/C base pairs. G/U base pairs will not usually be included in this simple type of analysis. As with matching DNA sequences, there are many random matches between the four bases in RNA, and the diagonals are difficult to visualize. A long window and a requirement for a large number of matches within this window are used to filter out these random matches.

An example of the RNA secondary structure analysis using a DNA matrix option of DNA Strider is shown in Figure 5.5. An analysis of the potato spindle tuber viroid is shown, using a window of 15 and a required match of 11. Note the appearance of a diagonal running from the center of the matrix to the upper left, and a mirror image of this diagonal running to the lower right. The presence of this diagonal indicates the occurrence of a large self-complementary sequence such that the entire molecule can potentially fold into a hairpin structure. An alternative dot matrix method for finding RNA secondary structure is to list the given RNA sequence across the top of the page and also down the side of the page and then to score matches of complementary bases (G/C, A/U, and G /U). Diagonals indicating complementary regions will go from upper right to lower left in this type of matrix. This is the kind of matrix used to produce an energy matrix (see Fig. 5.8, below).

MINIMUM FREE-ENERGY METHOD FOR RNA SECONDARY STRUCTURE PREDICTION

To predict RNA secondary structure, every base is first compared to every other base by a type of analysis very similar to the dot matrix analysis. The sequence is listed across the top and down the side of the page, and G/C, A/U, and G/U base pairs are scored (for an example using a dot matrix method to find hairpins, see Fig. 5.5). Just as a diagonal in a two-sequence comparison indicates a range of sequence similarity, a row of matches in the RNA matrix indicates a succession of complementary nucleotides that can potentially form a double-stranded region. The energy of each predicted structure is estimated by the nearest-neighbor rule by summing the negative base-stacking energies for each pair of bases in double-stranded regions and by adding the estimated positive energies of destabilizing regions such as loops at the end of hairpins, bulges within hairpins, internal bulges, and other unpaired regions. Representative examples of the energy values that are currently used are given in Table 5.2. To evaluate all the different possible configurations and to find the most energetically favorable, several types of scoring matrices are used. The complementary regions are evaluated by a dynamic programming algorithm to predict the most energetically stable molecule. The method is similar to the dynamic programming method used for sequence alignment (see Chapter 3).

To calculate the stacking energy of a row of base pairs in the molecule, the stacking energies similar to those shown in Table 5.2 are used. An illustrative example for evaluation of energy in a double-stranded region is shown in Figure 5.6. The sequence is listed down the side of the matrix, and a portion of the same sequence is also listed across the top of the matrix; matching base pairs have been identified within the matrix. The object is to find a diagonal row of matches that goes from upper right to lower left, and such a row is shown in the example. In Figure 5.6, a match of four complementary bases in a row produces a molecule of free energy −6.4 kcal/mole. In general, each matrix value is obtained by considering the minimum energy values obtained by all previous complementary pairs

Table 5.2. *Predicted free-energy values (kcal/mole at 37°C) for base pairs and other features of predicted RNA secondary structures*

A. Stacking energies for base pairs

	A/U	C/G	G/C	U/A	G/U	U/G
A/U	−0.9	−1.8	−2.3	−1.1	−1.1	−0.8
C/G	−1.7	−2.9	−3.4	−2.3	−2.1	−1.4
G/C	−2.1	−2.0	−2.9	−1.8	−1.9	−1.2
U/A	−0.9	−1.7	−2.1	−0.9	−1.0	−0.5
G/U	−0.5	−1.2	−1.4	−0.8	−0.4	−0.2
U/G	−1.0	−1.9	−2.1	−1.1	−1.5	−0.4

B. Destabilizing energies for loops

Number of bases	1	5	10	20	30
Internal	–	5.3	6.6	7.0	7.4
Bulge	3.9	4.8	5.5	6.3	6.7
Hairpin	–	4.4	5.3	6.1	6.5

(*Upper*) Stacking energy in double-stranded region when base pair listed in left column is followed by base pair listed in top row. C/G followed by U/A is therefore the dinucleotide 5′ CU 3′ paired to 5′ AG 3′. (*Lower*) Destabilizing energies associated with loops. Hairpin loops occur at the end of a double-stranded region, internal loops are unpaired regions flanked by paired regions, and a bulge loop is a bulge of one strand in an otherwise paired region (Fig. 5.2). An updated and more detailed list of energy parameters may be found at the Web site of M. Zuker (http://bioinfo.math.rpi.edu/~zuker/rna/energy/).

From Turner and Sugimoto (1988); Serra and Turner (1995).

A. Base comparisons

5'	A	C	G	U	3'
A					
C					
G					
U					
–					
–					
G		C/G		U/G	
C			G/C		
G		C/G		U/G	
U	A/U	C/U	G/U		
3'					

B. Free energy calculations

5'	A	C	G	U	3'
A					
C					
G					
U					
–					
–					
G				−6.4	
C			−5.2		
G		−1.8			
U					
3'					

Figure 5.6. Evaluation of secondary structure in RNA sequence by the method described in the text. The sequence is listed down the first column of *A* and *B* in the 5′→3′ orientation, and the first four bases of the sequence are also listed in the first row of the tables in the 5′→3′ direction. Several complementary base pairs between the first and last four bases that could lead to secondary structure are shown in *A*. The most 5′ base is listed first in each pair. The diagonal set of base pairs A/U, C/G, G/C, and U/G reveals the presence of a potential double-stranded region between the first and last four bases. The free energy associated with such a row of base pairs is shown in *B*. A C/G base pair following an A/U base pair has a base stacking energy of −1.8 kcal/mole (Turner and Sugimoto 1988). This value is placed in the corresponding position in *B*. Similarly, a C/G base pair followed by a G/C provides energy of −3.4, and a G/C followed by a U/G, −1.2 kcal/mole. Hence, the energy accumulated after stacking of these additional two base pairs is −5.2 and −6.4. The energy of this double-stranded structure will continue to decrease (become more stable) as more base pairs are added, but will be increased if the structure is interrupted by noncomplementary base pairs.

decreased by the stacking energy of any additional complementary base pairs or increased by the destabilizing energy associated with noncomplementary bases. The increase depends on the type and length of loop that is introduced by the noncomplementary base pair, whether internal loop, bulge loop, or hairpin loop, as shown in Table 5.2. This comparison of all possible matches and energy values is continued until all nucleotides have been compared. The pattern followed in comparing bases within the RNA molecule is illustrated in Figure 5.7.

SUBOPTIMAL STRUCTURE PREDICTIONS BY MFOLD AND THE USE OF ENERGY PLOTS

Originally, the FOLD program of M. Zuker predicted only one structure having the minimum free energy. However, changes in a single nucleotide can result in drastic changes in the predicted structure. A later version, called MFOLD, has improved prediction of non-base-paired interactions and predicts several structures having energies close to the minimum free energy. These predictions accurately reflect structures of related RNA molecules derived from comparative sequence analysis (Jaeger et al. 1989; Zuker 1989, 1994; Zuker et al. 1991; Zuker and Jacobson 1995). To find these suboptimal structures, the dynamic programming method was modified (Zuker 1989, 1991) to evaluate parts of a new scoring matrix in which the

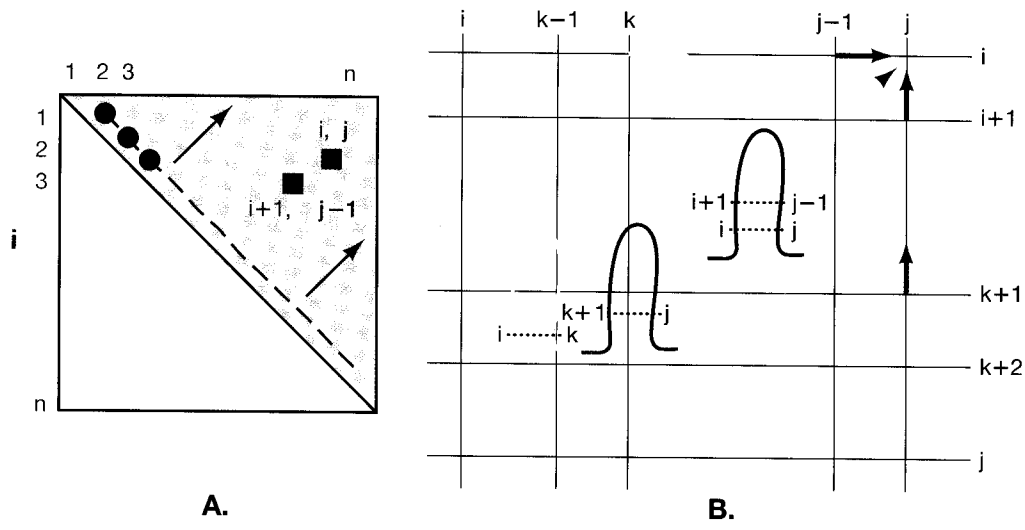

Figure 5.7. Method used in dynamic programming analysis for identifying the most energetically favorable configuration of a linear RNA molecule. (*A*) The sequence of an RNA molecule of length *n* bases is listed across the top of the page and down the side. The index of the sequence across the top is *j* and that down the side is *i*. The search only includes the upper right part of the matrix shown in gray and begins at the first diagonal line for matching base pairs. First positions $i = 1$ and $j = 2$ are compared for potential base-pairing, and if pairing can occur, an energy value is placed in an energy matrix *W* at position 1,2. Then, $i = 2$ and $j = 3$ base are compared, and so on, until all base combinations along the dashed diagonal have been made. Then, comparisons are made along the next upper right diagonal. As each pair of bases is compared, an energy calculation is made that is the optimal one up to that point in the comparison. In the simplest case, if $i+1$ pairs with $j-1$, and *i* pairs with *j*, and if this structure is the most favorable up to that point, the energy of the *i/j* base pair will be added to that of the $i+1/j-1$ base pair. Other cases are illustrated in *B*. The process of obtaining the most stable energy value at each matrix position is repeated following the direction of the arrows until the last position, $i = 1$ and $j = n$, has been compared and the energy value placed at this position in matrix *W*, the value entered in *W(1,n)*, will be the energy of the most energetically stable structure. The structure is then found by a trace-back procedure through the matrices similar to that used for sequence alignments. The method used is a combination of a search for all possible double-stranded regions and an energy calculation based on energy values similar to those in Table 5.2. The search for the most energetic structure uses an algorithm (Zuker and Stiegler 1981) similar to that for finding the structure with maximum base-pairing (Nussinov and Jacobson 1980). These authors recognized that there are three possible ways, illustrated here by the colored arrows, of choosing the best energy value at position *i,j* in an energy matrix *W*. The simplest calculation (*red arrow*) is to use the energy value found up to position $i-1, j-1$ diagonally below *i,j*. If *i* and *j* can form a base pair (and if there are at least four bases between them in order to allow enough sequence for a hairpin) and $i+1$ and $j-1$ also pair, then the stacking energy of *i/j* upon $i+1/j-1$ will reduce the energy value at $i+1, j-1$, producing a more stable structure, and the new value can be considered a candidate for the energy value entered at position *i,j*. If *i* and *j* do not pair, then another choice for the energy at *i,j* is to use the values at positions *i*, $j-1$ or $i+1$, *j* illustrated by the blue arrows. *i* and *j* then become parts of loop structures. Finally, *i* and *j* may each be paired with two other bases, *i* with *k* and *j* with $k+1$, where *k* is between *i* and *j* ($i < k < j$), illustrated by the structure shown in yellow and green, reflecting the location of the paired bases. The minimum free-energy value for all values of *k* must be considered to locate the best choice as a candidate value at *i,j*. Finally, of the three possible choices for the minimum free-energy value at *i,j* indicated by the four colored arrows, the best energy value is placed at position *W(i,j)*. The procedure is repeated for all values of *i* and *j*, as illustrated in *A*. Besides the main energy scoring matrix *W*, additional scoring matrices are used to keep track of auxiliary information such as the best energy up to *i,j* where *i* and *j* form a pair, and the influence of bulge loops, interior loops, and other destabilizing energies. An essential second matrix is *V(i,j)*, which keeps track of all substructures in the interval *i,j* in which *i* forms a base pair with *j*. Some values in the *W* matrix are derived from values in the *V* matrix and vice versa (Zuker and Stiegler 1981).

sequence is represented in two tandem copies on both the vertical and horizontal axes. The regions from $i = 1$ to n and $j = 1$ to n are used to calculate an energy $V(i,j)$ for the best structure that includes an i,j base pair and is called the included region. A second region, the excluded region, is used to calculate the energy of the best structure that includes i,j but is not derived from the structure at $i+1, j-1$ (Fig. 5.7). After certain corrections are made, the difference between the included and excluded values is the most energetic structure that includes the base pair i,j. All complementary base pairs can be sampled in this fashion to determine which are present in a suboptimal structure that is within a certain range of the optimal one.

An energy dot plot is produced showing the locations of alternative base pairs that produce the most stable or suboptimally stable structures, as illustrated in Figure 5.8. The program may be instructed to find structures within a certain percentage of the minimum free energy. Parameter d provides a measure of similarity between two structures. When MFOLD is established on a suitable local host machine, the window is interactive, and clicking a part of the display will lead to program output of the corresponding structure. The dot plot may be filtered so that only suboptimal regions with helices of a certain minimal length are shown. One of the predicted structures is shown in Figure 5.9.

Reliability of Secondary Structure Prediction

Three scores, *P*num (i), *H*num (i,j), and Ssum, have been derived to assist with a determination of the reliability of a secondary structure prediction for a particular base i or a base pair i,j. *P*num(i) is the total number of energy dots regardless of color in the ith row and ith column of the energy dot plot, and represents in an unfiltered dot plot the number of base pairs that the ith base can form with all other base pairs in structures within the defined energy range. The lower this value, the more well defined or "well determined" the local structure because there are few competitive foldings. *H*num(i,j) is the sum of *P*num(i) and *P*num(j) less 1 and is the total number of dots in the ith row and jth column and represents the total number of base pairs with the ith or jth base in the predicted structures. The *H*num for a double-stranded region is the average *H*num value for the base pairs in that helix. The lower this number, the more well determined the double-stranded region. In an analysis of tRNAs, 5S RNAs, ribosomal RNAs, and other published secondary structure models based on sequence variation (Jaeger et al. 1990; Zuker and Jacobson 1995), these methods correctly predict about 70% of the double-stranded regions. *S*num, also called ss-count, is the number of foldings in which base i is single-stranded divided by m, the number of foldings, and gives the probability that base i is single-stranded. If *S*num is approximately 1, then base i is probably in a single-stranded region, and if *S*num is approximately 0, then base i is probably not in such a region. This reliability information has been used to annotate output files of MFOLD and other RNA display programs (Zuker and Jacobsen 1998). Plots of these values against sequence position are given by the MFOLD program and the Zuker Web site.

OTHER ALGORITHMS FOR SUBOPTIMAL FOLDING OF RNA MOLECULES

A limitation of the Zuker method and other methods (Nakaya et al. 1995) for computing suboptimal RNA structures is that they do not compute all the structures within a given energy range of the minimum free-energy structure. For example, no alternative structures

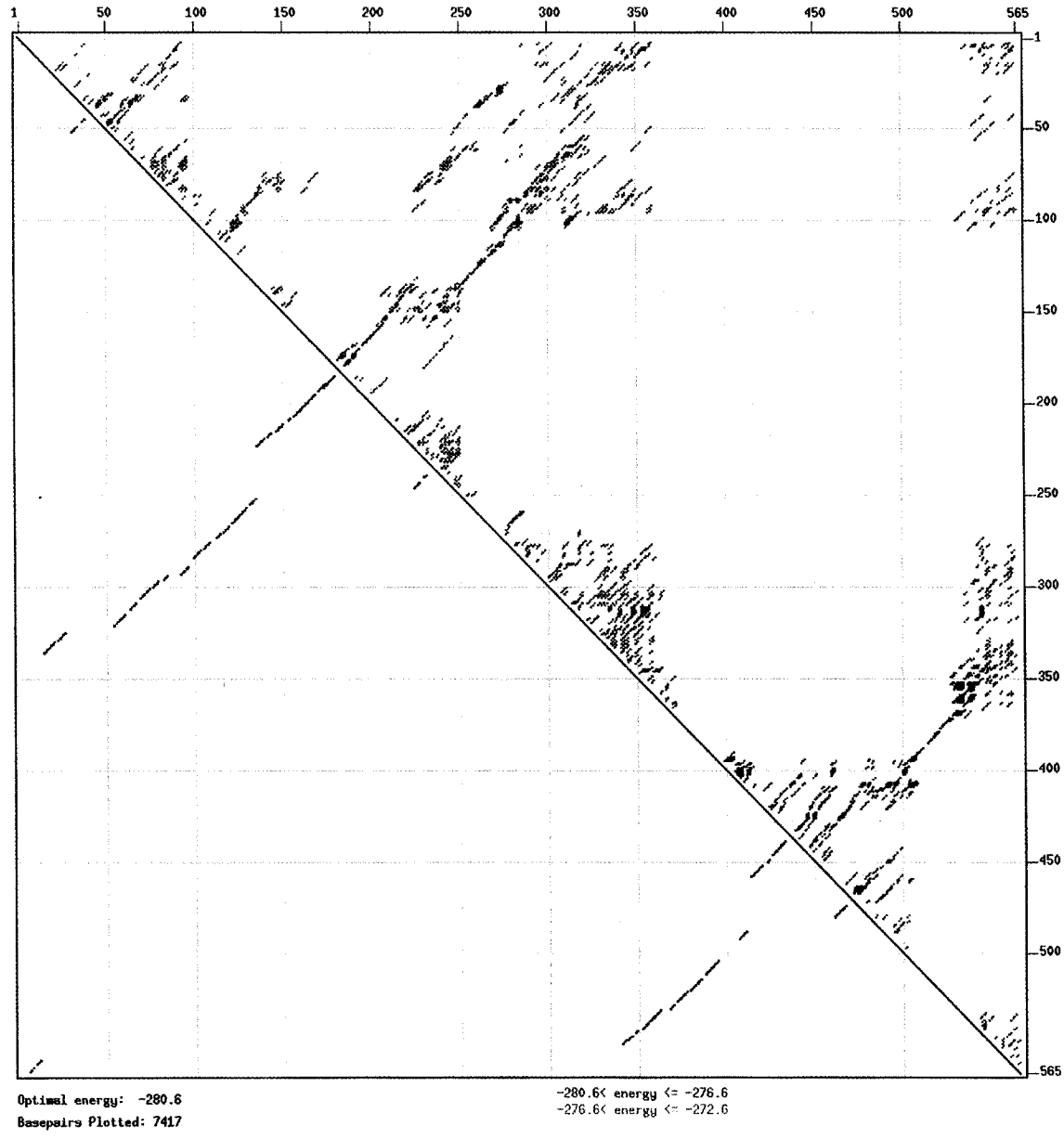

Figure 5.8. The energy dot plot (boxplot) of alternative choices of base pairs of an RNA molecule (Jacobson and Zuker 1993). The sequence is that of a human adenovirus pre-terminal protein (GenBank U52533) that is given by M. Zuker as an example on his Web site at http://bioinfo.math.rpi.edu/~zukerm. Foldings were computed using the default parameters of the MFOLD program at http://bioinfo.math.edu/~mfold/rna/form1.cgi (Mathews et al. 1999) using the thermodynamic values of SantaLucia (1998). The minimum energy of the molecule is −280.6 kcal/mole and the maximum energy increment is 12 kcal/mole. Black dots indicate base pairs in the minimum free-energy structure and are shown both above and the mirror image below the main diagonal. Red, blue, and yellow dots are base pairs in foldings of increasing 4, 8, and 12 kcal/mole energies greater than the minimum energy, respectively. A region with very few alternative base pairs such as the pairing of 370–395 with 530–505 is considered to be strongly predictive, whereas regions with many alternative base pairs such as the base-pairing in the region of 340–370 with 570–530 are much less predictive.

are produced that have the absence of base pairs in the best structure, and, if two substructures are joined by a stretch of unpaired bases, no structures are produced that are suboptimal for both structures. These factors limit the number of alternative structures predicted compared to known variations based on sequence variations in tRNAs (Wuchty et al. 1999).

These limitations have been largely overcome by using an algorithm originally described by Waterman and Byers (1985) for finding sequence alignments within a certain range of the optimal one by modifications of the trace-back procedure used in dynamic programming. This method efficiently calculates a large number of alternative structures, up to a very large number, within a given energy range of the minimum free-energy structure (see Fig. 5.10). The method has been used to demonstrate that natural tRNA sequences can form many alternative structures which are close to the minimum free-energy structure and that base modification plays a major role in this energetic stability (Wuchty et al. 1999). The method may also be used to assess the thermodynamic stability of RNA structures given expected changes in energies associated with base pairs and loops as a function of temperature. The RNA secondary structure prediction and comparison Web site at http://www.tbi.univie.ac.at/~ivo/RNA/ will fold molecules of length > 300 bases, and the Vienna RNA Package software for folding larger molecules on a local machine is available from this site.

PREDICTION OF MOST PROBABLE RNA SECONDARY STRUCTURE

In the above types of analyses, the energy associated with predicted double-stranded regions in RNA is used to produce a secondary structure. Stabilizing energies associated with base-paired regions and destabilizing energies associated with loops are summed to produce the most stable structure or suboptimal RNA secondary structure. A different way of predicting the structures is to consider the probability that each base-paired region will form based on principles of thermodynamics and statistical mechanics. The probability of forming a region with free energy ΔG is expressed by the Boltzmann distribution, which states that the likelihood of finding a structure with free energy $-\Delta G$ is proportional to [exp $(-\Delta G/kT)$] where k is the Boltzmann gas constant and T is the absolute temperature.

The Boltzmann constant k is 8.314510 J/mole/degree K.

Note that the more stable a structure, the lower the value of ΔG. Since ΔG is a negative number, the value of $\exp(-\Delta G/kT)$ increases for more stable structures and also grows exponentially with a decrease in energy. The probability of these regions forming increases in the same manner. Conversely, the effect of destabilizing loops that have a positive ΔG is to decrease the probability of formation. By using these probability calculations and a dynamic programming method similar to that used in MFOLD, it is possible to predict the most probable RNA secondary structures and to assess the probability of the base pairs that contribute energetic stability to this structure.

For a set of possible structural states, the likelihood of each may be calculated using this formula, and the sum of these likelihoods provides a partition function that can be used to normalize each individual likelihood, providing a probability that each will occur. Thus, probability of structure A of energy $-\Delta G_a$ is [exp $(-\Delta G_a/kT)$] divided by the partition function Q, where $Q = \Sigma_s$ [exp $(-\Delta G_s/kT)$], the sum of probabilities of all possible struc-

A.

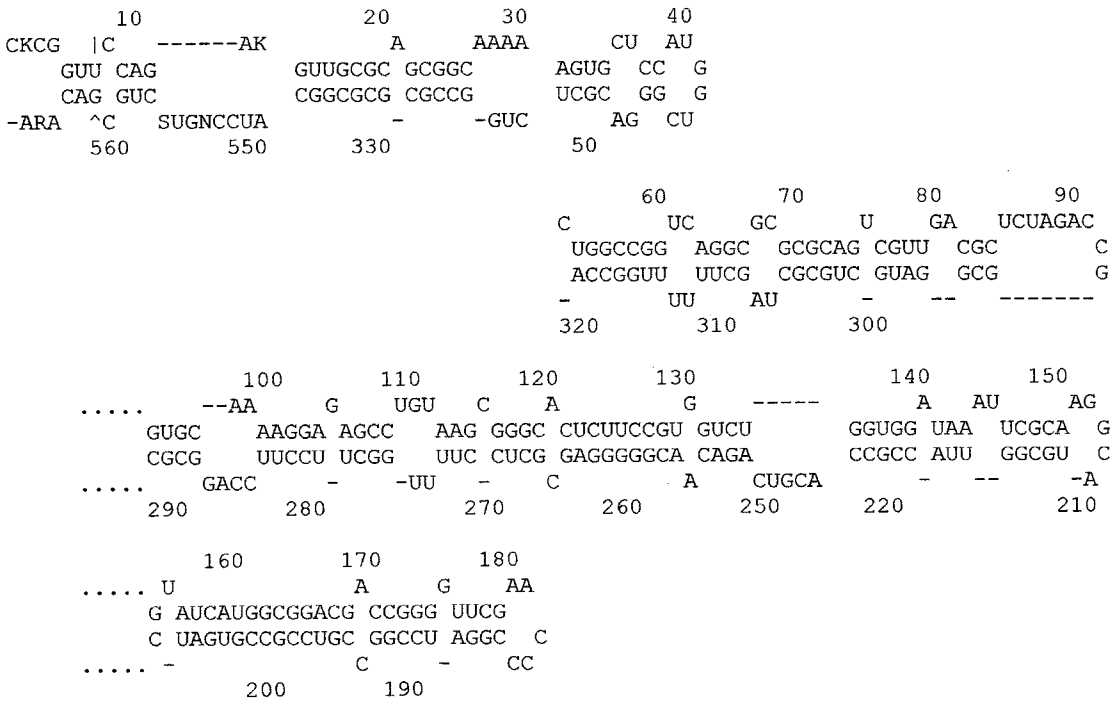

B.

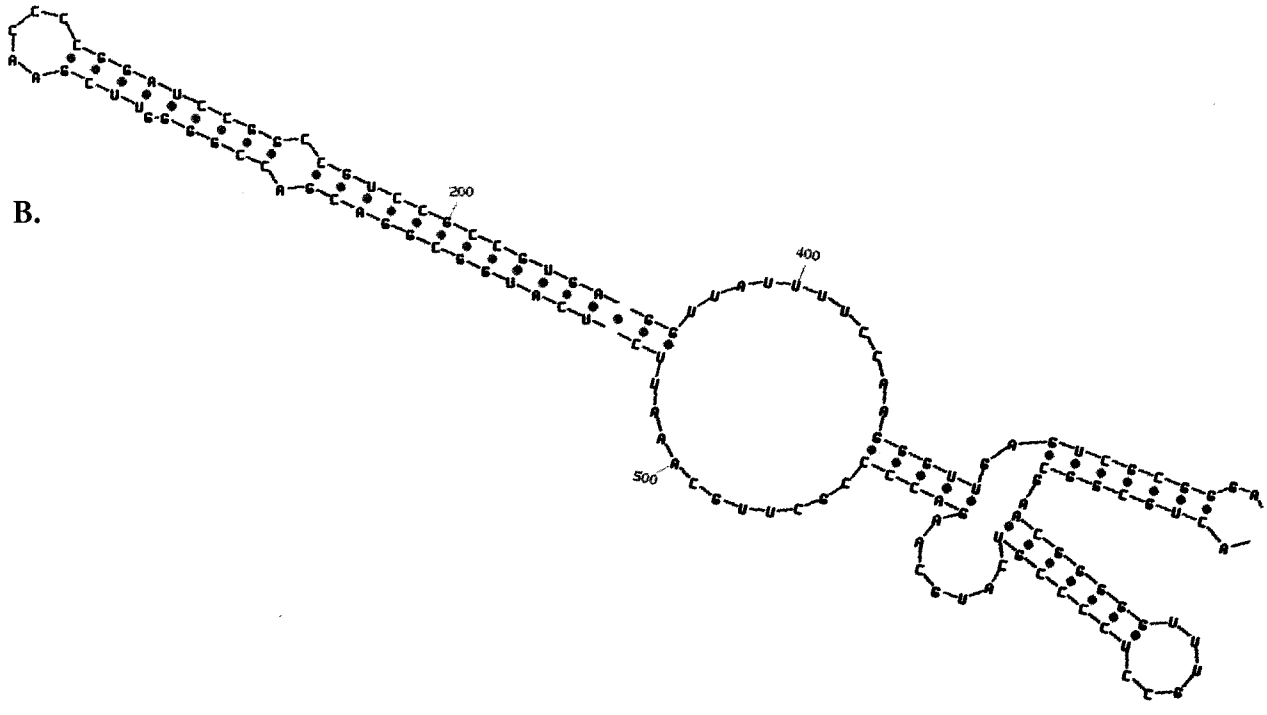

Figure 5.9. Model of RNA secondary structure of the human adenovirus pre-terminal protein. This model is one of several alternative structures represented by the above energy plot and provided as an output by the current versions of MFOLD. (*A*) Simple text representation of one of the predicted structures. Each stem-and-loop structure is shown separately and the left end of each structure is placed below the point of connection to the one above. (*B*) More detailed rendition of one part of the predicted structures. The structure continues beyond the right side of the page.

tures, s. This kind of analysis allows one to calculate the probability of a certain base pair forming.

The key to this analysis is the calculation of the partition function Q. A dynamic programming algorithm for calculating this function exactly for RNA secondary structure has been developed (McCaskill 1990). The algorithm is very similar to that used for computing an optimal folding by MFOLD. Complexity similarly increases as the cube of the sequence length, and the energy values used for base pairs and loops are also the same except that structures with very large interior loops are ignored. Just as the minimum free-energy value is given at $W(1,n)$ in the Zuker MFOLD algorithm, the value of the partition function is given at matrix position $Q(1,n)$ in the corresponding partition matrix.

As indicated above, the partition function is calculated as the sum of the probabilities of each possible secondary structure. Because there are a very large possible number of structures, the calculation is simplified by calculating an auxiliary function, $Q^b(i,j)$, which is the sum of the probabilities of all structures that include the base pair *i,j*. The partition function $Q(i,j)$ includes both these structures and the additional ones where *i* is not paired with *j*. An example illustrating the difference between the minimum free energy and the partition function methods should be instructive. Suppose that the bases at positions $i+1, j-1$ and *i,j* can both form base pairs. They then form a stack of two base pairs. In the minimum free-energy method, the energy of the *i,j* pair stacked on the $i+1, j-1$ pair will be added to $V(i+1, j-1)$ to give $V(i,j)$, where *V* is a scoring matrix that keeps track of the best structure that includes an *i,j* base pair. In contrast, the value for $Q^b(i,j)$ will be calculated by multiplying the matrix value $Q^b(i+1, j-1)$ by the probability of the base pair *i,j* given by the Boltzmann probability [exp $(-\Delta G/kT)$], where ΔG is the negative stacking energy of the *i,j* base pair on the $i+1, j-1$ base pair, and will be a large number reflecting the probability given the stability of the base-paired region.

For a hairpin structure with a row of successive base pairs, the probability will be the product of the Boltzmann factors associated with the stacked pair, giving a high number for the relative likelihood of formation. The procedure followed by the partition function algorithm is to calculate $Q^b(i,j)$ and $Q(i,j)$ iteratively in a scoring matrix similar to that illustrated in Figure 5.7A until $Q(1,n)$ is reached. This matrix position contains the value of the full partition function Q.

Both the partition function and the probabilities of all base pairs are computed by this algorithm, and the most probable structural model is thereby found. Information about intermediate structures, base-pair opening and slippage, and the temperature dependence of the partition function may also be determined. The latter calculation provides information about the melting behavior of the secondary structure.

A suite of RNA-folding programs available from the Vienna RNA secondary structure prediction Web site (http://www.tbi.univie.ac.at/~ivo/RNA/) uses this methodology to predict the most probable and alternative RNA secondary structures. An example of the folding of a 300-base RNA molecule is given in Figure 5.10. The probability of forming each base pair is shown in a dot matrix display in which the dots are squares of increasing size reflecting the probability of the base pair formed by the bases in the horizontal and vertical positions of the matrix. Secondary structure prediction is done by two kinds of dynamic programming algorithms: the minimum free-energy algorithm of Zuker and Stiegler (1981) and the partition function algorithm of McCaskill (1990).

A.

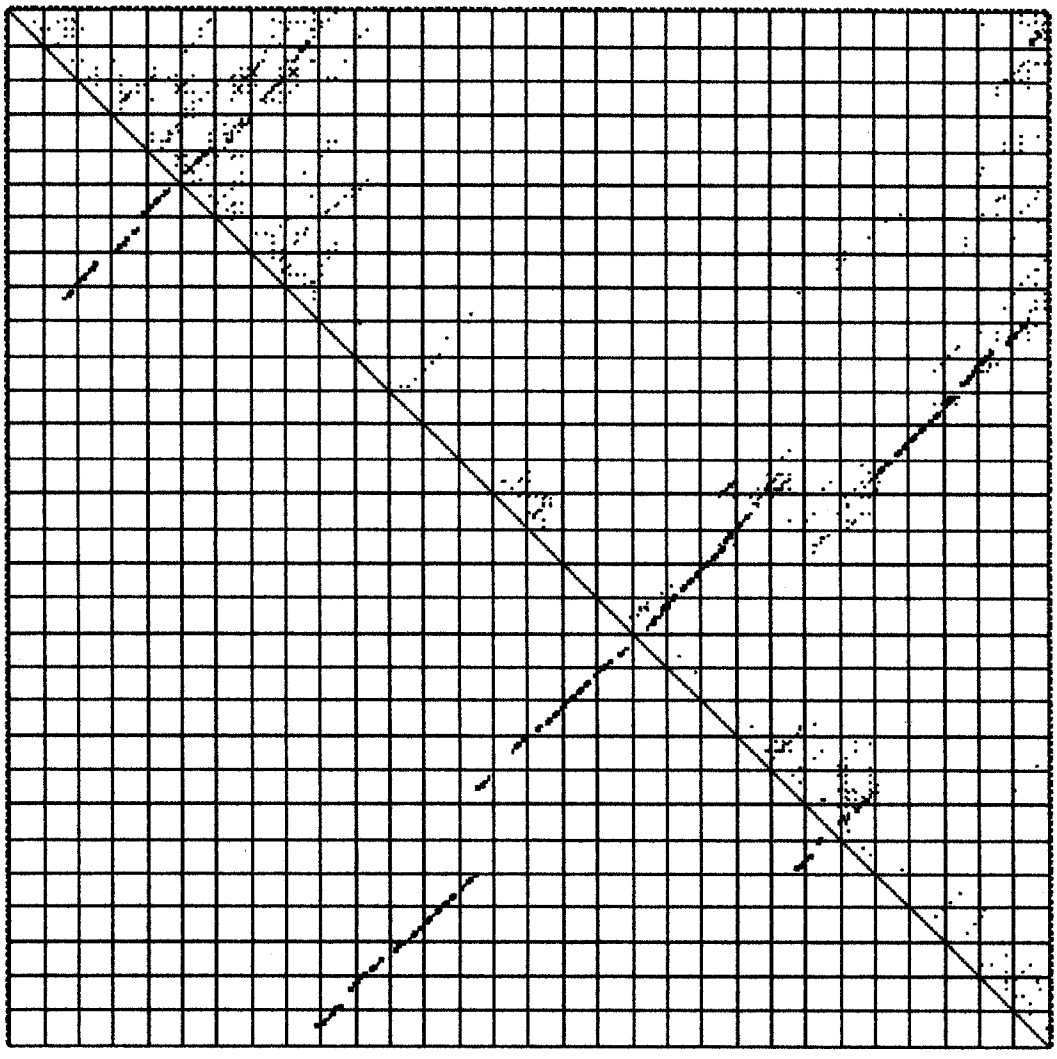

B.

```
CKCGGUUCCAGAKGUUGCGCAGCGGCAAAAAGUGCUCCAUGGUCGGGACGCUCUGGCCGGUC
AGGCGCGCGCAGUCGUUGACGCUCUAGACCGUGCAAAAGGAGAGCCUGUAAGCGGGCACUCU
UCCGUGGUCUGGUGGAUAAAUUCGCAAGGGUAUCAUGGCGGACGACCGGGGUUCGAACCCCG
GAUCCGGCCGUCCGCCGUGAUCCAUGCGGUUACCGCCCGCGUGUCGAACCCAGGUGUGCGAC
GUCAGACAACGGGGGAGCGCUCCUUUUGGCUUCCUUCCAGGCGCGGCGGAUG
.................(((((((((.....((((.((.(((((((.....)))))))
....)).))))...)))))))..)))....(.((((((..(((((.(((((...(((.(((
(.(((((((((.(((((((((.....((((..((.(((((((((((((.(((((..(
((.....))).)))))..)))))))))))))))..)))))).......)))).(((((.((.
...)).)))))..)))))..)))))))))..)))))))..)))))))))....)))))))
.....
```

Figure 5.10. Suboptimal foldings of an RNA sequence using probability distributions of base-pairings. The first 300 bases of the same adenovirus sequence used in Fig. 5.8 was submitted to the Vienna Web server. (*A*) The region shown represents structures within the range of bases 150–300 and may be compared to the same region in Fig. 5.8. The minimum free energy of this thermodynamic ensemble is −134.85 kcal/mole, compared to a minimum free energy of 125.46 kcal/mole. The size of the square box at highlighted matrix positions indicates the probability of the base pair and decreases in steps of 10-fold; i.e., order of magnitude decreases. The size variations shown in the diagram cover a range of ~4–6 orders of magnitude. Calculations of base-pair probabilities are discussed in the text. (*B*) The minimum free-energy structure representing base pairs as pairs of nested parentheses. A low-resolution picture was also produced (not shown).

USING SEQUENCE COVARIATION TO PREDICT STRUCTURE

The second major method that has been used to make RNA secondary structure predictions (Woese et al. 1983) and also tertiary structure analyses such as those shown in Figure 5.3 (Gutell et al. 1986) is RNA sequence covariation analysis. This method examines sequences of the same RNA molecules from different species for positions that vary together in a manner that would allow them to produce a base pair in all of the molecules. The idea is quite simple. On the one hand, for double-stranded regions in RNA molecules, sequence changes that take place in evolution should maintain the base-pairing. On the other hand, sequence changes in loops and single-stranded regions should not have such a constraint. The method of analysis is to look for sequence positions at which covariation maintains the base-pairing properties. The justification for this method is that these types of joint substitutions or covariations actually are found to occur during evolution of such genes. As shown in Figure 5.11, when one position corresponding to a base pair is changed, another position corresponding to the base-pairing partner will also change. For example, if two positions G and C form a base pair, then sequences that have C and G reversed, or A and T or T and A at the corresponding positions, would also be considered reasonable matches. Sequence covariability has been used to improve thermodynamic structure prediction as described in the above section (Hofacker et al. 1998). An example of using covariation analysis to decipher base-pair interactions in tRNA is shown in Figure 5.12.

One method of covariation analysis also examines which phylogenetic groups exhibit change at a given position. For each position, the base that generally predominates in one particular part of the tree is determined. These methods have required manual examination of sequences and structures for covariation, but automatic methods have also been devised and demonstrated to produce reliable predictions (Winker et al. 1990; Han and Kim 1993; see box below).

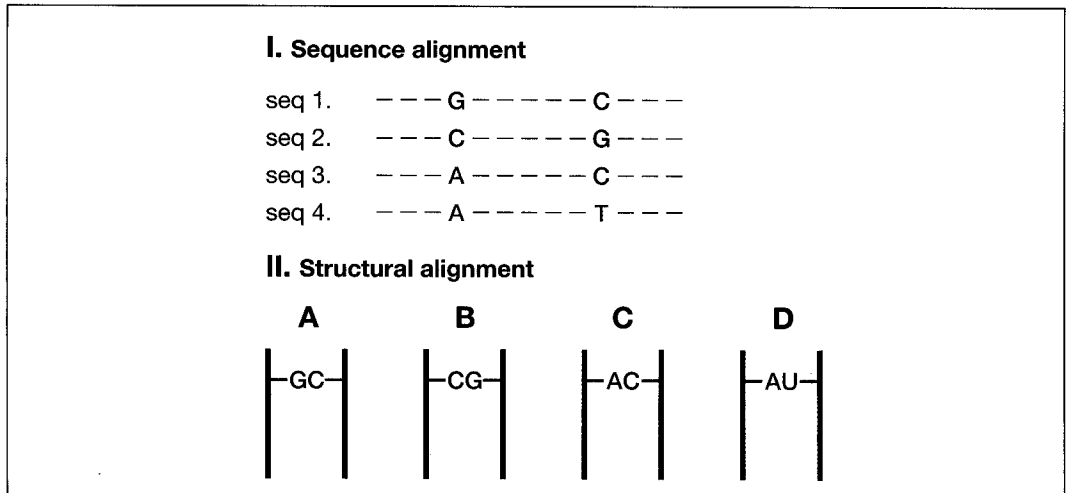

Figure 5.11. Conservation of base pairs in homologous RNA molecules influences structure prediction. The predicted structure takes into account sequence covariation found at aligned sequence positions, and may also use information about conserved positions in components of a phylogenetic tree. In the example shown, sequence covariations in A, B, and D found in sequences 1, 2, and 4, respectively, permit Watson–Crick base and G-U base-pairing in the corresponding structure, but variation C found in sequence 3 is not compatible. Sometimes correlations will be found that suggest other types of base interactions, or the occurrence of a common gap in a multiple sequence alignment may be considered a match. Positions with greater covariation are given greater weight in structure prediction. Molecules with only one of the two sequence changes necessary for conservation of the base-paired position may be functionally deleterious.

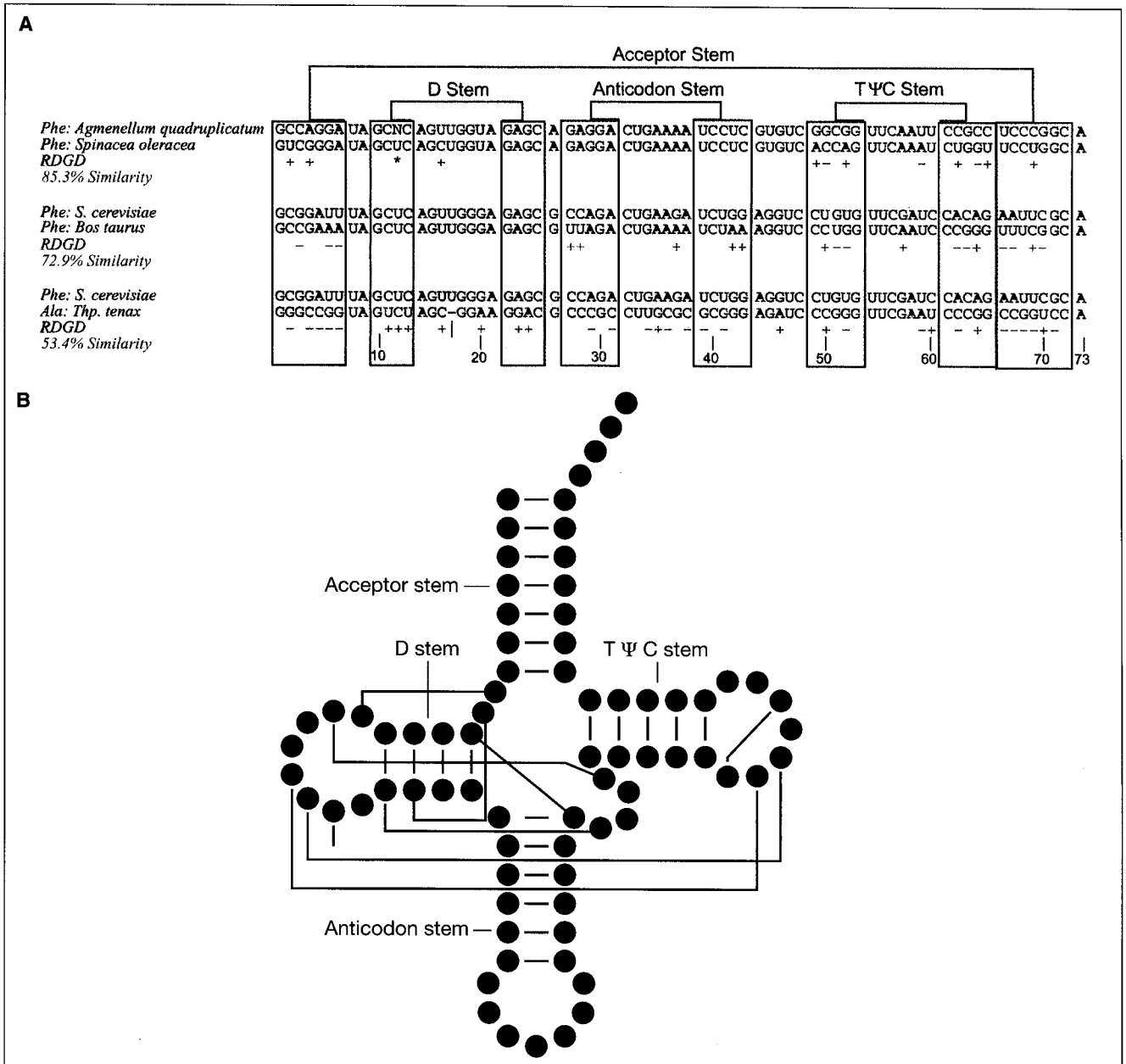

Figure 5.12. Covariation found in tRNA sequences reveals base interactions in tRNA secondary and tertiary structure. (*A*) Alignment of tRNA sequences showing regions of interacting base pairs. (+) Transition; (−) transversions; (|) deletion; (*) ambiguous nucleotide. (*B*) Diagram of tRNA structure illustrating base–base interactions revealed by a covariance analysis. Adapted from the Web site of R. Gutell at http://www.rna.icmb.utexas.edu.

Methods of Covariation Analysis in RNA Sequences

Secondary and tertiary features of RNA structure may be determined by analyzing a group of related sequences for covariation. Two sequence positions that covary in a manner that frequently maintains base-pairing between them provides evidence that the bases interact in the structure. Combinations of the following methods have been used to locate such covarying sites in RNA sequences (see R. Gutell for additional details and at http://www.rna.icmb.utexas.edu/METHODS/menu.html).

1. Optimally align pairs of sequence to locate conserved primary sequence, mark transitions and transversions from a reference sequence, and then visually examine these changes to identify complementary patterns that represent potential secondary structure.
2. Perform a multiple sequence alignment, highlight differences using one of the sequences as a reference, and visually examine for complementary patterns.
3. Mark variable columns in the multiple sequence alignment by numbers that mark changes (e.g., transitions or transversions) from a reference sequence; examine marked columns for a similar or identical number pattern that can represent potential secondary structure.
4. Perform a statistical analysis (Chi-square test) of the number of observations of a particular base pair in columns i and j of the multiple sequence alignment, compared to the expected number based on the frequencies of the two bases.
5. Calculate the mutual information score ($mixy$) for each pair of columns in the alignment, as described in the text and illustrated in Figure 5.13.
6. Score the number of changes in each pair of columns in the alignment divided by the total number of changes (the ec score), examine the phylogenetic context of these changes to determine the number of times the changes have occurred during evolution, and choose the highest scores that are representative of multiple changes.
7. Measure the covariance of each pair of positions in the alignment by counting the numbers of all 16 possible base-pair combinations and dividing by the expected number of each combination (number of sequence × frequency of base in first position × frequency of base in second position), choose the most prevalent pair, and examine remaining combinations for additional covariation; then sum frequency of all independently covarying sites to obtain covary score.

Mutual Information Content

A method used to locate covariant positions in a multiple sequence alignment is the mutual information content of two columns. First, for each column in the alignment, the frequency of each base is calculated. Thus, the frequencies in column m, $f_m(B_1)$, are $f_m(A)$, $f_m(U)$, $f_m(G)$, and $f_m(C)$ and those for column n, $f_n(B_2)$, are $f_n(A)$, $f_n(U)$, $f_n(G)$, and $f_n(C)$. Second, the 16 joint frequencies of two nucleotides, $f_{m,n}(B_1,B_2)$ one base B_1 in column m and the same or another base B_2 in column n are calculated. If the base frequencies in any two columns are independent of each other, then the

ratio of $f_{m,n}(B_1,B_2) / [f_m(B_1) \times f_n(B_2)]$ is expected to equal 1, and if the frequencies are correlated, then this ratio will be greater than 1. If they are perfectly covariant, then $f_{m,n}(B_1,B_2) = f_m(B_1) = f_n(B_2)$. To calculate the mutual information content $H(m,n)$ in bits between the two columns m and n, the logarithm of this ratio is calculated and summed over all possible 16 base-pair combinations.

$$H(m,n) = \Sigma_{B1,B2}\, f_{m,n}(B_1,B_2) \times \log_2 \{f_{m,n}(B_1,B_2) / [f_m(B_1)\, f_n(B_2)]\}$$

$H(m,n)$ varies from the value of 0 bits of mutual information representing no correlation to that of 2 bits of mutual information, representing perfect correlation (Eddy and Durbin 1994).

The mutual information content may be plotted on a motif logo (Gorodkin et al. 1997), similar to that described in Chapter 4, page 196, for illustrating a sequence motif. The example shown in Figure 5.13 shows the mutual information content M superimposed on the information content of each sequence position in an RNA alignment.

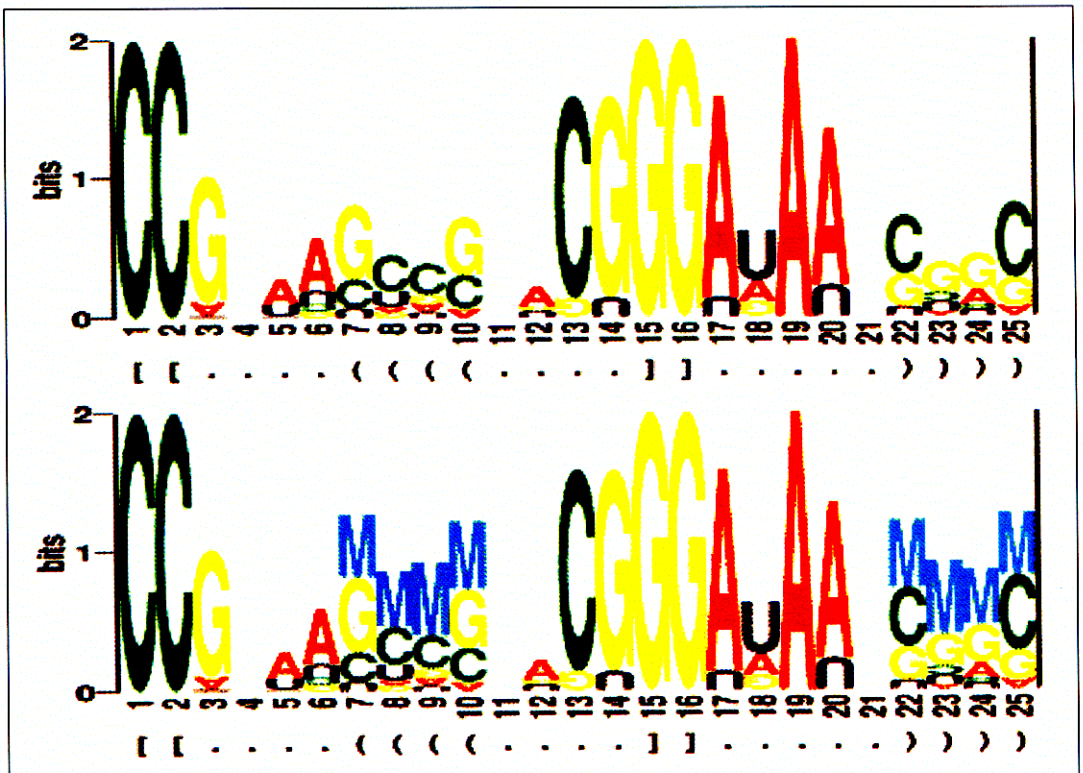

Figure 5.13. RNA structure logo. The top panel is the normal sequence logo showing the size of each base in proportion to the contribution of that base to the amount of information in that column of the multiple sequence alignment. The relative entropy method is used in which the frequency of bases in each column is compared to the background frequency of each base. Inverted sequence characters indicate a less than background frequency (see Chapter 4, page 196). The bottom panel includes the same information plus the mutual information content in pairs of columns. The amount of information is indicated by the letter M, and the matching columns are shown by nested sets of brackets and parentheses. All sequences have a C in column 1 and a matching G in column 16. Similar columns 2 and 15 can form a second base pair stacked upon the first. Columns 7–10 and 25–22 also can form G/C base pairs most of the time. Sequences with a G in column 7 frequently have a C in column 25, and those with a C in column 7 may have a G in column 25. Thus, there is mutual information in these two columns (Gorodkin et al. 1997 [using data of Tuerk and Gold 1990]).

A formal covariance model has been devised by Eddy and Durbin (1994). Although very accurate when used for identifying tRNA genes, the algorithm is extremely slow and unsuitable for searching through large genomes. Instead, the method has been used to screen through putative tRNA genes previously identified by faster methods (Lowe and Eddy 1997). The difficulty that is faced in modeling RNA molecules is to identify the potential base pairs in a set of related RNA molecules based on covariation at two sites. Recall from Chapter 4 that the hidden Markov model is used for capturing the types of variations observed in a sequence profile, including matches, mismatches, insertions, and deletions. This type of model assumes each sequence can be predicted by a series of states in the model, one after the other, as in a series of independent events in a Markov chain. The hidden Markov model does not analyze joint variations at sequence positions such as occur in RNA molecules. The model that is used for analyzing RNA secondary structure (but not tertiary structure) is an ordered tree model. A simplified tree representation of RNA secondary structure is shown in Figure 5.14.

The above assumes that we know which bases are paired in a model of RNA secondary structure, whereas the goal is to build a model that discovers this information. The task is achieved by constructing a more general model, training the model with a set of sequences,

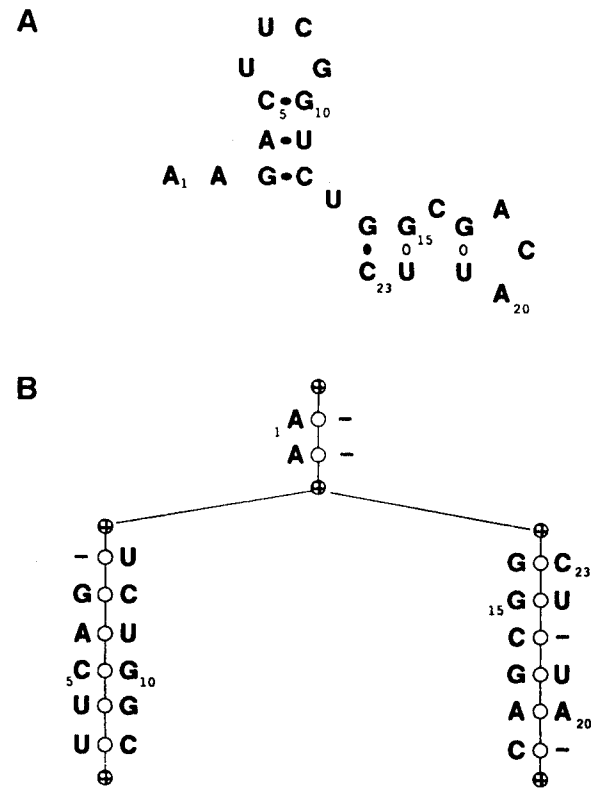

Figure 5.14. Tree model of RNA secondary structure. The model in *A* is represented by the ordered binary tree shown in *B*. This model attempts to capture both the sequence and the secondary structure of the RNA molecule. The tree is read like a sequence starting at the root node at the top of the model, then moving down the main branch to the bifurcation mode. Along the main trunk are nodes that represent matched or unmatched base pairs. Shown are two A's matching a "-," indicating no pairing with these bases. After the bifurcation mode, one then moves down the most leftward branch to the end node. Along the branch are unmatched bases, matched base pairs, and mismatched pairs. After the end node is reached, go back to the previous bifurcation node and follow the right branch. (Reprinted, with permission of Oxford University Press, from Eddy and Durbin 1994.)

and then having the model reveal the most likely base-paired regions. The approach is similar to training a hidden Markov model for proteins to recognize a family of protein sequences, thereby producing the most probable multiple sequence alignment. In the case of RNA secondary structure, a tree model is trained by the sequences, and the model may then be used to predict the most probable secondary structure. In addition, the model may also be used to search a database for sequences that produce a high score when aligned to the model. These sequences are likely to encode a similar type of RNA molecule such as tRNA or 5S RNA. Each model is derived by training a more general tree model with the sequences.

The general tree model needs to represent the types of variations that are found in aligning a series of related sequences, such as insertions, deletions, and mismatches. To allow for such variations, each node in the tree is replaced by a set of states that correspond to all of the possible sequence variations that might be encountered at that position. These states are illustrated in Figure 5.15.

The mutual information content of all sequence positions is used in designing the model, and the expectation maximization method (Chapter 4) is used to optimize the parameters of the model. A dynamic programming method is used to find a model that maximizes the amount of covariation. The structure of the model may subsequently be altered during training. Once a covariance model suitable for an RNA molecule has been established, the model is trained by the sequences. The methodology is similar to that of hidden Markov models and is described in detail in Chapter 4. Basically, the model is initialized by giving starting values to the base and dinucleotide frequencies in each MATCH and INS state and to the transition probabilities. All possible paths through the model are found for each sequence in the training set. The frequencies and transition probabilities are modified each time a particular path in the model is used. The base pairs are found from MATP (see Fig. 5.15), which gives probabilities to the 16 possible dinucleotides.

Once the model has been trained, the most probable path for each sequence provides a consensus structural alignment of the sequences. A dynamic programming algorithm is used that matches subsequence alignments to the nodes of the covariance model. The result is a log odds score of the sequence matching the covariance model. A similar method may be used to find sequences in a genomic database with high matching scores to the covariance model. The method was used to predict the structural alignment of representative sets of tRNA sequences, and it provided alignments that closely matched actual structural alignments based on other methods. The software for the COVELS program is available by request from the authors (Eddy and Durbin 1994).

STOCHASTIC CONTEXT-FREE GRAMMARS FOR MODELING RNA SECONDARY STRUCTURE

In the above section, we discussed the need to have models for RNA secondary structure that reflect the interaction among base pairs. Simpler models of sequence variation treat sequences as simple strings of characters without such interactions and are therefore not suitable for RNA. A general theory for modeling strings of symbols, such as bases in DNA sequences, has been developed by linguists. There is a hierarchy of these so-called transformational grammars that deal with situations of increasing complexity. The application of these grammars to sequence analysis has been extensively discussed elsewhere (Durbin et al. 1998). The context-free grammar is suitable for finding groups of symbols in different parts of the input sequence that thus are not in the same context. Complementary regions in sequences, such as those in RNA that will form secondary structures, are an

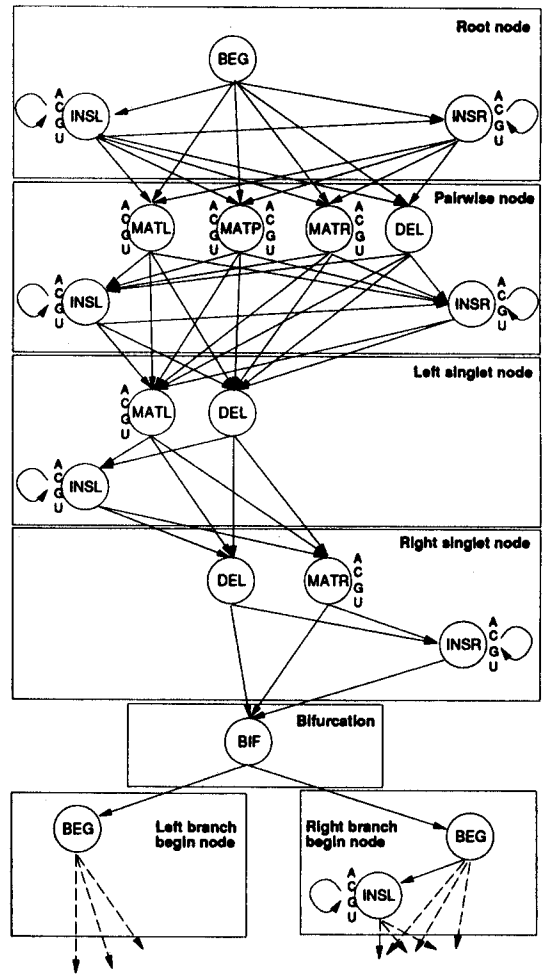

Figure 5.15. Details of tree model for RNA secondary structure. Each type of node in the tree shown in Fig. 5.14 is replaced by a pattern of states corresponding to the types of sequence variations that are expected in a family of related RNA sequences. These states each store a table of frequencies of 4 bases or of 16 possible dinucleotides. The seven different types of nodes are illustrated. BEG node includes insert states for sequence of any length on the right or left side of the node. The pair-wise node includes a state MATP for storing the 16 possible dinucleotide frequencies; MATL and MATR states for storing single base frequencies on either the left or right side of the node, respectively; a DEL state for allowing deletions; and INSL and INSR states that allow for insertions of any length on the left or right of the node. DEL does not store information. The other five node types have the same types of states. Each state is joined to other states by a set of transition probabilities shown by the arrows. These probabilities are similar to those used in hidden Markov models. BIF is a bifurcation state with transition probabilities entering the state from above and then leaving to one or the other of two branches. (Reprinted, with permission of Oxford University Press, from Eddy and Durbin 1994.)

example of such context-free sequences. Stochastic context-free grammars (SCFG) introduce uncertainty into the definition of such regions, allowing them to use alternative symbols as found in the evolution of RNA molecules. Thus, SCFGs can help define both the types of base interactions in specific classes of RNA molecules and the sequence variations at those positions. SCFGs have been used to model tRNA secondary structure (Sakakibara et al. 1994). Although SCFGs are computationally complex (Durbin et al. 1998), they are likely to play an important future role in identifying specific types of RNA molecules.

The application of SCFGs to RNA secondary structure analysis is very similar in form to the probabilistic covariance models described in the above section. For RNA, the symbols of the alphabet are A, C, G, and U. The context-free grammar establishes a set of rules called productions for generating the sequence from the alphabet, in this case an RNA molecule with sections that can base-pair and others that cannot base-pair. In addition to the sequence symbols (named terminal symbols because they end up in the sequence), another set of symbols (nonterminal symbols) designated S_0, S_1, S_2 . . . , determines intermediate production stages. The initial symbol is S_0 by convention. The next terminal symbol S_1 is produced by modifying S_0 in some fashion by productions indicated by an arrow. For example, the productions $S_0 \rightarrow S_1$, $S_1 \rightarrow C\ S_2\ G$ generate the sequence $C\ S_2\ G$ where S_2 has to be defined further by additional productions. The example shown in Figure 5.16 (from Sakakibara et al. 1994) shows a set of productions for generating the sequence CAUCAGGGAAGAUCUCUUG and also the secondary structure of this molecule. The productions chosen describe both features.

In this example of a context-free grammar, only one sequence is produced at each production level. In a SCFG, each production of a nonterminal symbol has an associated probability for giving rise to the resulting product, and there are a set of productions, each giving a different result. For example, the production $S_1 \rightarrow C\ S_2\ G$ could also be represented by 15 other base-pair combinations, and each of these has a corresponding probability. Thus, each production can be considered to be represented by a probability distribution over the possible outcomes. Note the identity of the SCFG representation of the predicted structure to that shown for the tree representation of the covariance model in Figure 5.14. The use of SCFGs in RNA secondary structure production analysis is in fact very similar to that of the covariance model, with the grammatical productions resembling the nodes in the ordered binary tree. As with hidden Markov models, the probability distribution of each production must be derived by training with known sequences. The algorithms used for training the SCFG and for aligning a sequence with the SCFG are somewhat different from those used with hidden Markov models, and the time and memory requirements are greater (Sakakibara et al. 1994: Durbin et al 1998).

SEARCHING GENOMES FOR RNA-SPECIFYING GENES

One goal in RNA research has been to design methods to identify sequences in genomes that encode small RNA molecules. Larger, highly conserved molecules can simply be identified based on their sequence similarity with already-known sequences. For smaller sequences with more sequence variation, this method does not work. A number of methods for finding small RNA genes have been described and are available on the Web (Table 5.1). A major problem with these methods in searches of large genomes is that a small false-positive rate becomes quite unacceptable because there are so many false positives to check out.

One of the first methods used to find tRNA genes was to search for sequences that are self-complementary and can fold into a hairpin like the three found in tRNAs (Staden 1980).

Figure 5.16. A set of transformation rules for generating an RNA sequence and the secondary structure of the sequence from the RNA alphabet (ACGU). (*A*) The set of production rules for producing the sequence and the secondary structure. These rules reveal which bases are paired and which are not paired. (*B*) Derivation of the sequence. (*C*) A parse tree showing another method for displaying the derivation of the sequence in *B*. (*D*) Secondary structure from applying the rules. (Redrawn, with permission of Oxford University Press, from Sakakibara et al. 1994.)

A. Productions

$P = \{ S_0 \rightarrow S_1,$ $S_7 \rightarrow G\,S_8,$
$S_1 \rightarrow C\,S_2\,G,$ $S_8 \rightarrow G,$
$S_2 \rightarrow A\,S_3\,U,$ $S_9 \rightarrow A\,S_{10}\,U,$
$S_3 \rightarrow S_4\ S_9,$ $S_{10} \rightarrow G\,S_{11}\,C,$
$S_4 \rightarrow U\,S_5\,A,$ $S_{11} \rightarrow A\,S_{12}\,U,$
$S_5 \rightarrow C\,S_6\,G,$ $S_{12} \rightarrow U\,S_{13},$
$S_6 \rightarrow A\,S_7,$ $S_{13} \rightarrow C$ $\}$

B. Derivation

$S_0 \rightarrow S_1 \rightarrow CS_2G \rightarrow CAS_3UG \rightarrow CAS_4S_9UG$
$\rightarrow CAUS_5AS_9UG \rightarrow CAUCS_6GAS_9UG$
$\rightarrow CAUCAS_7GAS_9UG \rightarrow CAUCAGS_8GAS_9UG$
$\rightarrow CAUCAGGGAS_9UG \rightarrow CAUCAGGGAAS_{10}UUG$
$\rightarrow CAUCAGGGAAGS_{11}CUUG$
$\rightarrow CAUCAGGGAAGAS_{12}UCUUG$
$\rightarrow CAUCAGGGAAGAUS_{13}UCUUG$
$\rightarrow CAUCAGGGAAGAUCUCUUG.$

C. Parse tree

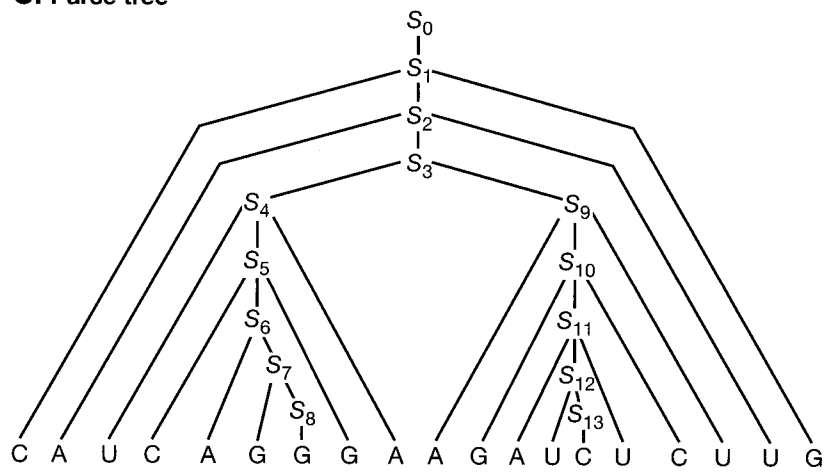

D. Secondary structure

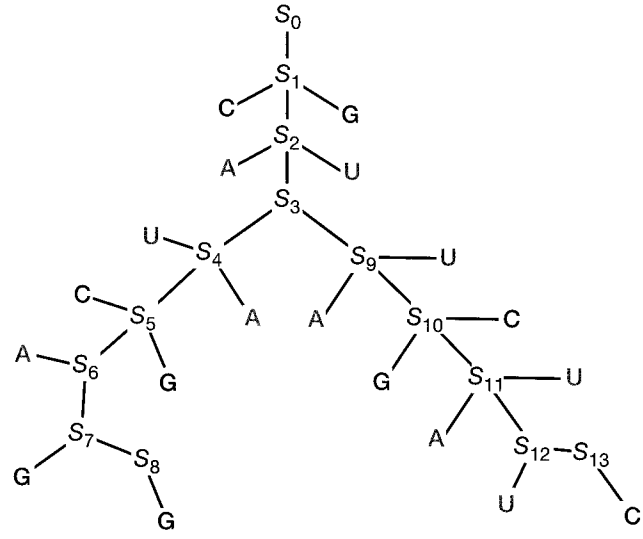

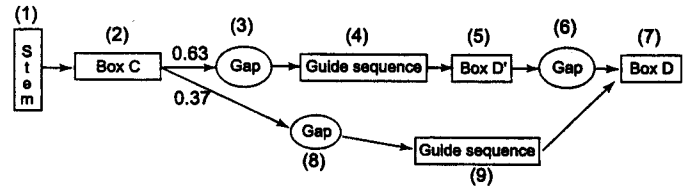

Figure 5.17. Probabilistic model of snoRNAs. The numbered boxes and ovals represent conserved sequence and structural features that have been modeled by training on snoRNAs. Secondary structural features of Stem were modeled with an SCFG. Boxes with ungapped hidden Markov models, the guide sequence with a hidden Markov model, and gapped regions (spacers) are shown by ovals. The guide sequence interacts with methylation sites on rRNA and is targeted in each search to a complementary sequence near one of those sites. The alignment of this model produces a log odds score that provides an indication of the reliability of the match. The transition probabilities are 1, except where the model bifurcates to allow identification of two types of target sequences. The model is highly specific and seldom identifies incorrect matches in random sequences. (Reprinted, with permission, from Lowe and Eddy 1999 [copyright AAAS, Washington, D.C.].)

Fichant and Burks (1991) described a program, tRNAscan, that searches a genomic sequence with a sliding window searching simultaneously for matches to a set of invariant bases and conserved self-complementary regions in tRNAs with an accuracy of 97.5%. Pavesi et al. (1994) derived a method for finding the RNA polymerase III transcriptional control regions of tRNA genes using a scoring matrix derived from known control regions that is also very accurate. Finally, Lowe and Eddy (1997) have devised a search algorithm tRNAscan-SE that uses a combination of three methods to find tRNA genes in genomic sequences—tRNAscan, the Pavesi algorithm, and the COVELS program based on sequence covariance analysis (Eddy and Durbin 1994). This method is reportedly 99–100% accurate with an extremely low rate of false positives.

The probabilistic model shown in Figure 5.17 was used to identify small nucleolar (sno) RNAs in the yeast genome that methylate ribosomal RNA. The model is not used to search genomic sequences directly. Instead, a list of candidate sequences is first found by searching for patterns that match the sequences in the model (Lowe and Eddy 1999). The probability model was a hybrid combination of HMMs and SCFGs trained on snoRNAs. These RNAs vary sufficiently in sequence and structure that they are not found by straightforward similarity searches. The RNAs found were shown to be snoRNAs by insertional mutagenesis.

APPLICATIONS OF RNA STRUCTURE MODELING

In summary, methods for predicting the structure of RNA molecules include (1) an analysis of all possible combinations of potential double-stranded regions by energy minimization methods and (2) identification of base covariation that maintains secondary and tertiary structure of an RNA molecule during evolution. Energy minimization methods have been so well refined that a series of energetically feasible models and the most thermodynamically probable structural models may be computed. Covariation analysis by C. Woese led to his building of detailed structural models for rRNAs. By examining the evolutionary variation in these structures, he was able to predict three domains of life—the Bacteria, the Eukarya, and a newly identified Archaea. Although a large amount of horizontal transfer among evolutionary lineages of other genes has added a great deal of noise to the evolutionary signal, the rRNA-based prediction is supported by other types of

genomic analyses. In addition to these uses of rRNA structural analysis, excellent probabilistic models of two small RNA molecules, tRNA and snoRNA, have been built, and these models may be used to search reliably through genomic sequences for genes that encode these RNA molecules. The successful analysis of these types of RNA molecules should be readily extensible to other classes of RNA molecules.

REFERENCES

Berman H.M., Zardecki C., and Westbrook J. 1998. The nucleic acid database: A resource for nucleic acid science. *Acta Crystallogr. D Biol. Crystallogr.* **54:** 1095–1104.

Brown J.W. 1999. The ribonuclease P database. *Nucleic Acids Res.* **27:** 314.

Burkhard M.E., Turner D.H., and Tinoco I., Jr. 1999a. The interactions that shape RNA secondary structure. In *The RNA world*, 2nd edition (ed. R.F. Gesteland et al.), pp. 233–264. Cold Spring Harbor Laboratory Press, Cold Spring Harbor, New York.

———. 1999b. Appendix 2: Schematic diagrams of secondary and tertiary structure elements. In *The RNA world*, 2nd edition (ed. R.F. Gesteland et al.), pp. 681–685. Cold Spring Harbor Laboratory Press, Cold Spring Harbor, New York.

Ceci L.R., Volpicella M., Liuni S., Volpetti V., Licciulli F., and Gallerani R. 1999. PLMItRNA, a database for higher plant mitochondrial tRNAs and tRNA genes. *Nucleic Acids Res.* **27:** 156–157.

Chan L., Zuker M., and Jacobson A.B. 1991. A computer method for finding common base paired helices in aligned sequences: Application to the analysis of random sequences. *Nucleic Acids Res.* **19:** 353–358.

Chen R.O., Felciano R., and Altman R.B. 1997. RIBOWEB: Linking structural computations to a knowledge base of published experimental data. *Ismb* **5:** 84–87.

Chetouani F., Monestié P., Thébault P., Gaspin C., and Michot B. 1997. ESSA: An integrated and interactive computer tool for analysing RNA secondary structure. *Nucleic Acids Res.* **25:** 3514–3522.

De Rijk P., Neefs J.M., Van de Peer Y., and De Wachter R. 1992. Compilation of small ribosomal subunit RNA sequences. *Nucleic Acids Res.* **20:** 2075–2089.

De Rijk P., Robbrecht E., de Hoog S., Caers A., Van de Peer Y., and De Wachter R. 1999. Database on the structure of large subunit ribosomal RNA. *Nucleic Acids Res.* **27:** 174–178.

Dong S. and Searls D.B. 1994. Gene structure prediction by linguistic methods. *Genomics* **23:** 540–551.

Durbin R., Eddy S., Krogh A., and Mitchison G., Eds. 1998. *Biological sequence analysis. Probabilistic models of proteins and nucleic acids*, chapters 9 and 10. Cambridge University Press, Cambridge, United Kingdom.

Eddy S. and Durbin R. 1994. RNA sequence analysis using covariance models. *Nucleic Acids Res.* **22:** 2079–2088.

Fichant G.A. and Burks C. 1991. Identifying potential tRNA genes in genomic DNA sequences. *J. Mol. Biol.* **220:** 659–671.

Freier S.M., Kierzek R., Jaeger J.A., Sugimoto N., Caruthers M.H., Neilson T., and Turner D.H. 1986. Improved free-energy parameters for predictions of RNA duplex stability. *Proc. Natl. Acad. Sci.* **83:** 9373–9377.

Gorodkin J., Heyer L.J., Brunak S., and Stormo G.D. 1997. Displaying the information contents of structural RNA alignments: The structure logos. *Comput. Appl. Biosci.* **13:** 583–586.

Gultyaev A.P., van Batenburg F.H., and Pleij C.W. 1995. The computer simulation of RNA folding pathways using a genetic algorithm. *J. Mol. Biol.* **250:** 37–51.

Gutell R.R. 1994. Collection of small subunit (16S- and 16S-like) ribosomal RNA structures *Nucleic Acids Res.* **22:** 3502–3507.

Gutell R.R., Noller H.F., and Woese C.R. 1986. Higher order structure in ribosomal RNA. *EMBO J.* **5:** 1111–1113.

Han K. and Kim H.-J. 1993. Prediction of common folding structures of homologous RNAs. *Nucleic Acids Res.* **21:** 1251–1257.

Hofacker I.L., Fekete M., Flamm C., Huynen M.A., Rauscher S., Stolorz P.E., and Stadler P.F. 1998. Automatic detection of conserved RNA structure elements in complete RNA virus genomes. *Nucleic Acids Res.* **26:** 3825–3836.

Jacobson A.B. and Zuker M. 1993. Structural analysis by energy dot plot of a large mRNA. *J. Mol. Biol.* **233:** 261–269.

Jaeger J.A., Turner D.H., and Zuker M. 1989. Improved predictions of secondary structures for RNA. *Proc. Natl. Acad. Sci.* **86:** 7706–7710.

———. 1990. Predicting optimal and suboptimal secondary structure for RNA. *Methods Enzymol.* **183:** 281–306.

Korab-Laskowska M., Rioux P., Brossard N., Littlejohn T.G., Gray M.W., Lang B.F., and Burger G. 1998. The organelle genome database project (GOBASE). *Nucleic Acids Res.* **26:** 138–144.

Lafontaine D.A., Deschenes P., Bussiere F., Poisson V., and Perreault J.P. 1999. The viroid and viroid-like RNA database. *Nucleic Acids Res.* **27:** 186–187.

Limbach P.A., Crain P.F., and McCloskey J.A. 1994. Summary: The modified nucleosides of RNA. *Nucleic Acids Res.* **22:** 2183–2196.

Lowe T.M. and Eddy S.R. 1997. tRNAscan-SE: A program for improved detection of transfer RNA genes in genomic sequence. *Nucleic Acids Res.* **25:** 955–964.

———. 1999. A computational screen for methylation guide snoRNAs in yeast. *Science* **283:** 1168–1171.

Maidak B.L., Cole J.R., Parker C.T., Jr., Garrity G.M., Larsen N., Li B., Lilburn T.G., McCaughey M.J., Olsen G.J., Overbeek R., Pramanik S., Schmidt T.M., Tiedje J.M., and Woese C.R. 1999. A new version of the RDP (ribosomal database project). *Nucleic Acids Res.* **27:** 171–173.

Martinez H.M. 1984. An RNA folding rule. *Nucleic Acids Res.* **12:** 323–334.

Mathews D.H., Sabina J., Zuker M., and Turner D.H. 1999. Expanded sequence dependence of thermodynamic parameters provides robust prediction of RNA secondary structure. *J. Mol. Biol.* **288:** 911–940.

McCaskill J.S. 1990. The equilibrium partition function and base pair binding probabilities for RNA secondary structure. *Biopolymers* **29:** 1105–1119.

Nakaya A., Yamamoto K., and Yonezawa A. 1995. RNA secondary structure prediction using highly parallel computers. *Comput. Appl. Biosci.* **11:** 685–692.

Notredame C., O'Brien E.A., and Higgins D.G. 1997. RAGA: RNA sequence alignment by genetic algorithm. *Nucleic Acids Res.* **25:** 4570–4580.

Nussinov R. and Jacobson A.B. 1980. Fast algorithm for predicting the secondary structure of single-stranded RNA. *Proc. Natl. Acad. Sci.* **77:** 6903–6913.

Pavesi A., Conterio F., Bolchi A., Dieci G., and Ottonello S. 1994. Identification of new eukaryotic tRNA genes in genomic DNA databases by a multistep weight matrix analysis of transcriptional control regions. *Nucleic Acids Res.* **122:** 1247–1256.

Pipas J.M. and McMahon J.E. 1975. Method for predicting RNA secondary structure. *Proc. Natl. Acad. Sci.* **72:** 2017–2021.

Rice P.M., Elliston K., and Gribskov M. 1991. DNA. In *Sequence analysis primer* (ed. M. Gribskov and J. Devereux), pp. 51–57. Stockton Press, New York.

Rozenski J., Crain P.F., and McCloskey J.A. 1999. The RNA modification database: 1999 update. *Nucleic Acids Res.* **27:** 196–197.

Sakakibara Y., Brown M., Hughey R., Mian I.S., Sjölander K., Underwood R.C., and Haussler D. 1994. Stochastic context-free grammars for tRNA modeling. *Nucleic Acids Res.* **22:** 5112–5120.

Samuelsson T. and Zwieb C. 2000. SRPDB (signal recognition particle database). *Nucleic Acids Res.* **28:** 171–172.

Sankoff D., Kruskal J.B., Mainville S., and Cedergren R.J. 1983. Fast algorithms to determine RNA secondary structures containing multiple loops. In *Time warps, string edits, and macromolecules: The theory and practice of sequence comparison* (ed. D. Sankoff and J.B. Kruskal), chap. 3, pp. 93–120. Addison-Wesley, Reading, Massachusetts.

SantaLucia J., Jr. 1998. A unified view of polymer, dumbbell, and oligonucleotide DNA nearest-neighbor thermodynamics. *Proc. Natl. Acad. Sci.* **95:** 1460–1465.

Schnare M.N., Damberger S.H., Gray M.W., and Gutell R.R. 1996. Comprehensive comparison of structural characteristics in eukaryotic cytoplasmic large subunit (23 S-like) ribosomal RNA. *J. Mol. Biol.* **256:** 701–719.

Serra M.J. and Turner D.H. 1995. Predicting thermodynamic properties of RNA. *Methods Enzymol.* **259:** 242–261.

Shapiro B.A. and Navetta J. 1994. A massively parallel genetic algorithm for RNA secondary structure prediction. *J. Supercomput.* **8:** 195–207.

Shumyatsky G. and Reddy R. 1993. Compilation of small RNA sequences. *Nucleic Acids Res.* **21:** 3017.
Simpson L., Wang S.H., Thiemann O.H., Alfonzo J.D., Maslov D.A., and Avila H.A. 1998. U-insertion/deletion edited sequence database. *Nucleic Acids Res.* **26:** 170–176.
Souza A.E. and Göringer H.U. 1998. The guide RNA database. *Nucleic Acids Res.* **26:** 168–169.
Spingola M., Grate L., Haussler D., and Ares M., Jr. 1999. Genome-wide bioinformatic and molecular analysis of introns of *Saccharomyces cerevisiae*. *RNA* **5:** 221–234.
Sprinzl M., Horn C., Brown M., Ioudovitch A., and Steinberg S. 1998. Compilation of tRNA sequences and sequences of tRNA genes. *Nucleic Acids Res.* **26:** 148–153.
Staden R. 1980. A computer program to search for tRNA genes. *Nucleic Acids Res.* **8:** 817–825.
Studnicka G.M., Rahn G.M., Cummings I.W., and Salser W.A. 1978. Computer method for predicting the secondary structure of single-stranded RNA. *Nucleic Acids Res.* **5:** 3365–3387.
Sühnel J. 1997. Views of RNA on the world wide web. *Trends Genet.* **13:** 206–207.
Szymanski M., Barciszewska M.Z., Barciszewski J., and Erdmann V.A. 1999. 5S ribosomal RNA Data Bank. *Nucleic Acids Res.* **27:** 158–160.
Tinoco I., Jr., Uhlenbeck O.C., and Levine M.D. 1971. Estimation of secondary structure in ribonucleic acids. *Nature* **230:** 362–367.
Tinoco I., Jr., Borer P.N., Dengler B., Levine M.D., Uhlenbeck O.C., Crothers D.M., and Gralla J. 1973. Improved estimation of secondary structure in ribonucleic acids. *Nat. New Biol.* **246:** 40–41.
Triman K.L. and Adams B.J. 1997. Expansion of the 16S and 23S ribosomal RNA mutation databases (16SMDB and 23SMDB). *Nucleic Acids Res.* **25:** 188–191.
Tuerk C. and Gold L. 1990. Systematic evolution of ligands by exponential enrichment: RNA ligands to bacteriophage T4 DNA polymerase. *Science* **249:** 505–510.
Tuerk C., Gauss P., Thermes C., Groebe D.R., Gayle M., Guild N., Stormo G., d'Aubenton-Carafa Y., Uhlenbeck O.C., Tinoco I., Jr., et al. 1988. CUUCGG hairpins: Extraordinarily stable RNA secondary structures associated with various biochemical processes. *Proc. Natl. Acad. Sci.* **85:** 1364–1368.
Turner D.H. and Sugimoto N. 1988. RNA structure prediction. *Annu. Rev. Biophys. Biophys. Chem.* **17:** 167–192.
von Heijne G. 1987. *Sequence analysis in molecular biology — Treasure trove or trivial pursuit*, pp. 58–72. Academic Press, San Diego, California.
Waterman M.S. and Byers T.H. 1985. A dynamic programming algorithm to find all solutions in a neighborhood of the optimum. *Math. Biosci.* **77:** 179–188.
Williams K.P. 1999. The tmRNA website. *Nucleic Acids Res.* **27:** 165–166.
Winker R., Overbeek R., Woese C., Olsen G.J., and Pfluger N. 1990. Structure detection through automated covariance search. *Comput. Appl. Biosci.* **6:** 365–371.
Woese C.R., Gutell R., Gupta R., and Noller H.F. 1983. Detailed analysis of the higher-order structure of 16S-like ribosomal ribonucleic acids. *Microbiol. Rev.* **47:** 621–669.
Wower J. and Zwieb C. 1999. The tmRNA database (tmRDB). *Nucleic Acids Res.* **27:** 167.
Wuchty S., Fontana W., Hofacker I.L., and Schuster P. 1999. Complete suboptimal folding of RNA and the stability of secondary structures. *Biopolymers* **49:** 145–165.
Zuker M. 1989. On finding all suboptimal foldings of an RNA molecule. *Science* **244:** 48–52.
———. 1991. Suboptimal sequence alignment in molecular biology. Alignment with error analysis. *J. Mol. Biol.* **221:** 403–420.
———. 1994. Predicting optimal and suboptimal secondary structure for RNA. *Methods Mol. Biol.* **25:** 267–294.
Zuker M. and Jacobson A.B. 1995. "Well-determined" regions in RNA secondary structure prediction: Analysis of small subunit ribosomal RNA. *Nucleic Acids Res.* **23:** 2791–2798.
———. 1998. Using reliability information to annotate RNA secondary structures. *RNA* **4:** 669–679.
Zuker M. and Sankoff D. 1984. RNA secondary structures and their prediction. *Bull. Math. Biol.* **46:** 591–621.
Zuker M. and Stiegler P. 1981. Optimal computer folding of large RNA sequences using thermodynamics and auxiliary information. *Nucleic Acids Res.* **9:** 133–148.
Zuker M., Jaeger J.A., and Turner D.H. 1991. A comparison of optimal and suboptimal RNA secondary structures predicted by free energy minimization with structures determined by phylogenetic comparison. *Nucleic Acids Res.* **19:** 2707–2714.
Zwieb C. 1997. The uRNA database. *Nucleic Acids Res.* **25:** 102–103.